SANTA CLARA UNIVERSITY

Department of Mechanical Engineering

I HEREBY RECOMMEND THAT THE THESIS PREPARED
UNDER MY SUPERVISION BY

Aja Hartman, Heather Montgomery, Shane Hereford, Grant Goyette

ENTITLED

PROOF OF CONCEPT PLANETARY LANDER TEST ARTICLE

BE ACCEPTED IN PARTIAL FULFILLMENT OF THE REQUIREMENTS
FOR THE DEGREE OF

BACHELOR OF SCIENCE
IN
MECHANICAL ENGINEERING

Thesis Advisor date

Department Chair date

PROOF OF CONCEPT PLANETARY LANDER TEST ARTICLE

By

Aja Hartman, Heather Montgomery, Shane Hereford, Grant Goyette

SENIOR DESIGN PROJECT REPORT

Submitted to
the Department of Mechanical Engineering

of

SANTA CLARA UNIVERSITY

in Partial Fulfillment of the Requirements
for the degree of
Bachelor of Science in Mechanical Engineering

Santa Clara, California

2015

Proof of Concept Planetary Lander Test Article

Aja Hartman, Heather Montgomery, Shane Hereford, Grant Goyette

Department of Computer Engineering
Santa Clara University
2015

Abstract

The goal of this proof of concept planetary lander is to safely deliver an exploration rover to a planet surface. This lander was designed to be used as the last stage of landing in the existing entry, descent, and landing procedures used in previous Mars missions. The design improved upon past missions to Mars by reducing risk of failure during landing by utilizing a passive system with no electronics or control systems while also increasing landing site accuracy. These goals were accomplished by incorporating external crushable materials and internal damping systems. Five drop tests of our final design were completed. The test results can be used for scaling the components of the modular design to suit different planet conditions.

Our scaled down test article design absorbed 7.40% of the energy absorbed by the previous Mars landing systems. The remote-controlled vehicle payload we used survived all of our tests. To scale up our design for a Spirit sized mission, we recommend using a crushable material design with 350 cylinders with the dimensions of 0.06 m radius, 0.00196 m thickness, and 0.1377 m height. Our design can be used for multiple payload landing applications, including care packages and supply deliveries.

Acknowledgments

We would like to sincerely thank our advisors Dr. Nikola Djordjevic and Dr. Timothy Hight. Without their help and guidance this project would not have been the fun and insightful learning experience it has been.

Although not our official advisors, Dr. Robert Marks, Dr. Calvin Tszeng, and Don MacCubbin were a huge help. Dr. Marks provided us with time in his material testing lab that was crucial to the success of our design. Dr. Tszeng provided very insightful guidance when we were in the process of analyzing our data. The designing and machining of our project would not have been possible without the expertise of Don MacCubbin.

Finally, we would like to thank Silicon Valley Glass, Inc. and Xchange Solutions, Inc. for their generous donation to our project that allowed us rent special equipment to successfully test our final design.

Table of Contents

Page

Chapter 1 - Introduction…….……....1

1.1 Background……1

1.2 Motivation……..2

1.3 Objective……3

1.4 Goals……..3

1.5 Review of Field Literature…….…3

Chapter 2 - Systems-Level Chapter…….…..…7

2.1 Customer Needs and System Level Requirements……7

2.2 System Level Sketch……...…...8

2.3 Functional Analysis……...……...…….8

2.4 Benchmarking Results……...……..10

2.5 Key Systems Level Issues……....12

2.6 Layout of System and Subsystems……...…...13

2.7 Team and Project Management…...……...…….14

Chapter 3 - Subsystem Chapters……..17

3.1 Guidance Parachute……..……...17

3.2 Internal Frame…….…….17

3.3 Internal Shock Absorption…….……..21

3.4 Shell……..……...26

3.5 Crushable Material……...……26

3.6 Design Comparison……...……...34

Chapter 4 - Modeling Cylindrical Shell Buckling……..…….36

Chapter 5 - System Integration and Test Results…….……38

5.1 Test Safety and Procedure……...…….……...38

5.2 Testing Results and Analysis for the First Round of Testing……...……...……38

5.3 Testing Results and Analysis for the Second Round of Testing……..…….……..41

5.4 Comparing Test Results to Goal……..……45

Chapter 6 - Cost Analysis……..…..47

Chapter 7 - Patent Search…….....48
7.1 General Purpose……..…….48
7.2 Possible Variants……..……48
7.3 Competing Technologies……..…….……49
7.4 Commercialization Possibilities……...……49
7.5 Inventors……...……...49
7.6 Key Dates…….49
7.7 Sketches……...……50
7.8 Summary of the Patent Classifications……50
7.9 Review of "Prior Art" ……...……..51
7.10 Patentability…….……..53
Chapter 8 - Scaling Up Our Design……54
Chapter 9 - Engineering Standards and Realistic Constraints…….……57
9.1 Economic Considerations……57
9.2 Environmental Impact……..57
9.3 Sustainability…….……...57
9.4 Manufacturability……...……..58
9.5 Health and Safety……..……...58
Chapter 10 – Arts…….59
Chapter 11 - Summary and Conclusions……...……..……60
11.1 Summary……60
11.2 Future Uses……...…….60
11.3 Lessons Learned…….60
Bibliography……..……..61
Appendix A: Detailed Calculations…….……64
Appendix B: Assembly Drawings……...……65
Appendix C: PDS/Requirements…….……78
Appendix D: Timelines……83
Appendix E: Decision Matrices……...……85
Appendix F: Detailed Parts List……...…86
Appendix G: Simulink Block Diagram……88

Appendix H: Copies of Important Patents……...……89
Appendix I: Technical Materials for Accelerometer……...…….106

List of Figures

Page

Figure 1 The system level sketch has brief descriptions of each system…….8
Figure 2 Finite element analysis for bending stress during flat impact…….……19
Figure 3 Finite element analysis for shear stress during flat impact……..19
Figure 4 Finite element analysis for bending stress during a corner load…….…20
Figure 5 Finite element analysis for shear stress during a corner load…….….20
Figure 6 Preliminary sketches for the suspension……..…21
Figure 7 The final suspension design modeled in Solidworks……..…22
Figure 8 A diagram showing a simplified geometry of the suspension…….…23
Figure 9 A diagram of a spring, mass, and damper system……...25
Figure 10 The response of the suspension to an impulse, modeled in Simulink……...25
Figure 11 Modeling set-up with pendulum and material……...27
Figure 12 The free-body diagram of the testing system.……...28
Figure 13 The amount of energy absorbed over the distance crushed……...31
Figure 14 The tall cans crushed after impact failed due to buckling…….31
Figure 15 The energy absorbed by one and two cans crushed at a time……32
Figure 16 Can configuration for the crushable base……..33
Figure 17 The final planetary landing capsule proof of concept test article.…….37
Figure 18 A photo from the testing site of the test set up……..38
Figure 19 The acceleration magnitude recorded during the 3 meter drop.……39
Figure 20 The acceleration magnitude recorded during the 6 meter drop. ……...39
Figure 21 The acceleration magnitude recorded during the 12 meter drop……...40
Figure 22 The acceleration magnitude recorded during the second test 12 meter drop……42
Figure 23 The acceleration magnitude recorded during the third test 12 meter drop……42
Figure 24 Shock response spectra……..43
Figure 25 Typical chip end conditions……...44
Figure 26 Free body diagram of the capsule as it experiences free fall…….45
Figure 27 A sketch of the planetary lander utilizing cylindrical tubes……..50
Figure 28 The bottom view of the planetary landing capsule crushable base……...50

Figure 29 Relationship between the buckling force and thickness of the buckling cylinder……55
Figure 30 Relationship between the buckling force and the radius of the buckling cylinder……55

List of Tables

Page

Table 1 Customer needs in tabular form ordered vertically by importance……...…….……7

Table 2 6061-T6 Al properties provided by the SolidWorks material database……18

Table 3 List of parameters used to create the suspension system model……...24

Table 4 Modeling results for each loading condition.……..……..……..30

Table 5 Material properties of silicon……44

Table 6 Impact energy comparison…..……..46

Table 7 The five iterations of cylinder geometry design solutions ……...56

Table 8 List of team members and one of their drawing locations…….…...59

Table 9 Priority matrix based on customer analysis……...……...85

Table 10 Design rating matrix used to choose between possible design solutions……...85

Chapter 1 Introduction

1.1 Background

Existing Entry, Descent, and Landing

Landing a Rover on another planet was accomplished using three different stages. In the first stage, entry, the landing capsule began to enter the planet's atmosphere and used a heat shield to protect the capsule from heat damage. After this stage was completed, the heat shield was released and a large parachute was enabled, enacting the descent stage and slowly lowering the capsule. Once the descent stage was completed, the landing capsule was released and experienced free fall for 12m before landing on the planet surface [19].

Current Problems

Landing rovers on a different planet is challenging. It is impossible to have direct control over landing operations because of communication lag due to the large distance between mission control and the planet where the mission is being carried out. This means that all electronic components related to landing must use complicated control systems to land autonomously. Space and weight is limited due to current rocket technology, therefore a more compact and lightweight design is always desirable. The rover must be fully operational after the landing capsule has stopped acceleration, meaning that it is unharmed, upright, and has access to the planet surface. If the rover payload is not operational, for example its sensors, data collection hardware, or transmitter are broken, then the mission is a failure and all of the funds and time used to prepare for the mission are wasted.

Current Solutions

NASA has landed multiple rovers on Mars, which include Pathfinder, Spirit, Opportunity, and Curiosity. The landing capsule that delivered the most rovers to the surface of Mars used airbag retraction actuator technology. The airbags surrounded the landing capsule and absorbed energy

while bouncing across the surface of Mars [1][4]. The newest landing capsule design was implemented for the Curiosity rover. It used multiple reverse thrusters and lowered the Curiosity rover with cables to the surface of Mars [13].

Current Solution Drawbacks

The airbag retraction actuator technology was expensive, and dangerous. If the airbag released too soon, it could damage the other components of the rover carrier used for the entry and descent landing procedures. If the airbag system did not deploy, then the unprotected rover and capsule would be subjected to all of the impact force. The airbag retraction actuator caused the landing capsule to bounce long distances, over a kilometer for the Mars landers, which caused the landing location to be inaccurate and unpredictable. The reverse propulsion system was also very risky because it relied on a complicated control system that made the reverse thrusters hover. This meant that there was a high failure risk if the control system malfunctioned or hardware malfunctioned that could cause the whole mission to fail.

1.2 Motivation

Space exploration and science have, historically, been government controlled. In order to have a just society, space exploration needs to be open to a diverse population. There is a need to create a cost effective planetary landing capsule that will be more economically available.

Space is used for communications, remote sensing, navigation, science and exploration. Space is the final frontier, and needs to be explored. There is a lot to learn about space and there is the potential that scientific findings can be used to improve human life.

In order to pursue knowledge of other planetary environments, and history of previous life, we need to land robots equipped for testing on different planets. Humans are not well suited for missions to other planets because they require expensive and complicated life support systems that regulate breathable atmosphere, temperature, balanced nutrition, and caloric input. Also, return capability is needed because leaving a human on another planet to die is unethical. These

issues are avoided by using unmanned rovers to explore other planets instead of humans.

The world has an expanding population, and population growth is expected to continue. We live on a planet that will not be able to support this estimated population growth, which means our current trajectory leads to an inhumane and unsustainable world population. There is a need to land robots equipped for testing on different planets, in order to have a better understanding of the environment and be able to design ways to sustain human life on these other planets as a solution to overpopulation.

1.3 Objective

Our objective was to create a more compact and lightweight, passive landing device. Our team designed and built a planetary landing capsule proof of concept test article that safely delivered a functioning payload to Earth. Afterwards, our modular design could be scaled up or down for different applications.

1.4 Goals

Our team goals were to work efficiently throughout the entire year to finish our Planetary Landing Capsule in a timely manner. Our goal was to follow our timeline with few alterations in deadlines. We were aiming to learn about aerospace, and how to apply our mechanical engineering skills. We wanted to make our design experience fun, grow together as a team, and as individual engineers. We also wanted to improve our problem solving skills and learn how to make our ideas come to life. We intended for our final project to be complete and functioning, and earn a good grade. All of these goals have been achieved.

1.5 Review of Field Literature

Paul Withers applied simple physics concepts and college level calculus to analyze the descent of a landing spacecraft on Mars in his article, "Landing Spacecraft on Mars and Other Planets: An

Opportunity to Apply Introductory Physics" [29]. The author aimed to inform readers about the criticality of the designs and descent stages chosen by NASA. The article was broken into four main sections: entry descent and deceleration, decent and impact without parachutes, descent and impact with parachutes, and design considerations for descents through alien atmospheres that are much thicker than Mars'. The author developed a set of equations using elementary physics, and college calculus. These equations described the velocities throughout the various descent stages in terms of the Martian atmospheric conditions. It was concluded that a parachute used in conjunction with retrorockets was crucial in landing any spacecraft safely on Mars. This knowledge of the first NASA solution to planetary landing was crucial to our design because we needed to understand the issues and current technology related to planetary landing before brainstorming new solutions.

Adam Steltzner detailed the various complicated systems that were new to the Curiosity's entry, descent, and landing system, and discusses the design challenges they presented in his article,"Mars Science Laboratory Entry, Descent, And Landing System Development Challenges" [23]. Before Curiosity, the landing systems of Mars rovers were relatively simple because they utilized airbags and other systems that required less programming and computer control. The Curiosity landing sequence featured a new heat shield material to shed weight, a thruster control system that could react to the entry and descent conditions, a new parachute that could accommodate the huge weight of Curiosity (the heaviest rover to date), mobility deployment systems, and the SkyCrane. The thrusters used during the Curiosity rover were deployed shortly after the parachute. These thrusters were upgraded from previous designs to correct the descent trajectory and improve landing site accuracy. The mobility deployment system was a completely new system that jettisoned after the parachute and thrusters had done their job. This module held the Curiosity rover and gently decelerated it to about 0.42 m/s at 20 m above the Martian surface using 8 computer controlled thrusters. At this altitude the all new SkyCrane lowered the rover to the planet surface. The mobility deployment system then cut its cord to Curiosity and flew away. This knowledge of the newest NASA solution to planetary landing helped our design process because we needed to understand the new technology that

enabled accurate landing before brainstorming new solutions to this issue.

Kurng Chang reported the findings of an experiment to test the shock reactions of various components on Mars Exploration Rover (MER) landers and Airbag Retraction Actuators (ARA) in his article, "Mars Exploration Rover (MER) Airbag Retraction Actuator (ARA) Pyroshock Test Results" [1]. During entry, descent, and landing, MER landers experienced shock from a variety of different sources. These included shocks generated to begin entry, deploy the parachute, detach the heat shield, fire retrorockets, deploy ARAs, detach landing capsule, and touchdown itself. Shock was simulated using a variety of equipment on various sensitive components making up the landing capsule. The report concluded that the sensitive components successfully survived the simulated shocks without damage. The simulated shocks were set to be more aggressive than the estimated shock to be experienced during landing. Understanding the importance of shock and how acceleration data was used was essential to designing our testing procedure and project design specifications.

Ellie Zolfagharifard discussed one of the proposed landing systems for the ExoMars rover to be launched by the European Space Agency (ESA) in 2018 in her article, "Soft Landings" [31]. The proposed system utilized vented airbags that deflated in a controlled manner upon touchdown to the Martian surface. This new design was much lighter than the airbag systems used by American landers before Curiosity, and increased the landing site accuracy by not bouncing. The design was a giant donut shaped airbag with very complicated, computer controlled pressure valves to precisely deflate the airbag upon touch down. The article also presented the challenges associated with this new design and how the company proposing it was overcoming them with new technologies. The ESA solution to landing on Mars was a strong inspiration for our final design, our final design deformed material, like the ExoMars airbag, to absorb impact and eliminate bouncing.

Brian Dunbar explained the design and testing of the airbag systems used in the Pathfinder lander in his article, "Mars Pathfinder Air Bag Landing Tests." The reason for developing the airbags were to reduce contamination of the Martian surface created by using a purely powered

descent and landing. This powered landing utilized rockets whose exhaust chemicals would contaminate any soil or rock to be tested around the landing site. The article chronicles the tests and how the final design of the airbags was arrived at. The rigor of the tests was also emphasized by detailing the conditions that were created in testing chambers. Non-powered landing was found to be very important to Mars landing missions and was used as one of our design specifications during the design process to reflect this issue.

Chapter 2 Systems-Level Chapter

2.1 Customer Needs and System Level Requirements

The needs listed in the customer needs section were derived from the three interviews [11][12][22]. The importance of each item on the list of needs was deciphered using the opinions from the interviews, our team's product design specifications, and our team's preferences. The needs were grouped into three main categories: the ability to carry out the objective, cost to be within the budget, and the system level requirements that need to be met. A table reflecting this importance of needs based hierarchy organization is shown in Table 1.

Table 1: Customer needs in tabular form ordered vertically by importance.

Main Needs	Sub Needs
Ability to carry out objective	
	Low risk
	Lands on planet
	Protects payload
	Opens upright
	Meets performance requirements
	Meets reliability requirements
	Meets quality requirements
Cost within Budget	
	High technical performance
	Meets volume constraints
	Meets weight constraints
	Is legal
Meets Requirements	
	Meets safety requirements
	Able to be manufactured
	Meets maintenance requirements
	Meets environmental constraints
	Meets time scale requirements
	Stands against competition
	Meets shelf storage requirements

2.2 System Level Sketch

The subsystems and their placement on the planetary landing capsule are shown in Figure 1. The user scenario and explanation for how the system works is explained in Figure 1 as well.

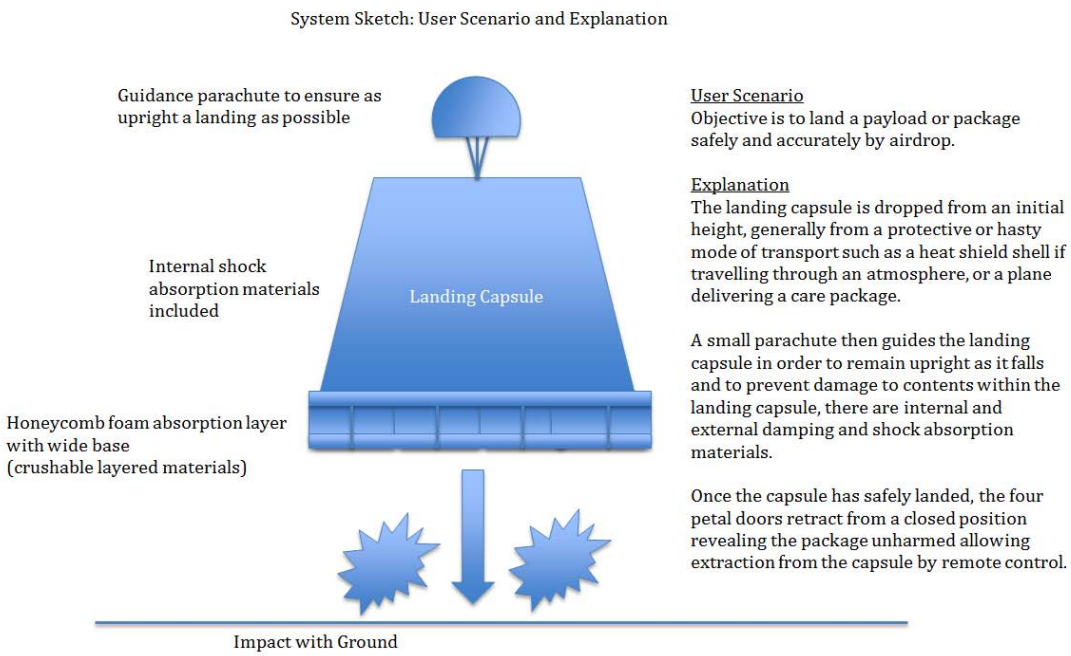

Figure 1. The system level sketch has brief descriptions of each system.

2.3 Functional Analysis

Customer Need

The customer required us to develop a proof of concept test article to safely deliver a functioning

payload to Earth.

Mission Statement

Our mission was to build a small-scale planetary landing capsule that improved upon the Opportunity and Spirit Lander airbag technology while increasing the accuracy of the landing site.

Functional Decomposition

The functional requirements described the behaviors that the planetary landing capsule needed to accomplish in order to fulfill the mission statement. The functional requirements could not be compromised throughout the design process of the planetary landing capsule test article. A list of these functional requirements is provided below:

- Land Safely
- Minimize Weight
- Minimize Size
- Absorb Shock
- Stop Acceleration
- Stop Motion
- Land Upright
- Open
- Provide Payload Planet Access

List of Inputs/Outputs and Constraints

The inputs of the planetary landing capsule are listed below:

- Force
- Shock
- Gravity
- Planet Surface

- Electrical Energy

The outputs of the planetary landing capsule are listed below:

- Shock Absorption
- Stopping Motion
- Landing Upright
- Opening

The constraints of the planetary landing capsule are listed below:

- Maximum Acceleration
- Shock Levels
- Size
- Weight
- Deceleration Time
- Safety
- Cost
- Time
- Able to be Manufactured
- Intellectual Property
- No Maintenance Required
- Durability
- Reliability
- Compact Ability
- PDS Compliance

2.4 Benchmarking Results

There have been three major rover deliveries to Mars in the past two decades. The first, in 1997, delivered the Pathfinder Lander. This lander used airbags in the last stage of landing in order to touch down safely on the surface of Mars. The Pathfinder was designed to stay stationary, while

a very small rover (~65 cm long) would be able to travel some distance away from the Pathfinder [21]. In 2004 the twin rovers, Spirit and Opportunity, were delivered to Mars [27]. The last stage of landing for these landers used the same airbag technology from the Pathfinder lander. Most recently, in 2012, the Curiosity rover was sent to Mars. The lander for this rover used completely different technology. Airbags were removed from the design and a complex system of retro thrusters and a lowering cable were used to deliver Curiosity to the surface.

All three of these missions were successful, but some were much more costly than the others. The Pathfinder mission spent $171 million, Spirit and Opportunity $400 million each, and Curiosity $2.5 billion [27]. The huge increase in cost for Curiosity is due to many things, such as more scientific equipment on board, more accurate equipment, upgraded power systems, better optics, state of the art communication tools, and the new landing technology that used computer controlled rocket thrusters.

The goal of this design project was to present a proof of concept of a new last stage landing system. This system utilized external and internal damping. The Pathfinder and Spirit/Opportunity landers did not use internal damping, only the external air bags [4]. The external shock absorption in our design was achieved by using crushable materials. Internally, a spring dashpot suspension system was used to absorb the remaining energy.

Our new last stage landing system had two goals to improve over the Curiosity, Pathfinder, and Spirit/Opportunity landers. First, our design utilized passive systems. Passive systems have a smaller chance of failure and are much cheaper than computer and sensor controlled systems. Second, our design accomplished a more accurate landing. The Curiosity design veered from the airbags design because of this; the airbag system bounced the landing pod and rover hundreds of meters away from initial touchdown. By using crushable materials to dampen impact, we aimed to reduce bouncing in order to more accurately deliver a rover.

2.5 Key Systems Level Issues

Impact Orientation

After examining various design ideas, affixing external damping material on the bottom of the lander shell was chosen to be most effective. This design decision was the cheapest and lowered the center of gravity, forcing the impact orientation to be upright. A pyramid shaped shell design allowed for a square base and four petals that opened to release the rover. This shape was simple to manufacture and affix crushable material to the bottom. Some designs proposed affixing crushable material on all sides of the lander, but this was deemed too expensive and complex. Instead, a pilot parachute was decided to be used to maintain the proper orientation of the lander so that the impact occurred on the bottom side.

Shock Absorption

Our main goal was to incorporate external damping and internal damping to increase landing accuracy and decrease cost and complexity of a landing capsule. Using exclusively crushable material externally was the best option because it drastically reduced the amount the lander might bounce after touchdown. There were various ideas for the internal damping, which all incorporated a "floating frame." This frame held the rover and other essential equipment. The design differences were regarding how to "float" the frame in the shell. One idea was to suspend the frame on all sides by springs, another would use soft foam to encapsulate the frame, and the last design would utilize a suspension system that connected the frame to the bottom of the shell. We decided that the suspension system was the best option because of the low cost and complexity it entailed.

Achieving Upright Position

This system level issue was solved when choosing the shape of the lander. The Pathfinder and Spirit/Opportunity landers all used a tetrahedral shaped lander. This design enabled the lander to orient itself upright from any orientation when the petals were opened. We chose a pyramid shape, instead of a tetrahedral, because a square base was easier to design and manufacture than

a triangular base. A square base was easier to affix crushable materials to cover the entire base, and helped prevent the capsule from falling over after touchdown. One design idea was to use a cylinder shaped capsule, but manufacturing a cylinder would be more complex than the two dimensional geometric shapes that make up a pyramid.

Delivering Rover

Once the lander had halted all movement and the petals were opened, the rover must be released. A couple design ideas to accomplish this were considered. All of the designs must contain and support the rover during impact, and then be able to release it when necessary. One design proposed using a servo that latched or de-latched a mechanism that held the rover in place. The servo was activated after the petals opened. A simpler design used the same encapsulating foam that supported the floating frame. This foam was retracted as the petals were opening. The third design utilized an L-bracket attached to the frame and a pin that attached the payload to the L-bracket. When the petal doors opened, the pin would release the payload from the L-bracket. This design reduced complexity and chances for error, which is why it was chosen as the delivering rover mechanism.

2.6 Layout of System and Subsystems

Our main system was a planetary landing capsule test article that delivered a payload safely from freefall to the planet surface.

The subsystems were the: guidance parachute, internal frame, internal suspension, external shell, and crushable material. A pictorial layout of both the main system and subsystems is shown in Figure 1 on Page 8. The parachute was located at the top of the planetary landing capsule and induced drag to ensure the planetary landing capsule landed upright. The internal frame was located inside the planetary landing capsule and was used as the structural foundation. The internal suspension attached the frame to the shell and was used to absorb residual impact forces that the crushable material did not absorb. The shell was made up of four petal doors and a base, which fully encapsulated the payload and frame. The crushable material was attached to the

bottom of the shell and was used to absorb initial impact energy.

2.7 Team and Project Management

Project Challenges and Constraints

There were multiple challenges encountered in this project. All of the functional requirements were considered challenges, which included landing safely, minimizing weight, minimizing size, absorbing shock, stopping acceleration, stopping motion, landing upright, opening, and providing payload access to planet. The overall challenge encountered by this project was finding a way for the capsule to land safely without harming the payload. There were several constraints that had to be complied with in order for the mission statement to be accomplished. The project constraints were maximum acceleration, shock levels, size, weight, deceleration time, safety, cost, time, able to be manufactured, intellectual property, no maintenance required, durability, reliability, compact ability, and PDS compliance.

Budget

One of the main budgetary issues was that we were on a $2000 budget and the total cost of this project exceeded our budget by $200. For testing purposes, $800 was donated by Silicon Valley Glass Inc. and Xchange Solutions Inc. for boomlift rentals and did not cover any of our budget expenses. There were four components budgeted for including the shell material, accelerometer, testing equipment and frame parts. Our detailed parts list, which is in Appendix F, has specific items that we needed to purchase to guarantee that we could build a mock up, model, and final design test article.

Timeline

Following our timeline was necessary in order to stay on task and and complete general milestones and benchmarks accordingly. Our timeline was flexible and could be fleshed out in detail as more information about building and testing was acquired. Our final timeline can be seen in Appendix D.

Design Process

Our team began the design process by identifying our problem, and coming up with a problem definition. We began to research past landing capsule designs to learn about problems with existing designs. This research led to our own generation of ideas that involved many brainstorming sketches. The sketches were broken up by function. The four functions we designed for were stopping motion and acceleration, absorbing shock, landing upright, and opening. After collaborating over the sketches, we made a priority matrix that led us to our design choice, which can be seen in Appendix E. This design choice was evaluated and tested for effectiveness and changed based on these tests. We made a model capsule and mock up capsule to test our design ideas and sensor equipment. We used what we learned from both physical capsules to design and build our final design iteration of a proof of concept planetary landing capsule.

Risks and Mitigations

One of the biggest risks for this project was safety. Some safety issues included sharp edges, shattering parts, and pinch points. There also was an inherent safety risk with the necessary testing of our project by dropping it 12 m. Our project was tested off campus, so the safety of the Santa Clara University community was ensured. We tested our project at Silicon Valley Glass. Our safety plan was a collaboration of multiple advisors so that the safety of the Silicon Valley Glass community was maintained. Only non-shattering materials were used in our design. Protective coverings over all components that could cause bodily harm were affixed. We also designed our crushable material base to be easily affixed and dismounted without touching sharp deformed materials. We filed down any sharp edges to prevent injury during manufacturing and testing.

Team Management

Our team was strict with each other when it came to accomplishing tasks and making sure everything was completed on time. We had defined roles in the team, which were Heather

Montgomery as team leader, Aja Hartman as team facilitator, Grant Goyette as team documenter, and Shane Hereford as team code of cooperation enforcer. However, our roles sometimes overlapped, which worked well for our team. There were no issues with team management. We respected each other, and were all passionate about our project, which created a positive environment for our team to work in.

Chapter 3 Subsystem Chapters

3.1 Guidance Parachute

The purpose of the guidance parachute was to to help ensure that the landing capsule landed in an upright position. There were multiple parachute design ideas. The first idea was a parachute made of cloth material attached by string to the top of the planetary landing capsule. The second possible design was an umbrella approach where the parachute had a stiff structure and was only attached to the planetary landing capsule by one component. After testing the mockup design, we found that landing upright was easily obtained without a parachute at our drop height; therefore, the parachute subsystem was eliminated from the planetary landing capsule design.

3.2 Internal Frame

The purpose of the internal frame was that it provided the structure to the planetary landing capsule. This subsystem was included in all of the designs proposed in the design rating matrix shown in Appendix E. After the final planetary landing capsule design was chosen, we analyzed the internal frame using finite element analysis.

The finite element analysis of the internal frame was accomplished by applying a 15973 N force to the frame in two cases. One case assumed that there was a perfectly flat impact with the ground and the frame. The other case assumed that the frame impacted the ground on one corner. The 15973 N force was obtained by taking 10% of the impact energy the Spirit capsule experienced, and then dividing that energy by the sum of the can crushing distance and the travel of the internal suspension.

The drop test analyses shown in Figures (2) and (3) was made by assuming a perfectly uniform and flat impact where the forces were evenly distributed throughout the frame after being transmitted through the crushable material and the internal suspension. The force transmitted to the frame was done in the same orientation as the shocks at a 45-45-90 triangle geometry.

Applying the bending stress setting for the stress analysis showed no expected failures within the frame. The maximum bending stress and shear stress experienced anywhere in the frame was 158 MPa and 14.17 MPa, respectively. There was a Factor of Safety of 1.74 and 19.4 for bending stress and shear stress, respectively, which was found by comparing the maximum stress results to the maximum yield stress of 275 MPa as shown in Table 2.

For the analyses in Figures (4) and (5), it was assumed that the capsule landed on a corner, therefore applying the stress in the frame to a localized area. This was the assumed worst case scenario for our drop testing. As was done for the perfectly flat impact analyses, bending stress and shear stress were analyzed throughout the frame. It was found that the maximum bending and shear stress were about 1088 MPa and 10.74 MPa. This analysis showed that the frame had a Factor of Safety of 25.4 in terms of shear, but was 3.95 times the yield stress expected at the top of the frame for bending, indicating that there would be imminent failure in the top of the frame should the capsule land on a corner. This meant that the impact orientation of the capsule was very important and must be completely upright for our design to function properly.

Table 2: 6061-T6 Al properties provided by the SolidWorks material database.

Property	Value	Units
Elastic Modulus	6.900000067e+010	N/m^2
Poisson's Ratio	0.33	N/A
Shear Modulus	2.600000013e+010	N/m^2
Mass Density	2700	kg/m^3
Tensile Strength	310000002.1	N/m^2
Compressive Strength		N/m^2
Yield Strength	275000000.9	N/m^2
Thermal Expansion Coefficient	2.4e-005	/K
Thermal Conductivity	166.9	W/(m·K)
Specific Heat	896	J/(kg·K)
Material Damping Ratio		N/A

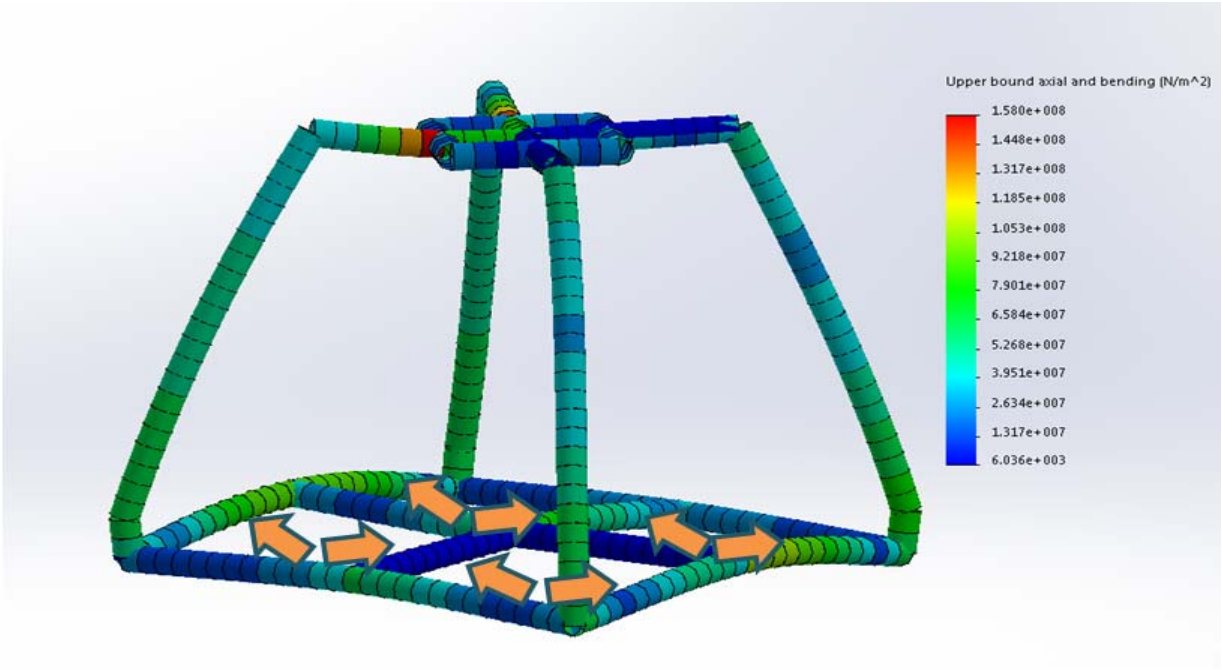

Figure 2. Finite element analysis for bending stress during a perfectly flat impact of 15,973 N force split diagonally 45-45-90 [6.036 x 10^3 to 1.580 x 10^8] (Goyette 2015).

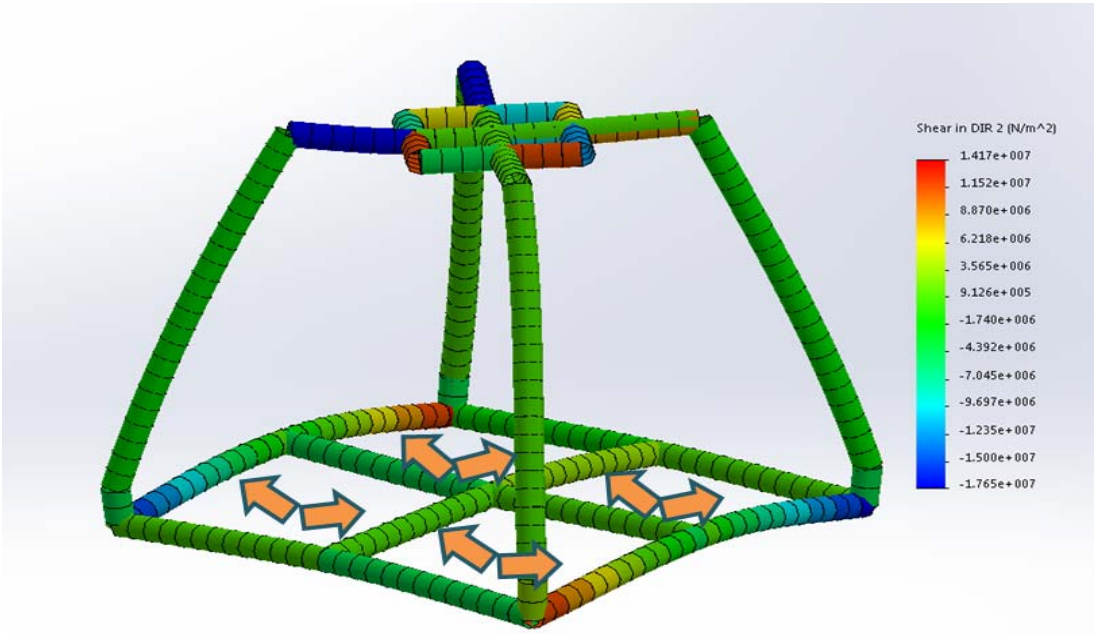

Figure 3. Finite element analysis for shear stress during a perfectly flat impact of 15973 N force split diagonally 45-45-90. [-1.765 x 10^7 to 1.417 x 10^7]

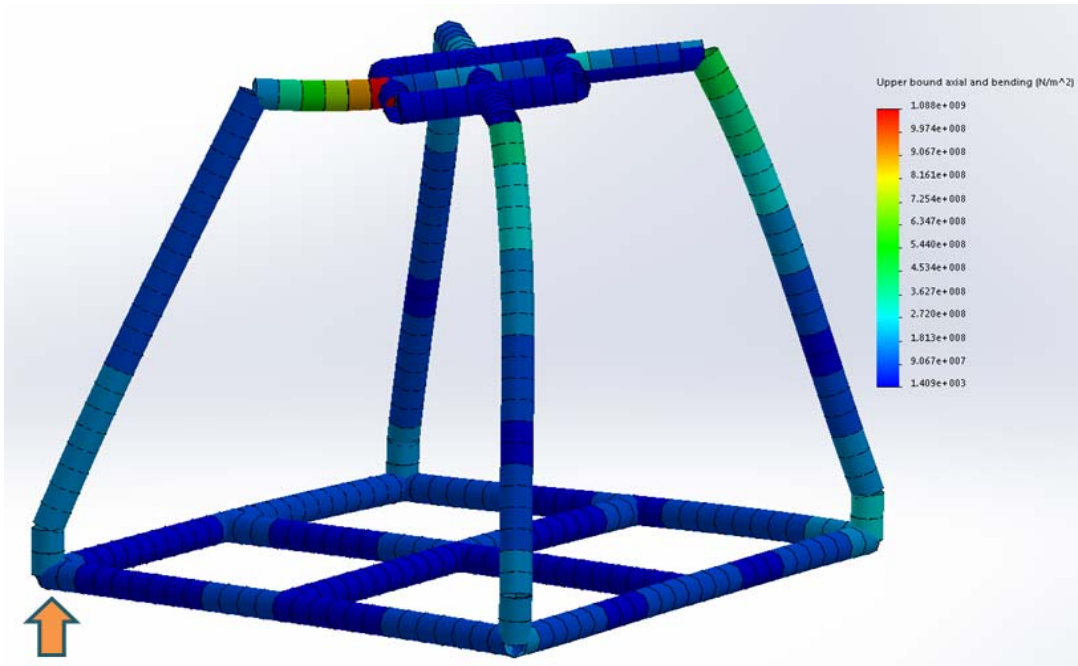

Figure 4. Finite element analysis for bending stress during a corner load of 15973 N force. [1.409 x 10^3 to 1.088 x 10^9]

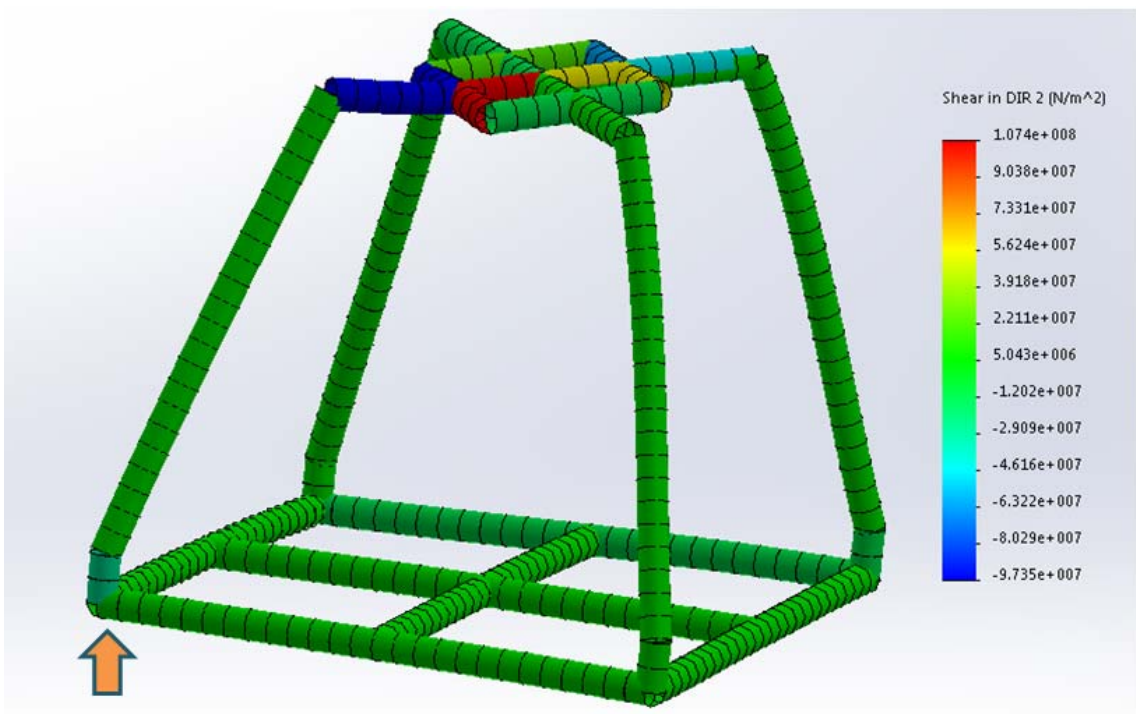

Figure 5. Finite element analysis for shear stress during a corner load of 15973 N force. [-9.735 x 10^7 to 1.074 x 10^8]

3.3 Internal Shock Absorption

The purpose of the internal damper was to absorb residual energy that the crushable material did not absorb. There were two internal shock absorption designs that we considered. The first design used the natural damping properties of foam material encapsulating the payload to absorb residual shock. The second design used an internal shock absorption system consisting of a suspension system. The suspension system utilized mechanical spring dampers to absorb residual energy not absorbed by the crushable base. We chose the suspension system that utilized mechanical spring dampers because we found off-the-shelf bicycle shocks that were inexpensive and performed adequately for the internal shock absorption subsystem needs.

After deciding to use an internal dampening system made up of bicycle shocks, we designed the suspension system. We decided to use DNM-22 bicycle shocks because they were inexpensive mountain bike shocks that included both a spring and a dashpot. Our design utilized four bicycle shocks so that the suspension system could symmetrically absorb energy in the vertical direction. The problem we had to overcome was that each shock was designed for an 80 kg person riding on rough terrain. Since the final design was estimated to weigh 43 kg, we needed to design the suspension in a way that would expose each shock to the type of forces that it was designed for. Pictures of design sketches for the suspension system are shown in Figure 6.

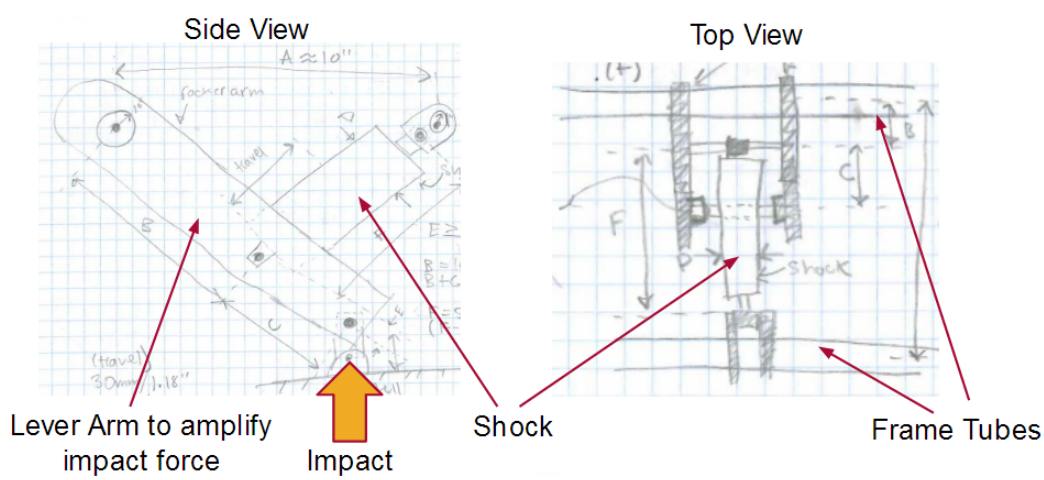

Figure 6. Preliminary sketches for the suspension. Four of these assemblies were used (Hereford

2015).

As seen in Figure 6, the suspension featured a primary lever arm that amplified the impact force, thereby increasing the force experienced by the bicycle shock. The final design is shown in Figure 7.

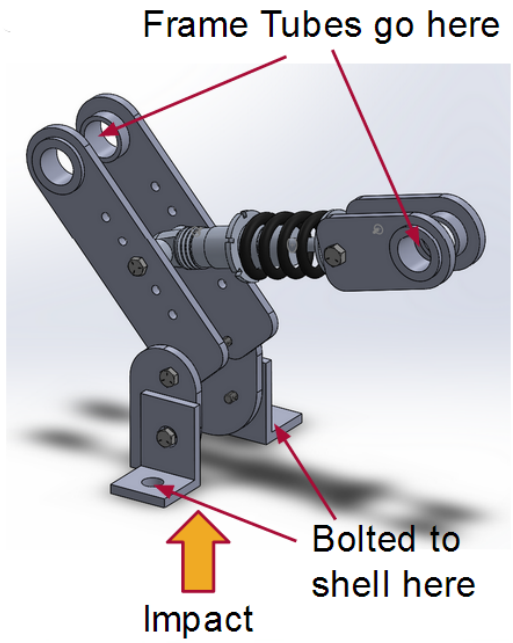

Figure 7. The final suspension design modeled in Solidworks. Four of these assemblies were used. (Hereford 2015)

There were multiple holes for the shock to connect to along the primary lever arm as shown in Figure 7. These were included in case fine tuning of the mechanical advantage given to the impact was needed during testing. The frame connected through the holes at the top of the assembly, and the bottom of the assembly was bolted to the base of the shell through the holes in the L-brackets. There were two advantages to this suspension system: one; each bicycle shock was exposed to forces they were design for, and two; the effective travel of the suspension was doubled. The shocks alone had about 8.75 cm of travel, while the final assembly had a full travel distance of 18.42 cm. This increased travel is due to the new geometry achieved using the lever arm.

In order to predict the assembly's response to an impact, and to test whether it would bottom out during an impact, we performed dynamic analysis on one of the suspension assemblies. An estimated impact force can be found by dividing the impact energy to be dissipated 5,142 J, by the distance over which it was dissipated. The distance over which energy was dissipated was the can height, 0.1377 m, plus the full travel of the suspension, 0.1842 m. The equations used for calculating the impact force are Equations (1) through (3).

$$F_{impact} = \frac{Impact\ Energy}{Can\ Height + Suspension\ Travel} \tag{1}$$

$$F_{impact} = \frac{5{,}141.3}{0.1377 + 0.1842} \tag{2}$$

$$F_{impact} = 15{,}972.79\ N \tag{3}$$

The impact force value was then divided by four, to get the force experienced by each single shock assembly, then multiplied by the lever arm factor provided by the suspension geometry. See Figure 8. The force experienced during impact for each assembly was found to be 3,993 N.

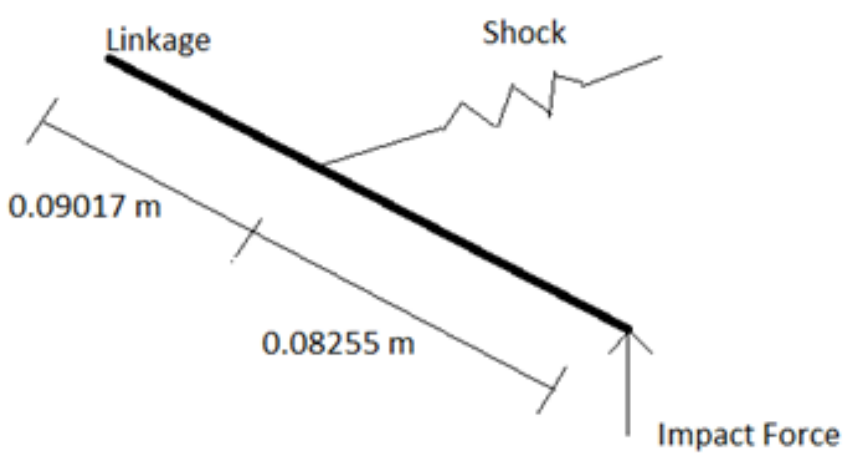

Figure 8. A diagram showing a simplified geometry of the suspension.

Knowing the suspension geometry, we calculated how much the impact force was increased

when going into the bicycle shock. The increase in shock force was calculated using Equation (4) and found to 1.92 times the impact force. Equation (4) balanced the moment about the left side of the lever arm created by the impact force.

$$0.09017F_{shock} = (0.09017 + 0.08225)F_{impact/shock} \tag{4}$$

The force experienced by the shock was about twice the impact force, making the force experienced by each shock 7,667 N.

When calculating the response of a spring, mass, and damper system, the spring constant, damping ratio, system mass, and forcing function must be known. We knew the system mass and forcing function. The forcing function was an impulse with amplitude of the force experienced by one shock. The spring constant and damping ratio were provided by the manufacturer of the shocks. All parameters and characteristics used in this simulation are listed in Table 3.

Table 3: List of parameters used to create the suspension system model.

Parameter	Expected or Calculated Value
Energy Dissipated	5,141.6 Joules
Mass (m)	43 kg
Drop Height	12 m
Impact Force (per shock)	7,666.94 N
Spring Constant (k)	131 kN/m
Damping Ratio (ζ)	0.707

The response of the suspension system was modeled using Simulink. A simple block diagram that represents a spring, mass, and damper system, excited by an impulse is shown in Figure 9.

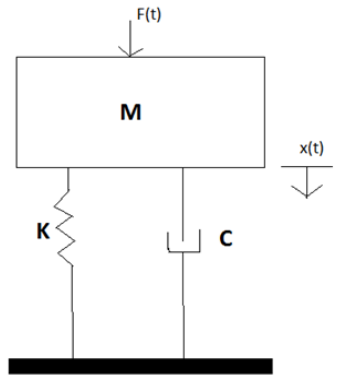

Figure 9. A diagram of a spring, mass, and damper system used to model the suspension system.

After the Simulink Block Diagram was set up, the values from Table 3 were inputted, and the simulation was run. The block diagram can be viewed in Appendix G.

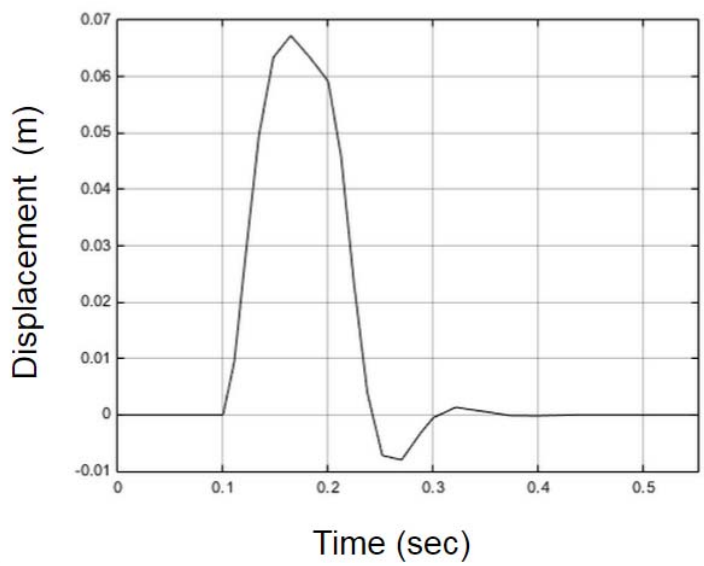

Figure 10. The displacement of the mass (frame) to an impulse, modeled in Simulink.

This simulation showed that the shocks responded very quickly to the input, and that the maximum amplitude of the shock position did not exceed the maximum suspension travel. Looking at Figure 10, the suspension reacted to the impact and settled within 0.4 seconds. There were only two oscillations, the second of which was less than a centimeter. The maximum travel the suspension could handle was 0.1842 m. The simulation had a displacement peak of 0.066 m,

well below the maximum travel distance of 0.1842 m.

This simulation proved, theoretically, that the suspension design was able to handle the expected impact forces. This meant that the shocks would respond quickly and would not bottom out during impact.

3.4 Shell

The purpose of the shell was to encapsulate the payload and open to provide the payload with safe access to the planet surface. We used the design rating matrix shown in Appendix E to choose an initial shell shape. After choosing the initial shell shape, there were several possible designs that opened the petal doors, providing the payload with access to the planet surface. Our first design opened the petal doors using linear actuators. Since they were symmetrically located around the four sides of the landing capsule, should the landing capsule tip over during landing, any of the petal doors could open individually in order to upright the craft onto its base. The second design utilized spring loaded petal doors and an impact pin. The spring loaded petal doors were forced closed using the pin, which broke during impact, releasing the spring-loaded doors. Our third design used weak magnets to hold the doors closed during free fall and disconnected during impact, allowing for the impact to force the petal doors open. We chose to utilize the third design because it was a passive system and the spring loaded hinges were too difficult to work with.

3.5 Crushable Material

The purpose of the crushable material was to absorb the initial impact forces. The shock absorption on the bottom side of the craft was a key factor in our design because it was subjected to the direct impact force. There was a need for sufficient shock absorption and frequency vibration mitigations to protect the payload. We tested different materials to see which could absorb the most energy. The three different materials were egg cartons, tall cans, and short cans.

The test crushable material was attached to a steel plate which would not allow any deformation. The steel plate was against a wall to ensure stability. The material was attached to the plate using packaging tape adhesives only on the outside of the test material. The pendulum of the impact testing device was then raised to a specific height and dropped to crush the material at the bottom of its swing. A picture of the test set up is shown in Figure 11.

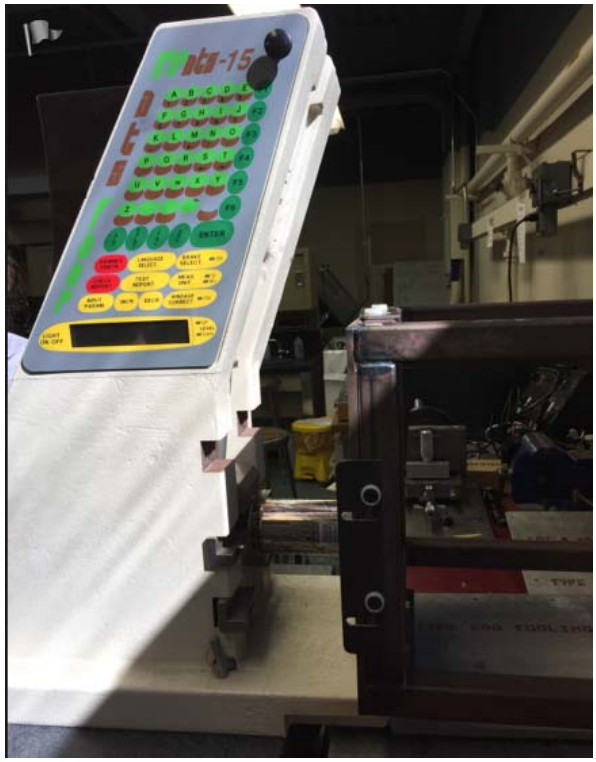

Figure 11. Modeling set-up with pendulum and material (can) held against a wall.

The crushable materials were tested using a pendulum machine. A pendulum with a mass of 4.2kg was raised to various heights and released in order to crush the material that was propped against a wall when the pendulum reached the bottom. The material height was measured before and after crushing in order to find how much the material crushed. The energy absorption was calculated using the potential energy equation, Equation (5).

$$PE = mgh \tag{5}$$

The mass of the pendulum rod was assumed to be negligible. The pendulum was assumed to crush the material at the bottom of its swing. However, as the pendulum crushed the material, it moved away from the bottom of its swing. This slight distance variation was determined to be negligible because not much height was recovered and, therefore, the potential energy did not change a significant amount. There was a small amount of oscillation after initial impact of the pendulum, which we assume to be negligible and, therefore, the deformation of the test material was assumed to absorb all of the potential energy.

Figure 12 shows a simple free-body diagram of the system. There was one degree of freedom. The force applied to the material was supplied through a pendulum.

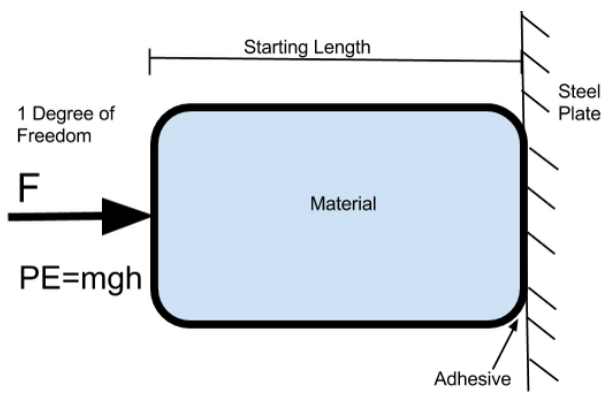

Figure 12. The free-body diagram of the testing system.

The testing materials used were egg cartons made of recycled paper and molded pulp, tall cans made of aluminum, and short cans made of aluminum. The pendulum was made of non-ductile metal and the wall was made of a non-ductile steel plate.

There were several simplifying elements used during this test procedure. The pendulum hit the test material perpendicularly, which was a simplification of how the crushable material on the prototype was oriented during impact. This test did not use other simplifying elements because it was a physical material test and not computer modeled. Physical testing was chosen over computer modeling analysis because deformation and crushing was very complicated to model,

and the purpose of this test was to compare different materials.

The load applied to the material was from the moving pendulum. The mass of the pendulum was 4.2 kg. The pendulum was released at different heights to provide a variety of potential energy values to be absorbed.

The tall can was expected to absorb the most energy over the largest distance because it had more material and length to absorb impact than both the egg carton and shorter can. We measured crushing distance and potential energy absorbed by each material. The material that absorbed the most energy with the largest deformation was determined to be the best material for absorbing impact because impact energy is a function of force and distance.

There were several problems that were encountered during testing. The first problem was accuracy. Making sure the materials were all placed in the same location and the pendulum started from the same height was difficult. By marking the placement of the material on the steel plate and the height of the pendulum using a permanently placed ruler, we overcame this problem. Measuring the final height of the crushed material accurately was also difficult. This problem was solved by taking the average of the highest and lowest measurements of the unevenly crushed material surface.

Figure 12 illustrates the hand calculation model. The external conditions were the steel plate used as a wall, the adhesive connection between the material and the wall, and the pendulum force exerted on the material. The crushable material was constrained to only moving in one direction; therefore the system had only one degree of freedom. There were no hypothesized hand calculations because deformation of the materials are not known, predictable, or easily calculable.

The egg carton absorbed the least amount of energy and deformed the least, which can be seen in both Table 4 and Figure 13. The egg carton material initial height was too short to have a large

crushing distance. The short can absorbed the same amount of energy as the tall can and deformed more on average, which can be seen in Figure 13 by the triangles on the right of the squares. The testing results were reasonable and repeatable to a certain degree, which can be seen in Figure 14 by the similar crushing heights of the two front tall cans exposed to the same amount of energy. The implications of the results were that the egg carton was not usable for the planetary landing capsule crushable material and the short can was the most suitable material for this application.

Table 4: Modeling results for each loading condition.

Material	Material Start h (ft)	Material End h (ft)	Pendulum Drop h (ft)	Energy (mgh) (J)	Amount Crushed (ft)	Energy Absorbed Per Single Crushed Item (J)
4 egg, carton	0.10833	0.06667	0.60000	5.57756	0.04167	1.39439
4 egg, carton	0.10833	0.08333	0.60000	5.57756	0.02500	1.39439
4 egg, carton	0.10833	0.10000	0.60000	5.57756	0.00833	1.39439
2 egg, carton	0.10833	0.05000	0.60000	5.57756	0.05833	2.78878
2 egg, carton	0.10833	0.06667	0.35000	3.25358	0.04167	1.62679
1 egg, carton	0.10833	0.04167	0.10000	0.92959	0.06667	0.92959
1 egg, carton	0.10833	0.05833	0.10000	0.92959	0.05000	0.92959
1 tall can	0.42500	0.37500	0.35000	3.25358	0.05000	3.25358
1 tall can	0.42500	0.33333	0.35000	3.25358	0.09167	3.25358
1 tall can	0.42500	0.32500	0.60000	5.57756	0.10000	5.57756
1 tall can	0.42500	0.32500	0.60000	5.57756	0.10000	5.57756
1 tall can	0.42500	0.32500	0.60000	5.57756	0.10000	5.57756
1 tall can	0.42500	0.27083	0.85000	7.90155	0.15417	7.90155
1 tall can	0.42500	0.29167	0.85000	7.90155	0.13333	7.90155
1 tall can	0.42500	0.29167	1.10000	10.22553	0.13333	10.22553
1 tall can	0.42500	0.22917	1.10000	10.22553	0.19583	10.22553
1 short can	0.40208	0.28650	0.60000	5.57756	0.11558	5.57756
1 short can	0.40208	0.30208	0.60000	5.57756	0.10000	5.57756
1 short can	0.40208	0.21333	0.85000	7.90155	0.18875	7.90155
1 short can	0.40208	0.23542	0.85000	7.90155	0.16667	7.90155
1 short can	0.40208	0.23000	1.10000	10.22553	0.17208	10.22553
1 short can	0.40208	0.23833	1.10000	10.22553	0.16375	10.22553

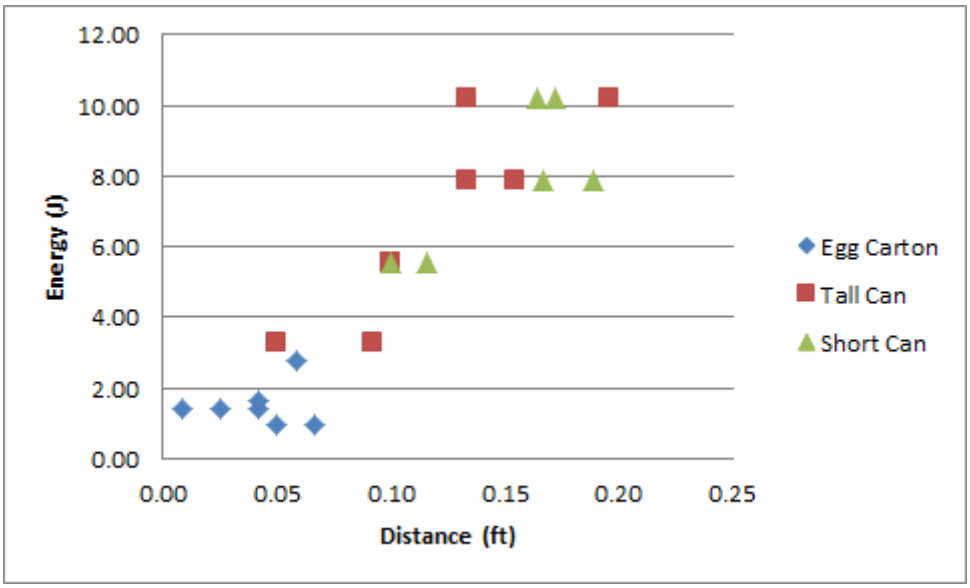

Figure 13. The amount of energy absorbed over the distance the testing material crushed for an egg carton, tall can, and short can.

Figure 14. The tall cans crushed after impact failed due to buckling.

When two cans were crushed versus one, the crush distance was reduced by two. This phenomena is shown in Figure 15. This meant that we could assume that deformation was linear and that adding more cans increased the buckling force linearly, which can be used for scaling up our design.

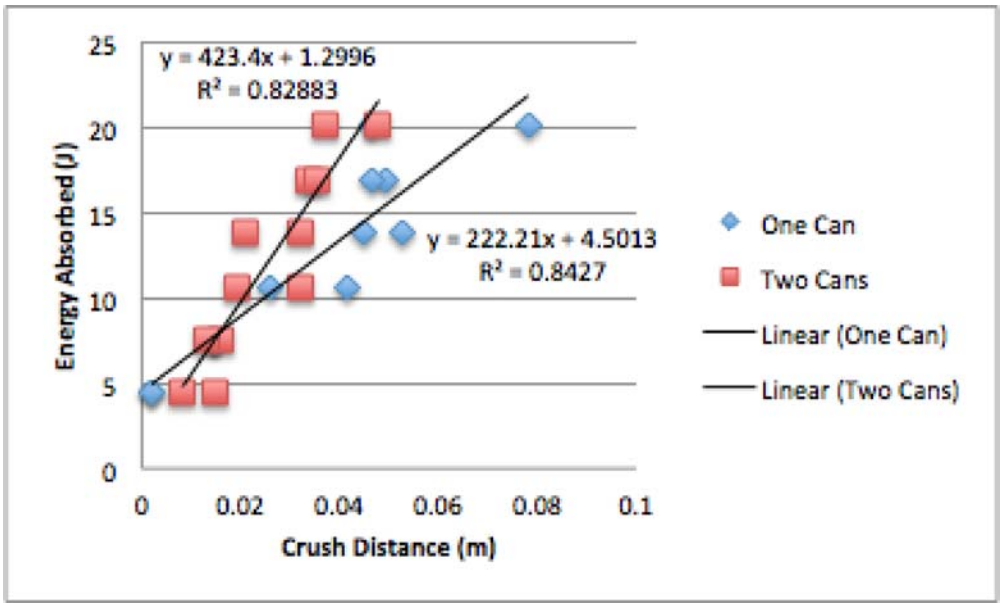

Figure 15. The energy absorbed by one and two cans crushed at a time using the pendulum set up for both crush tests.

The egg carton could not deform enough nor absorb enough energy to be considered for the planetary landing capsule crushable material. The short cans were easier to acquire and absorbed the same amount of energy as the tall cans, which was why they were used as the crushable material on the planetary landing capsule base. A drawing of the configuration of short cans on the base of the planetary lander can be seen in Figure 16. The deformation was linear, which allowed us to use the buckling force for calculations because it was assumed to be a constant. The relationship between crushing distance and energy absorbed was needed in order to decide how many cans were necessary for absorbing the target amount of energy. This was done using a cylindrical shell buckling model.

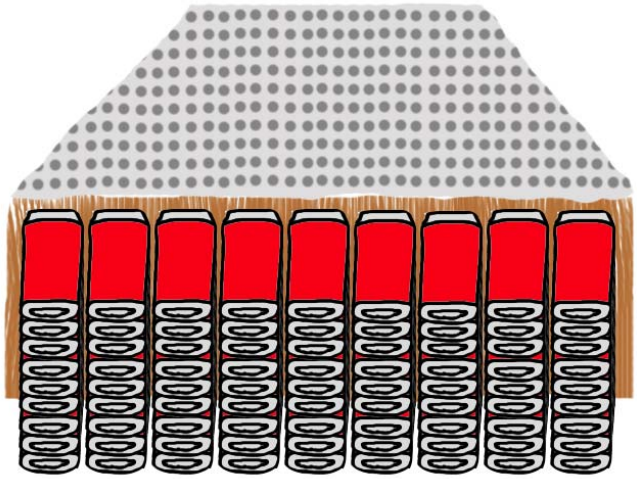

Figure 16. A drawing of an array of crushable short cans affixed to a removable plate attached to the bottom of the planetary lander (Hartman 2015).

3.6 Design Comparison

Our design ideas were based off of three main critical parameters: energy absorption, reliability and accuracy. The goal was to come up with a design that best suited the above parameters. The main ideas we brainstormed were crushable material covering the entire capsule similar to that of the spirit/opportunity and then we focused on designs with crushable material only on the bottom of the capsule. We looked into different capsule geometries such as a pyramid, cylinder and an egg shape, but in the end decided to go with a pyramid shape with crushable material fixed to the bottom of the frame due to nice symmetry and a large base to affix crushable material. The problem with the cylinder or pyramid with crushable material only on the base was that it if it did not land perfectly on its base, there was a high potential to damage the payload due to insufficient energy absorption. To combat this problem, we decided we were going to attached a pilot parachute to the top of the frame to induce drag and help keep the capsule upright through its flight. The issue with the egg shape is that it would be a complicated geometry to manufacture and it had a small base so not as much crushable material could be attached and would present a geometrically complicated platform for payload extraction. For payload extraction using a cylinder design, the capsule would have to fall onto its side and this wasn't an ideal scenario and

was the main reason the cylinder idea was rejected. In order for payload extraction using the pyramid geometry, fabric was attached from the internal frame to the edge of the petal doors, which acted as a platform for the payload to disembark from the landing capsule.

Chapter 4 Modeling Cylindrical Shell Buckling

During material testing, we found that the cans failed due to cylindrical shell buckling. We assumed perfect plastic deformation, which allowed us to assume a constant impact force. Using this impact force we were able to calculate the energy absorption, time of buckling, and expected acceleration. Using Equations (6) through (12) we are able to model the cylindrical shell buckling where D was the wall flexural stiffness per unit width, Z was the curvature parameter for an isentropic cylinder, k_x was the buckling coefficient of a cylinder subjected to axial loading, N_x was the axial loading per circumference, γ was the correction factor, φ was based on radius r and thickness t, l was the height of the can, E was the Young's modulus, and μ was Poisson's ratio [20].

$$D = \frac{Et^3}{12(1-\mu^2)} \tag{6}$$

$$Z = \frac{l^2}{rt}\sqrt{1-\mu^2} \tag{7}$$

$$k_x = \frac{4\sqrt{3}}{\pi^2}\gamma Z \tag{8}$$

$$k_x = \frac{4\sqrt{3}}{\pi^2}\gamma Z \tag{9}$$

$$N_x = k_x \frac{\pi^2 D}{l^2} \tag{10}$$

$$\gamma = 1 - 0.901(1 - e^{-\phi})$$

(11)

$$\phi = \frac{1}{16}\sqrt{\frac{r}{t}} \quad for \left(\frac{r}{t} < 1500\right)$$

(12)

The height of one can was 0.1227 m, the radius was 0.033 m, the thickness was 1.19 mm, the Young's modulus was 6.9E10 N/m^2, and the Poisson's ratio was 0.334. The gradual load force required to buckle one can, N_x, was 1582 N. The impact force required to buckle one can was half of the gradual load, 792 N. This meant that the energy one can can could absorb was 97 J. Assuming that the crushable base was evenly crushed we needed 53 cans on the base of our planetary landing capsule design to absorb 10% of the impact force the Spirit capsule experienced.

Chapter 5 System Integration and Test Results

5.1 Test Safety and Procedure

The completed design is shown in Figure 17. The accelerometer used was a YEI-Technologies 3-Space Bluetooth Sensor. The technical brief can be viewed in Appendix J. The settings used for these tests included a QCOMP filter, sampling rate of 185 Hz, and the corrected acceleration was recorded. Corrected acceleration means that the accelerometer put the data through extra scaling and averaging that smoothed it out.

Figure 17. The final planetary landing capsule proof of concept test article.

A very strict testing procedure was implemented in accordance with similarly strict health and safety considerations. Everyone involved with testing wore high visibility vests, hard hats, and safety glasses. In addition, anyone on the boom lift also wore a safety harness fixed to the railing. The testing procedure was as follows:

- Secure test article with quick release to boom lift

- Check accelerometer functionality
- Lift test article to predetermined height
- Initiate drop with quick release
- Collect data
- Inspect and remove crushable base
- Recycle base sustainably
- Repeat at 3, 6, and 12 m drop heights

Figure 18. A photo from the testing site of the test set up.

The quick release mechanism was a rope that was looped through the capsule and tied to the boom lift. The knots on the boom lift were quick release knots that could be undone by one pull. After the capsule was secured, and the accelerometer was functioning, the capsule was raised to the desired test height and dropped while recording the acceleration. The testing procedure was repeated for three heights including 3 m, 6 m, and 12 m.

5.2 Testing Results and Analysis for the First Round of Testing

The acceleration data recorded during the three drops are presented in Figures (19) through (21).

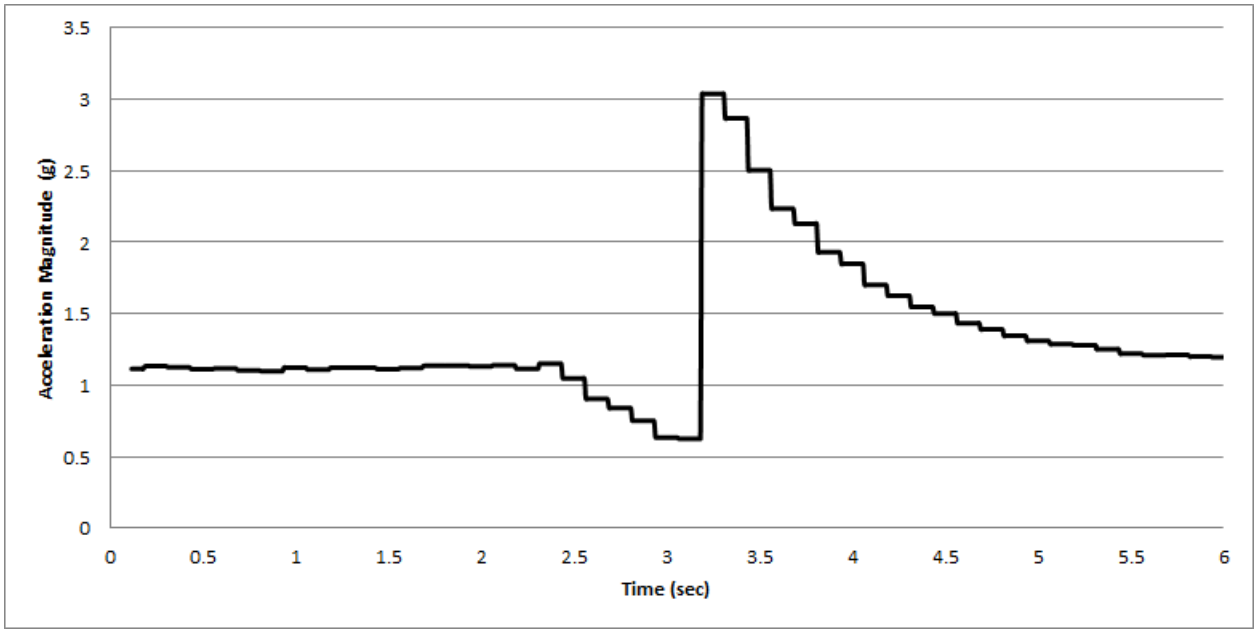

Figure 19. The acceleration magnitude recorded during the 3 meter drop.

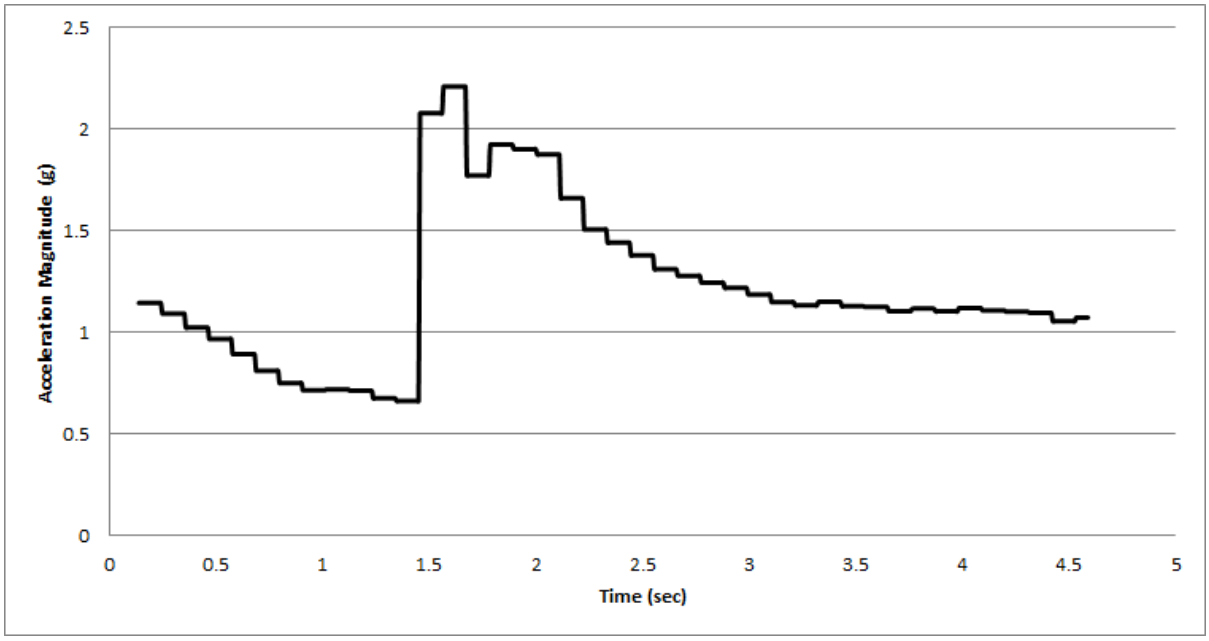

Figure 20. The acceleration magnitude recorded during the 6 meter drop.

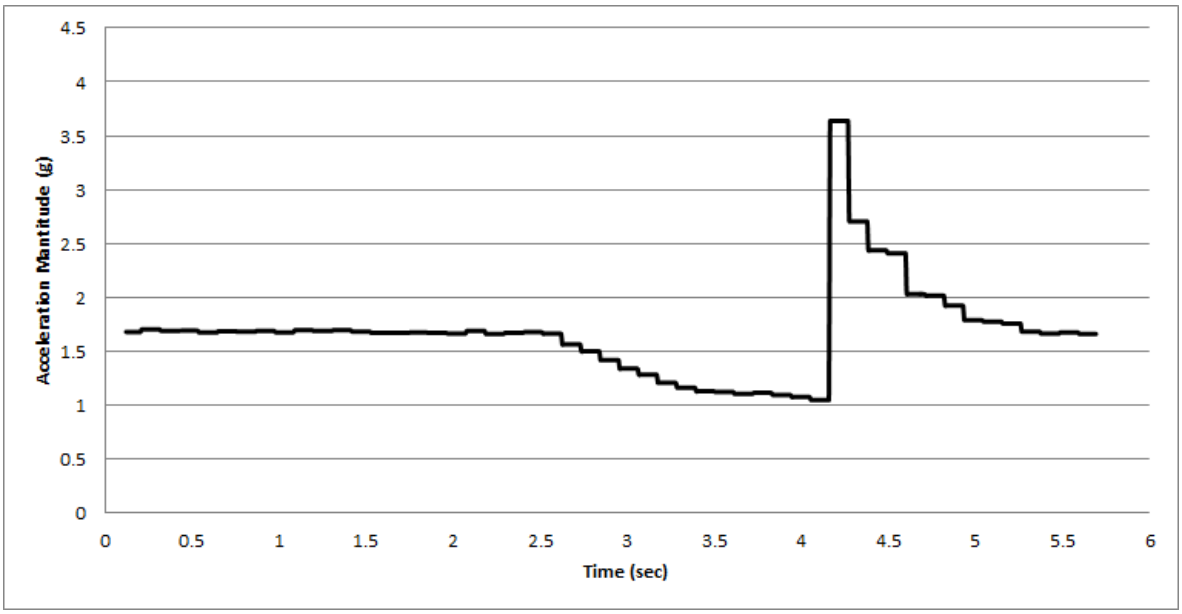

Figure 21. The acceleration magnitude recorded during the 12 meter drop.

Figures 19 through 21 showed that when the capsule was dropped, the acceleration started to decrease steadily. The acceleration began to decrease because once the capsule was dropped it was exposed to an upward force: air resistance. At the bottom of this steady decrease was a sharp jump in acceleration; this was where impact happened. The highest acceleration magnitude recorded was 3.6g.

What we learned from these tests was that the RC car payload functioned after every drop, indicating that the crushing aluminum cans and the suspension dampened the impact enough for the onboard electronics to survive. The capsule was also mostly unharmed throughout all tests. Only one cast aluminum joint broke on the last drop because a gust of wind made the capsule land on its corner, the worst case scenario.

After looking at the raw data recorded, Figures 19 through 21, we were able to see that the actual sampling frequency during these tests was only 145 Hz, which was lower than the maximum sampling rate of 185 Hz. A rough estimate of the peak acceleration expected for the capsule to experience can be found by dividing the estimated impact force by the mass of the capsule,

which is shown in Equations 13 through 15.

$$a_{expected} = \frac{F_{impact}}{M} \tag{13}$$

$$a_{expected} = \frac{15{,}972.9}{37.6} \tag{14}$$

$$a_{expected} = 424.81 \frac{m}{s} \text{ --> } 43.35\ G \tag{15}$$

The maximum measured acceleration was only 3.6g, over one whole order of magnitude smaller than the expected peak acceleration. Because of this, we suspected that the sampling rate used was insufficient to measure the peak accelerations experienced by the capsule.

A different setting on the accelerometer, in IMU mode, could reach a sampling rate of 600 Hz. In the first tests corrected acceleration was measured, instead of raw acceleration. This meant that the filter used by the accelerometer put the data through extra scaling and averaging that smoothed it out. We hoped that using this higher sampling frequency while recording raw acceleration would allow us to record the actual peak impact accelerations experienced by the capsule. Knowing how fast the capsule decelerated would help support our claims that our impact dampening design was viable if sensitive electronics were on board.

5.3 Testing Results and Analysis for the Second Round of Testing

Since the data recorded in the first round of testing was deemed insufficient, a second round of testing was done. Only two drops were made, both from 12 meters. The goal was to more accurately measure the acceleration during impact using different accelerometer settings that would increase the sampling rate. The acceleration plots can be seen in Figures 22 through 23.

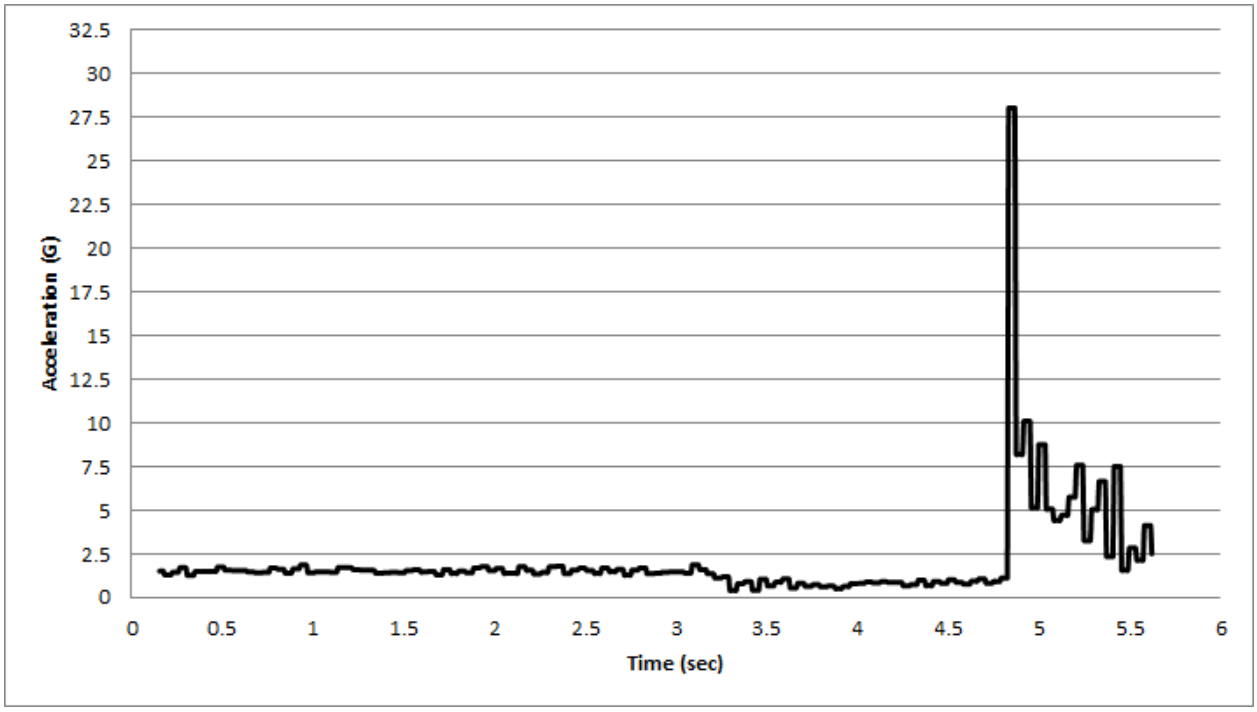

Figure 22. The first drop from the second round of testing. Dropped from 12 meters. The acceleration peaked at 28.04 G.

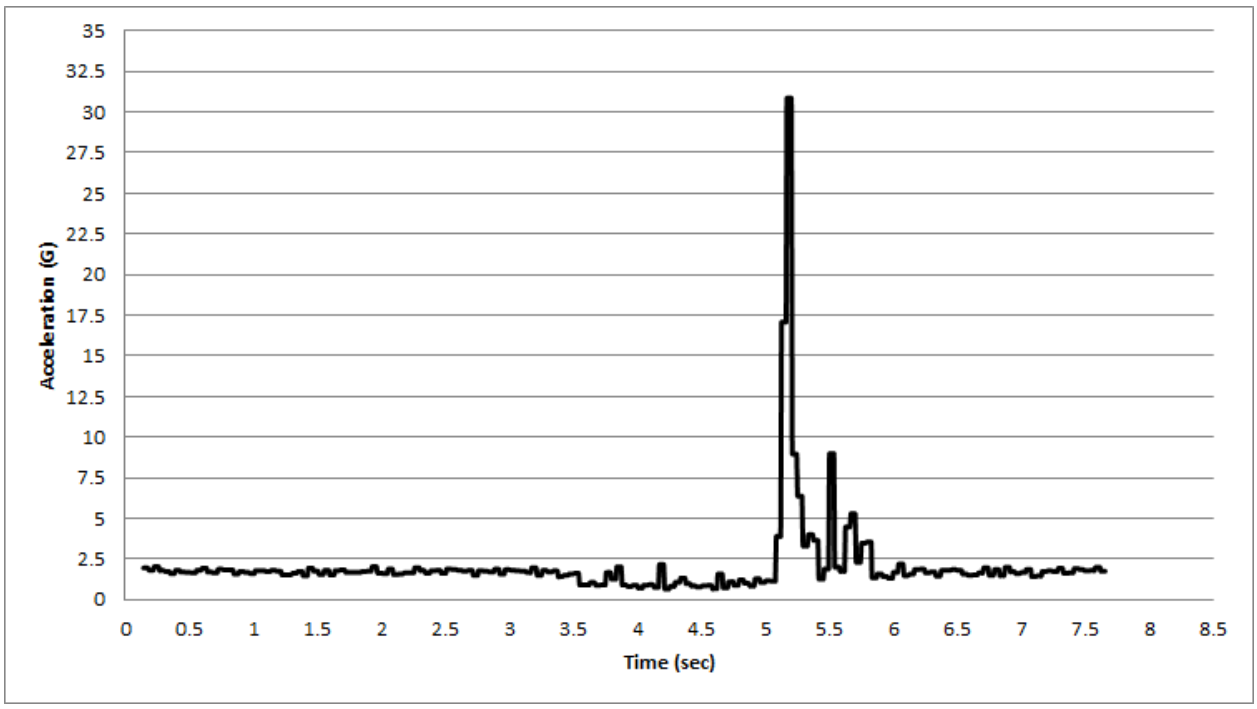

Figure 23. The second drop from the second round of testing. Dropped from 12 meters as well. The acceleration peaked at 30.87 G.

The data presented in Figures 22 and 23 was much more indicative of the actual accelerations experienced by the capsule. The peaks were not as square, and the accelerometer seemed to have picked up many more small changes. This indicated that the sampling rate was fast enough to capture the actual accelerations experienced during impact.

A paper by Tom Irvine, a NASA engineer, outlines a method for how to estimate how much mechanical shock electronic components can experience before being damaged [9]. The paper cites previous sources, and summarizes the findings. The mechanical shock limits for electronic components can be found through the peak accelerations expected and the natural frequency of the components themselves.

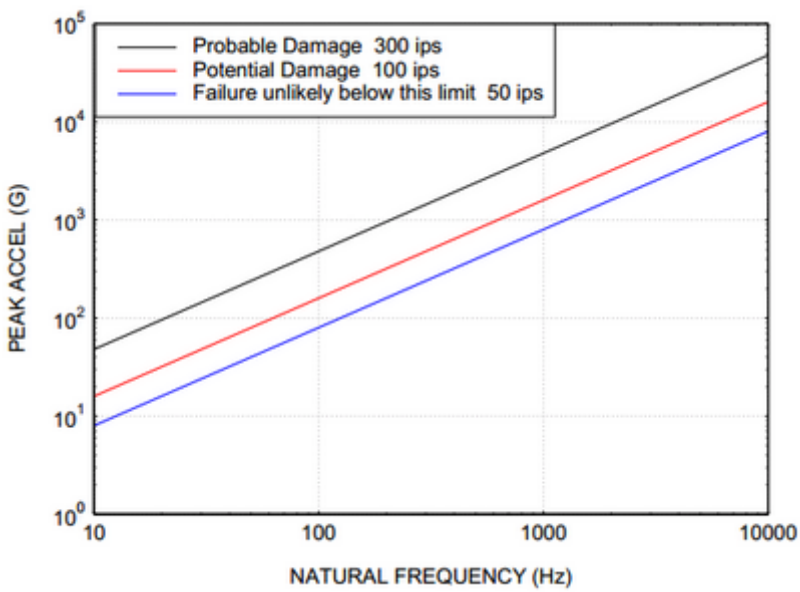

Figure 24. Shock response spectra and damage thresholds from electronics based on their natural frequency and peak acceleration [9].

Irvine goes further to show that a typical chip's natural frequency, of end conditions fixed-free-fixed-free, can be found by first finding the plate stiffness of the chip. The plate stiffness is calculated using the material properties of the chip. An example chip made from silicon will be used to compare its damage threshold, according to the shock spectra above, to the actual acceleration measured during our testing.

The material properties of silicon can be seen in Table 5.

Table 5: The material properties of silicon used to calculate a chip's mechanical shock limits [18].

Young's Modulus, E (Pa)	Poisson's Ratio, μ	Density, ρ (kg/m^3)
150*10^9	0.17	2,330

The following chip geometry will be used here as an example, of typical chip size and shape today.

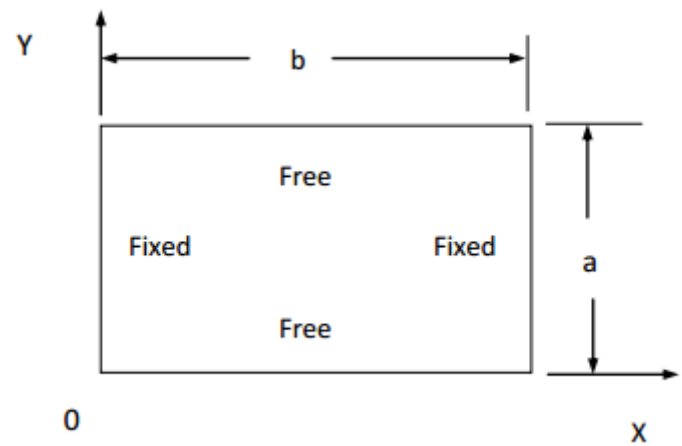

Figure 25. A typical chip's end conditions. For this example b = a = 5 mm, and the thickness will be 0.5 mm [9].

Using the above information the, plate stiffness, and consequently, the natural frequency of the chip can be calculated [9].

$$D = \frac{Et^3}{12(1-\mu^2)} \tag{16}$$

Where D is the plate stiffness of the chip, E is Young's Modulus, t the thickness of the chip, and μ being Poisson's ratio.

$$D = \frac{(150*10^9)(0.0005)^3}{12(1-\ 0.17^2)} \tag{17}$$

$$D = 1.609\ N/m \tag{18}$$

Next, the natural frequency of the chip can be calculated [9].

$$f_n = \frac{3.55}{b^2}\sqrt{\frac{D}{\rho}} \tag{19}$$

Where f_n is the natural frequency, b is the free side length of the chip, and ρ is the chip's density.

$$f_n = 3,731.5\ Hz \tag{20}$$

Using this natural frequency, and Figure 24, we see that the required acceleration for potential damage is about 2,000 G. The highest recorded acceleration was only 30.87 G, suggesting that sensitive electronics would not be damaged on the landing capsule built for this project.

5.4 Comparing Test Results To Goal

In order to compare the impact energy during our testing to our impact energy goal of 5,141.6 J, we calculated the impact velocity during our tests using Equations (21) through (26). Using the free body diagram shown in Figure 26, the velocity and distance from impact as a function of time could be found. Detailed calculations can be seen in Appendix A.

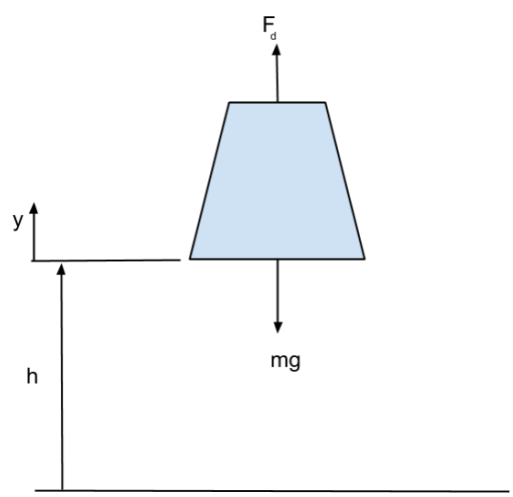

Figure 26. Free body diagram of the capsule as it experiences free fall.

$$v(0) = 0\frac{m}{s} \tag{21}$$

$$y(0) = h \tag{22}$$

$$F_d - mg = ma \tag{23}$$

$$cv^2 - mg = m\frac{dv}{dt} \tag{24}$$

$$\rightarrow v(t) = \sqrt{\frac{mg}{c}}tanh[-gt\sqrt{\frac{c}{mg}}] \tag{25}$$

$$\rightarrow y(t) = \frac{m}{c}ln[cosh(-gt\sqrt{\frac{c}{mg}})] + h \tag{26}$$

Using the initial conditions above, the differential equation resulting from applying Newton's second law to the free body diagram could be solved yielding an equation for velocity and distance from the ground as a function of time. Table 6 shows the results from our second round of testing compared to our goals. The impact velocity was found by using Equation (25).

Table 6: Impact energy from testing compared to the impact energy goal of 10% of Spirit's impact energy.

	Imact Velocty	Mass	Impact Energy	% of Spirit Impact Energy
Expected	15.47 m/s	43 kg	5,141.6 J	10%
Actual	14.24 m/s	37.6 kg	3,812.2 J	7.40%

Solving equations (25) and (26), the actual impact velocity was 14.24 m/s, and the final capsule weight was 37.6 kg. Finding the impact energy using these values gave us an impact energy of 3,812.2 J which is 7.4% of Spirit's impact energy. This is close to our goal of 10% of Spirit's impact energy.

Chapter 6 Cost Analysis

The main expenses of our design were the outer pyramid shell, accelerometer, testing equipment, frame, and crushable materials. Polycarbonate was used for the pyramid shell because the shell needed to be light and strong. The accelerometer was an expensive part in our budget because accelerometers that fulfill our testing requirement sampling rate and maximum acceleration measurement are at least $350. The boom used to drop our test was $400 per day of testing and we had two days of testing. In order to ensure health and safety, the boom was a necessary piece of testing equipment. The frame was made of standardized sch 40 cast aluminum pipe and fittings, known for its structural integrity. We used recycled cans as our crushable material to maintain a sustainable building procedure and save money.

The four components including the shell, accelerometer, testing equipment, and frame took up the majority of our budget, about two-thirds. The rest of the budget was used for replacing broken parts, making a mockup, and manufacturing components required to put the capsule together, such as hinges, latches, and bolts.

Chapter 7 Patent Search

Our design of an array of thin-walled cylinders for crushable impact dampening is a patentable idea. The design improves upon current solutions by decreasing cost and risk while increasing accuracy. The array of thin-walled cylinders for crushable impact dampening absorbs the energy upon initial impact from the proof of concept planetary landing capsule hitting a surface during landing. Upon impact, the cylinders deform due to buckling. This deformation is assumed to be linear. During buckling, the cylinders absorb the energy from impact, which protects the payload and prevents the capsule from rebounding. This idea has not been used before, and is patentable.

7.1 General Purpose

The purpose of the array of thin-walled cylinders for crushable impact dampening is to absorb the energy upon initial impact from the proof of concept planetary landing capsule hitting the planet surface during landing. Impact dampening protects the payload within the capsule, which is a necessity. Upon impact, the cylinders deform linearly due to buckling. During buckling, the cylinders absorb the energy from impact and protect the payload. The cylinders, which are cans, are placed in an array on a piece of cardboard with an adhesive. The cardboard is attached to the bottom of the capsule with the cans facing downwards. The shock absorption on the bottom side of the craft is the key factor in our design, as it will take the force of the impact directly. There will need to be sufficient shock absorption and frequency vibration mitigation to protect the payload.

7.2 Possible Variants

Possible variants for thin-walled cylinders for crushable impact dampening are to use different geometry cylinders or different material. The cans used for our design were an average soda can with diameter of 0.066 m, thickness of 0.00019 m, height of 0.1227 m and aluminum properties. Changing the diameter, wall thickness, height, or using a different material would have different

impact dampening results. A different shape would also provide another variant, such as a hexagonal shape.

7.3 Competing Technologies

Currently, the competing technology is the newest landing capsule design that was implemented for the Curiosity rover. It used multiple reverse thrusters and lowered the Curiosity rover with cables to the Mars surface, which gave it high accuracy.

7.4 Commercialization Possibilities

Commercialization possibilities could potentially be with any space company (i.e. NASA, SpaceX, Virgin Galactic, etc.). The company can scale up the components of the modular design to suit different planet conditions in order for it to fit their needs. Also, using thin-walled cylinders for crushable impact dampening can be applied to areas outside of space. These areas could be delivering care packages or supplies from an aircraft.

7.5 Inventors

Grant Goyette

Aja Hartman

Shane Hereford

Heather Montgomery

7.6 Key Dates

Invented: November 17, 2014

Publicized: May 14, 2015

7.7 Sketches

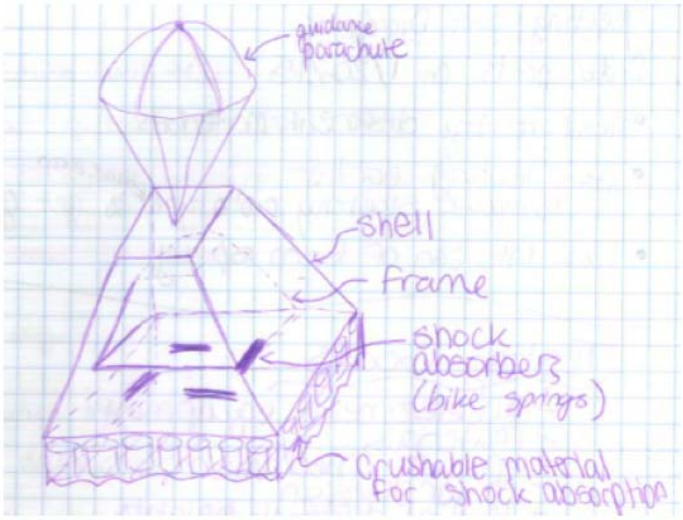

Figure 27. A sketch of the planetary lander utilizing cylindrical tubes as crushable base (Montgomery 2015).

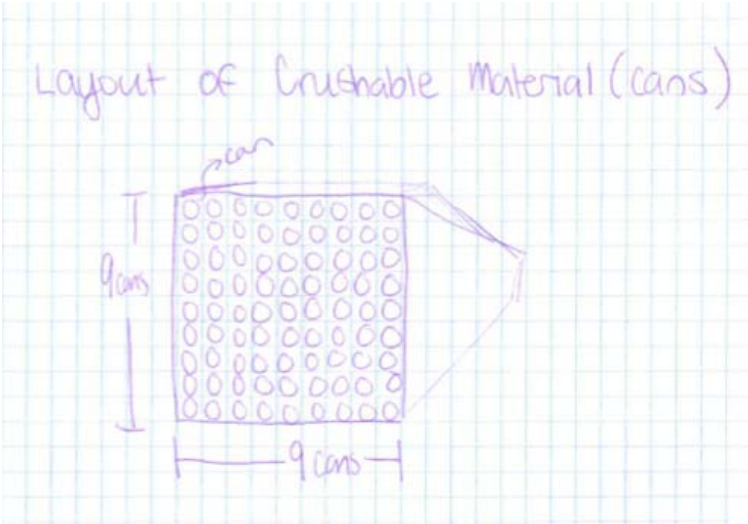

Figure 28. The bottom view of the planetary landing capsule crushable base with placement of crushable cylinders shown (Montgomery 2015).

7.8 Summary of the Patent Classifications

A summary of the patent classifications found to be applicable to this concept are:

“Devices attached to vehicles for the purpose of catching and retaining the same hits from other vehicles or objects.” As well as, “machines or structures adapted to be propelled and guided or stabilized through the air.” Along with, “means for retarding the motion of or stopping machines, including vehicles, both rail and road, and shafts, wheels, pulleys, or other moving mechanisms, by friction, by positive engagement of elements, or by the internal resistance of a fluid or a field of force.”

7.9 Review of “Prior Art”

The patents summarized below can be found in Appendix H.

Impact energy absorbing system utilizing fracturable material

Publication number: US3637051 A

Publication date: Jan 25, 1972

A patent for “impact energy absorbing system utilizing fracturable material” uses a multitude of brittle spheres arranged in a way that absorbs energy upon impact. The brittle materials prevents the payload from rebounding. Our design using cans for impact dampening is similar. The cans are crushable, and absorb energy upon impact. They also prevent the capsule from rebounding. However, the geometry of our cans is a cylinder, not a sphere. Both materials are hollow and lightweight. Another difference between the materials is that the spheres are brittle and do not experience plastic deformation, while the cans are plastic.

Space craft soft landing system

Publication number: US3181821 A

Publication date: May 4, 1965

A patent for “space craft soft landing system” relates to spacecraft energy absorbing systems, like shock impact, that are capable of absorbing large amounts of kinetic energy at a constant rate of deceleration force applied per unit of stroke distance. The energy absorber is embodied in the landing gear of the system. The energy absorber has a conical shape unlike our cylindrical shape.

Energy absorbing air drop pallet

Publication number: US5039036 A

Publication date: Aug 13, 1991

A patent for an “energy absorbing air drop pallet” uses struts to absorb shock and prevent the cargo being dropped from rolling over. The pallet has shock absorbers between its upper and lower surfaces to protect the cargo after being dropped. Our design uses its weight to maintain an upright position, so our impact dampening material is not meant for uprighting. Similar to our cans, the pallet deforms in a controlled way upon impact in order to absorb energy.

Energy absorbing bumper

Publication number: US4078837 A

Publication date: Mar 14, 1978

A patent for an “energy absorbing bumper” is placed on the front of vehicles to collapse upon impact without increasing in its density in order to absorb almost all the energy. The bumper uses a low density foam plastic with a semi-rigid cellular structure. Our design is similar in the way that our crushable material (cans) also collapse upon impact in order to absorb the energy. The material of the cans is aluminum, which differs from foam plastic. The geometry of the cans is also different from the bumper.

Safety seat

Publication number: US20140239684 A1

Publication date: Aug 28, 2014

A patent for a “safety seat” has an energy-absorbing arrangement which connects the base and displaceable member. The energy-absorbing arrangement uses a plastically deformable absorbing element in response to stresses greater than a predetermined threshold stress. The purpose of the safety seat is to ensure that the passenger does not experience more than the maximum acceptable impulse. Our design does the same for our payload. Cans are also perfectly plastic, and deform after the threshold force is achieved. Through this deformation, the energy upon impact is being absorbed which protects the payload.

7.10 Patentability

Our design of an array of thin-walled cylinders for crushable impact dampening is a patentable idea that improves upon current solutions by decreasing cost and risk while increasing accuracy. The array of thin-walled cylinders for crushable impact dampening absorbs the energy upon initial impact from the proof of concept planetary landing capsule hitting a surface during landing. This idea has not been used before, and is patentable.

Chapter 8 Scaling Up Our Design

We scaled up our design so that it could absorb 100% of the Spirit lander impact energy by assuming that the crushable materials were evenly spaced cylinders that failed due to buckling. By making this assumption we could calculate the energy absorbed by multiplying the buckling force by the crush distance. By changing the cylinder geometry or material we could control the threshold force, which is the force required to begin buckling the thin walled cylinder. We designed several solutions for a scaled up design that absorbs the same amount of energy as the Spirit lander while maintaining the same size lander.

The shape of the Spirit landing capsule was a tetrahedron made up of equilateral triangles with side lengths of 3.45 meters [27]. This meant that the bottom area available on the Spirit lander to implement our crushable material design was 5.15 m^2. The calculated thickness of the deflated airbag actuator assembly on the Spirit lander was 0.1377 m [27]. We set the height of the cylinders for our crushable material to be the same as the Spirit lander assembly height to maintain the same size of the landing capsule.

How the geometric parameters of the cylinders affect the buckling force are shown in Figures (29) and (30).

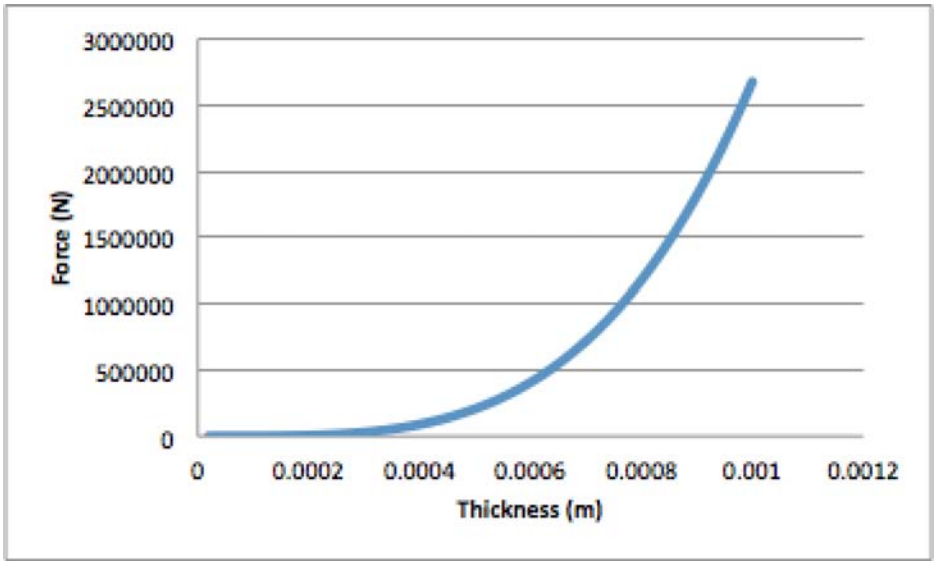

Figure 29. The relationship between the buckling force and thickness of the buckling cylinder.

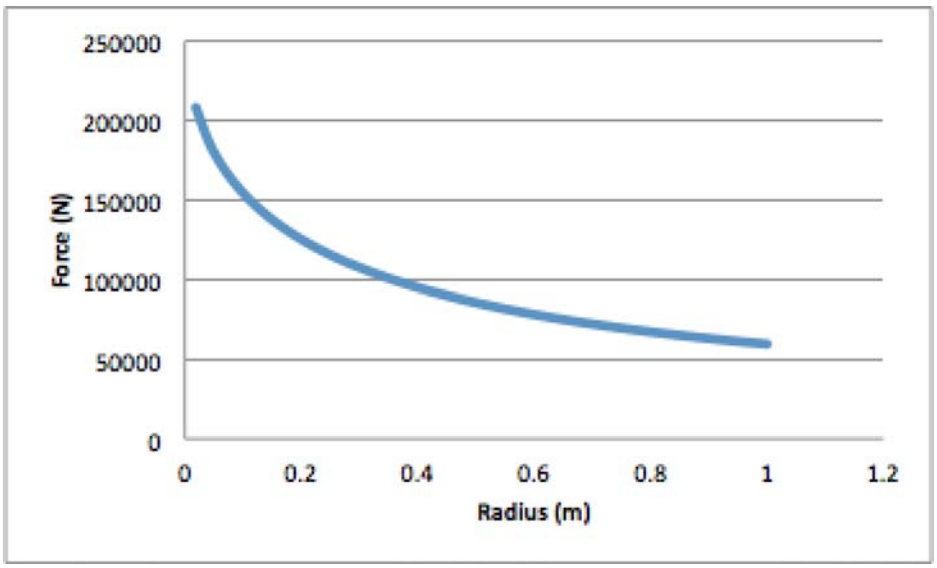

Figure 30. The relationship between the buckling force and the radius of the buckling cylinder.

Aluminum cylinders of different geometries were used for all five of our solutions for a scaled up design, which is shown in Table 7. The solutions used the cylindrical buckling Equations (6) through (12). All of our solutions absorbed slightly more than the impact force the Spirit lander was subjected to. The crushable base for the solutions is made from a grid of cylinders touching in four places. As the radius of the cylinders increased, fewer cylinders were able to fit on the

5.15 m^2 base of the lander. As the radius of the cylinders increased, the thickness of the cylinders also increased in order for the same amount of energy to be absorbed. The solution that was best for implementing on the Spirit sized lander is the 5th iteration because it used the least amount of volume of material and was the easiest to manufacture and therefore the cheapest design.

Table 7: The five iterations of cylinder geometry design solutions for the crushable base to absorb the same amount of energy as the Spirit lander.

Parameters	1nd	2rd	3th	4th	5th
Total Energy Absorbed (J)	51452.0308	51927.29126	51514.82334	51750.67172	51736.62733
Radius (m)	0.008	0.01	0.02	0.04	0.06
Thickness (m)	0.00178	0.0018	0.00184	0.00191	0.00196
# Cylinders	20000	12500	3200	800	350
Volume of Material	0.218994601	0.177148598	0.097198593	0.051618168	0.035029757
Area (m^2)	5.12	5	5.12	5.12	5.04

Chapter 9 Engineering Standards and Realistic Constraints

9.1 Economic Considerations

The ultimate constraints when dealing with space are weight and cost. The current average for sending one pound into Low Earth Orbit is $10,000, and even more so when travelling to other planets [16]. The cost of the most recent NASA endeavour, Curiosity, was $2.5 billion. Since the government funds NASA, this means that the cost of this mission came directly from taxes. Using the people's money to advance human exploration could be seen as a good way to spend the money, but $2.5 billion dollars could easily be spent on matters of our own planet that more directly affect humanity in the short term. There are plenty of things such as education and medical research that government funding could be spent on. For our project, we aimed to stick to basics in terms of design and make it as simple and cost effective as possible. We aimed to have a product that could land safely and accurately without breaking the bank so that government funding could be spent elsewhere to benefit society.

9.2 Environmental Impact

Pollution is an environmentally damaging practice. Our design had reusable parts that could be used for every test run. This will allowed us to test our design multiple times and not produce waste that was harmful to the environment. We used recycled cans as our crushable base. This approach reduced our project's carbon footprint. The goal of our project was to have a positive environmental impact rather than a negative one.

9.3 Sustainability

A sustainable design project can be explained as a project that helps people in the present without harming future generations ability to meet their own needs, as well as using Earth's resources at a slower rate than they are replaced. Our design acknowledged sustainable practices. Our design utilized recycled and reusable parts. This allowed us to reuse parts of our design

multiple times during the testing process so that our test procedure was a sustainable practice. The goal of our project is to help future generations — not harm them.

9.4 Manufacturability

This project was a proof of concept, so manufacturing the testing prototype was only done once. Our design used readily available materials and off-the-shelf parts, so the manufacturing process was mostly assembly. We had access to two machine shops: Santa Clara University machine shop and Silicon Valley Glass machine shop. Between both of these machine shops we had access to all of the machines needed to manufacture our design.

9.5 Health and Safety

Our project was impacted by many health and safety considerations. The testing of our project was risky because it involved the dissipation of 5,141 J of energy. We planned on reaching this energy level by accelerating a heavy object using Earth's gravity. We did not want any people or property harmed during this testing procedure. This affected not only our final design but our testing procedure as well. The importance of health and safety considerations to our project was huge and can be seen in our design matrix and project design specifications provided in Appendix E and C respectively. Safety was the most important factor of our design, which can be seen in our design matrix. Our project design specifications included the absence of sharp edges, shattering parts, pinch points, and exposed gears. We did not want anyone harmed during the production, testing or use of our test article, which was a major consideration in our design. There also was a safety risk with the necessary testing of our project by dropping it 12 m. Only non-shattering materials were used in our design. Protective coverings over all components that could cause bodily harm were affixed. We also designed our crushable material base to be easily affixed and dismounted without touching sharp deformed materials. We filed down any sharp edges to prevent injury during manufacturing and testing.

Chapter 10 Arts

As part of satisfying the Santa Clara University Core Arts and Humanities requirements, members of this team have all contributed original drawings, sketches, or CAD models to this project. Table 8 lists a sampling of at least one such artifact, and a reference to it, for each of the team members.

Table 8: List of team members and one of their drawing locations.

Team Member	Description	Location
Aja Hartman	Drawing of removable crushable base can configuration	Figure 16
Heather Montgomery	Preliminary sketch of cylinders as crushable base	Figure 27
Shane Hereford	Preliminary sketch of suspension	Figure 6
Grant Goyette	CAD model of frame	Figure 2

Chapter 11 Conclusions

11.1 Summary

We successfully designed, built and tested our planetary landing capsule. The remote-controlled vehicle payload we used survived all five of our drop tests. To scale up our design for a Spirit sized mission, the crushable material would need to use 350 cylinders with the dimensions of 0.06 m radius, 0.00196 m thickness, and 0.1377 m hight. An array of cylinders with these dimensions would fit on the bottom of the Spirit landing capsule and would be able to absorb 51,736.6 J, more than the impact energy experienced by Spirit during its arrival to Mars.

11.2 Future Uses

Our design could be used for multiple payload landing applications, including, but not limited to supply deliveries and car packages.

11.3 Lessons Learned

We learned that using crushable materials for impact dampening works when the payload is electronic equipment. This means that the electronic payload was not damaged during impact, the design used was inexpensive, the landing was accurate, and recorded acceleration data suggests that more sensitive electronics would also not be damaged. Our design utilized cylinder shaped aluminum to create an array of crushable objects, but further study could reveal a better shape or geometry. We were also able to scale up our design and suggest a cylinder geometry that would be able to handle the full impact energy experienced by the Spirit lander using equations for thin-walled cylinder buckling.

Appendix

Bibliography

[1] Chang, Kurng Y.1. "Mars Exploration Rover (MER) Airbag Retraction Actuator (ARA) Pyroshock Test Results." Journal Of The IEST 48.1 (2005): 114-126. Applied Science & Technology Source. Web. 9 Oct. 2014.

[2] Dawson, Donna. "COMPOSITES CARRY THE CURIOSITY ROVER TO A SAFE MARS LANDING. (Cover Story)." High Performance Composites 22.3 (2014): 78-80. Academic Search Complete. Web. 9 Oct. 2014.

[3] Do, Sydney, and Olivier de Weck. "A Personal Airbag System For The Orion Crew Exploration Vehicle." Acta Astronautica 81.1 (2012): 239-255. Academic Search Complete. Web. 9 Oct. 2014.

[4] Dunbar, Brian. "Mars Pathfinder Air Bag Landing Tests." NASA. NASA, 21 Mar. 2013. Web. 13 Oct. 2014.

[5] Fasanella, Edwin L. "Multiterrain Earth Landing Systems Applicable For Manned Space Capsules." Journal Of Aerospace Engineering 22.3 (2009): 201-213. Academic Search Complete. Web. 9 Oct. 2014.

[6] Harris, D. K., D. C. Wilson, and J. Rade. "Thermal Design And Analysis Of The Mars Exploration Rover Surface Impact Airbags." Journal Of Spacecraft & Rockets 44.2 (2007): 445-452. Applied Science & Technology Source. Web. 9 Oct. 2014.

[7] Haug, E., et al. "Industrial Design And Analysis Of Structural Membranes." International Journal Of Space Structures 24.4 (2009): 191-204. Academic Search Complete. Web. 9 Oct. 2014.

[8] Inman, D. J. *Engineering Vibration*. Upper Saddle River, NJ: Pearson, 2014. Print.

[9] Irvine, Tom. "Shock Severity Limits for Electronic Components." *Vibrationdata*. N.p., 16 June 2014. Web. 28 May 2015.

[10] Johnson, Andrew, Reg Willson, and Yang Cheng. "Design Through Operation Of An Image-Based Velocity Estimation System For Mars Landing." International Journal Of

Computer Vision 74.2 (2007): 319-341. Applied Science & Technology Source. Web. 9 Oct. 2014.

[11] Karwon, Jeff: Omega, 1 (888) 826-6342 extension 2282, jkarwon@omega.com

[12] Kitts, Christopher: NASA Ames, (408) 554-4382, ckitts@scu.edu

[13] Kornfeld, Richard P., et al. "Verification And Validation Of The Mars Science Laboratory/Curiosity Rover Entry, Descent, And Landing System." Journal Of Spacecraft & Rockets 51.4 (2014): 1251-1269. Academic Search Complete. Web. 9 Oct. 2014

[14] Lewis, Wendy. "New Thermal Vacuum Chamber Will Increase Production Capacity, Efficiency At SSL." New Thermal Vacuum Chamber Will Increase Production Capacity, Efficiency At SSL. Space Systems Loral, 7 Aug. 2013. Web. 13 Oct. 2014. <http://sslmda.com/html/pressreleases/pr20130807.html>.

[15] Lockheed Martin. "Space Based Infrared System Geosynchronous (GEO-1) Thermal Vacuum Testing." Space Based Infrared System (n.d.): n. pag. Lockheedmartin.com. Lockheed Martin. Web. 13 Oct. 2014.

[16] Lord, Morgan. "How To Land On Mars." Popular Mechanics 186.7 (2009): 15. Academic Search Complete. Web. 9 Oct. 2014.

[17] Maier, Sharon. "Space Power Facility (SPF)." Space Power Facility (SPF). NASA, 13 Dec. 2013. Web. 14 Oct. 2014. <http://facilities.grc.nasa.gov/spf/>.

[18] McEntee, Jarlath. "Properties of Silicon." *Properties of Silicon*. N.p., n.d. Web. 28 May 2015.

[19] NASA. "Step-by-Step Guide to Entry, Descent, and Landing" *Mars Exploration Rover Mission: The Mission*. NASA, n.d. Web. 12 May 2015.s

[20] NASA. "Buckling of Thin-Walled Circular Cylinders." (n.d.): n. pag. NASA, 1968. Web. 10 May 2015.

[21] NASA. "NASA Facts: Mars Pathfinder." NASA. Jet Propulsion Laboratory, n.d. Web.

[22] Shepard, John: Moog Inc., jtshepard@gmail.com

[23] Steltzner, Adam D.1, et al. "Mars Science Laboratory Entry, Descent, And Landing System Development Challenges." Journal Of Spacecraft & Rockets 51.4 (2014): 994-1003. Applied Science & Technology Source. Web. 9 Oct. 2014.

[24] United States. Congress. House. Committee on Science. Subcommittee on Space and Aeronautics. A Review of Vertical Takeoff and Landing Technology in the National Airspace System Hearing before the Subcommittee on Space and Aeronautics, Committee on Science, House of Representatives, One Hundred Seventh Congress, First Session, May 9, 2001. Washington: U.S. G.P.O., 2001. Print.

[25] Weisbin, Charles R. Rover and Telerobotics Technology Program: Accomplishments and Technology Transfer. Pasadena, CA: Jet Propulsion Laboratory, 1997. Print

[26] Wen, Jinpeng, Bin Li, and Zhichun Yang. "Study On Cushioning Characteristics Of Soft Landing Airbag With Elastic Fabric." International Journal Of Applied Electromagnetics & Mechanics 33.3/4 (2010): 1535-1545. Academic Search Complete. Web. 9 Oct. 2014.

[27] Williams, Dave R., Dr. "Mars Fact Sheet." Mars Fact Sheet. NASA, 25 Apr. 2013. Web. 13 Oct. 2014. <http://nssdc.gsfc.nasa.gov/planetary/factsheet/marsfact.html>.

[28] Williams, Dave R., Dr. "Mars Pathfinder Atmospheric Entry Strategy." Mars Pathfinder Entry Strategy. NASA, 30 Dec. 2004. Web. 14 Oct. 2014. <http://nssdc.gsfc.nasa.gov/planetary/marsentry.html>.

[29] Withers, Paul. "Landing Spacecraft on Mars and Other Planets: An Opportunity to Apply Introductory Physics." American Journal of Physics 81.8 (2013): 565. Web.

[30] Zubrin, Robert, and Richard Wagner. The Case for Mars: The Plan to Settle the Red Planet and Why We Must. London: Simon & Schuster, 1996. Print.

[31] Zolfagharifard, Ellie. "Soft Landings." *Engineer (00137758)* 296.7855 (2014): 47-48. *Applied Science & Technology Source*. Web. 4 Nov. 2014.

Appendix A: Detailed Calculations

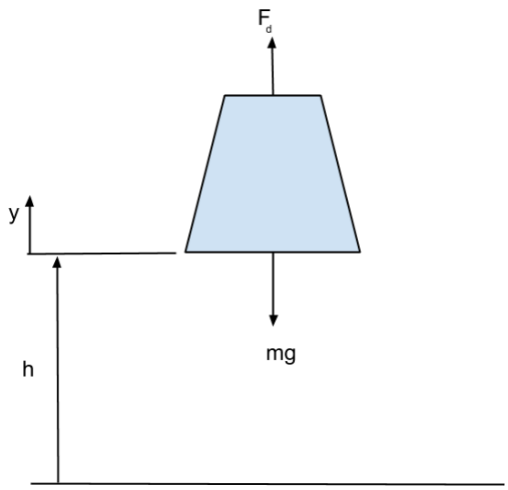

$v(0) = 0\frac{m}{s}$

$y(0) = h$

$F_d - mg = ma$

$cv^2 - mg = m\frac{dv}{dt}$

$\rightarrow v(t) = \sqrt{\frac{mg}{c}}tanh[-gt\sqrt{\frac{c}{mg}}]$

$\rightarrow y(t) = \frac{m}{c}ln[cosh(-gt\sqrt{\frac{c}{mg}})] + h$

$\Sigma F = ma$

$F_d - mg = ma$

$cv^2 - mg = m\frac{dv}{dt}$

$\frac{c}{m}v^2 - g = \frac{dv}{dt}$

$-g(1 - \frac{c}{gm}v^2) = \frac{dv}{dt}$

$\int -gdt = \int \frac{dv}{(1-\frac{c}{gm}v^2)}$

Using u substitution...

$u = \sqrt{\frac{c}{mg}}v$

$du = \sqrt{\frac{c}{mg}}dv$

$-g\int dt = \int \sqrt{\frac{mg}{c}}\frac{du}{1-u^2}$

$-gt + C_1 = \sqrt{\frac{mg}{c}}tanh^{-1}(\frac{v}{\sqrt{\frac{mg}{c}}})$

I.C: $[v(0) = 0]$

$-> v(t) = \sqrt{\frac{mg}{c}}tanh[\sqrt{\frac{c}{mg}}(-gt)]$

$y(t) = \int v(t)dt = \int \sqrt{\frac{mg}{c}}tanh[\sqrt{\frac{c}{mg}}(-gt)]dt$

I.C: $[d(0) = h]$

$-> y(t) = \frac{m}{c}ln[cosh(-gt\sqrt{\frac{c}{mg}})] + h$

Appendix B: Assembly Drawings

Shell Assembly

S01

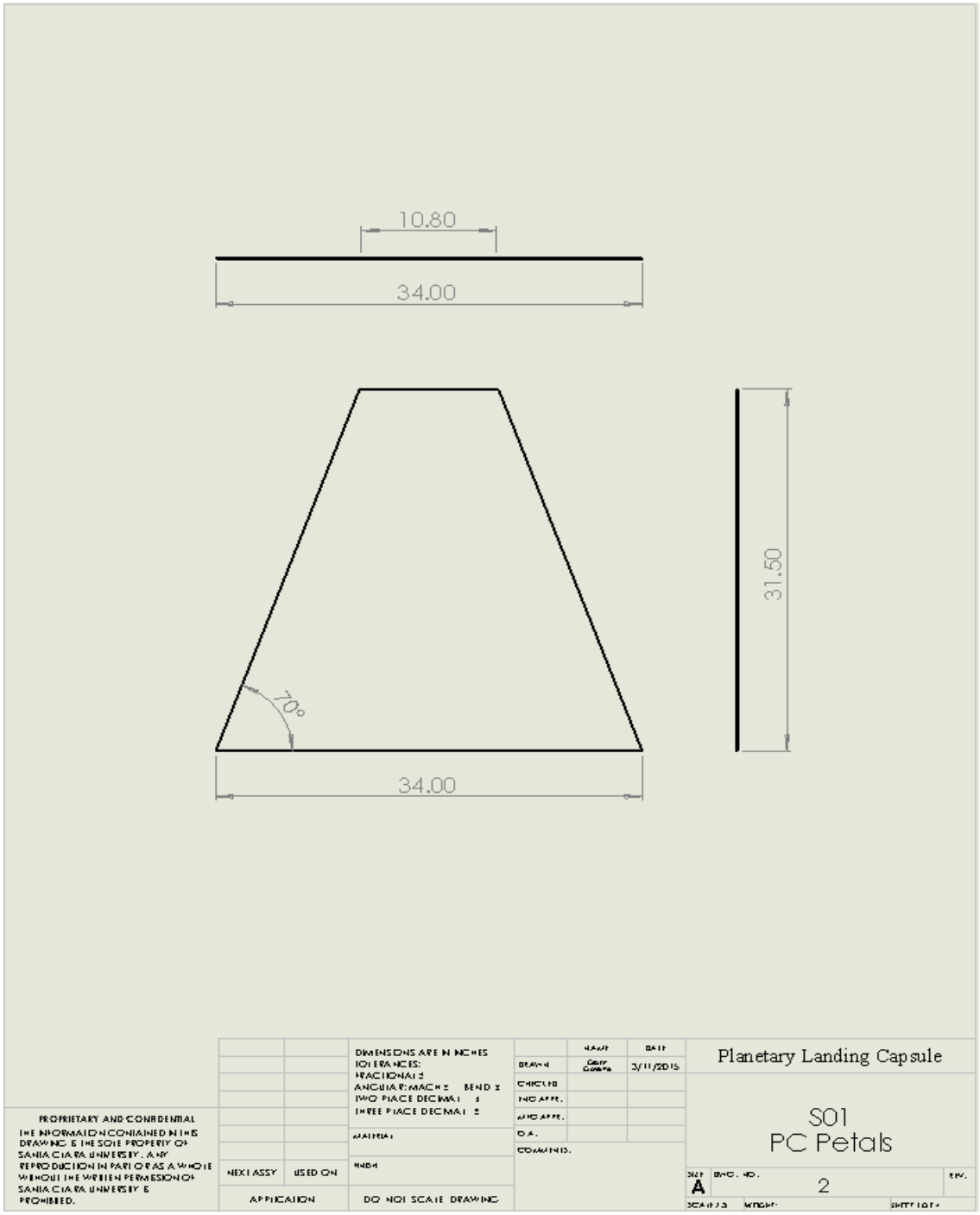

S02

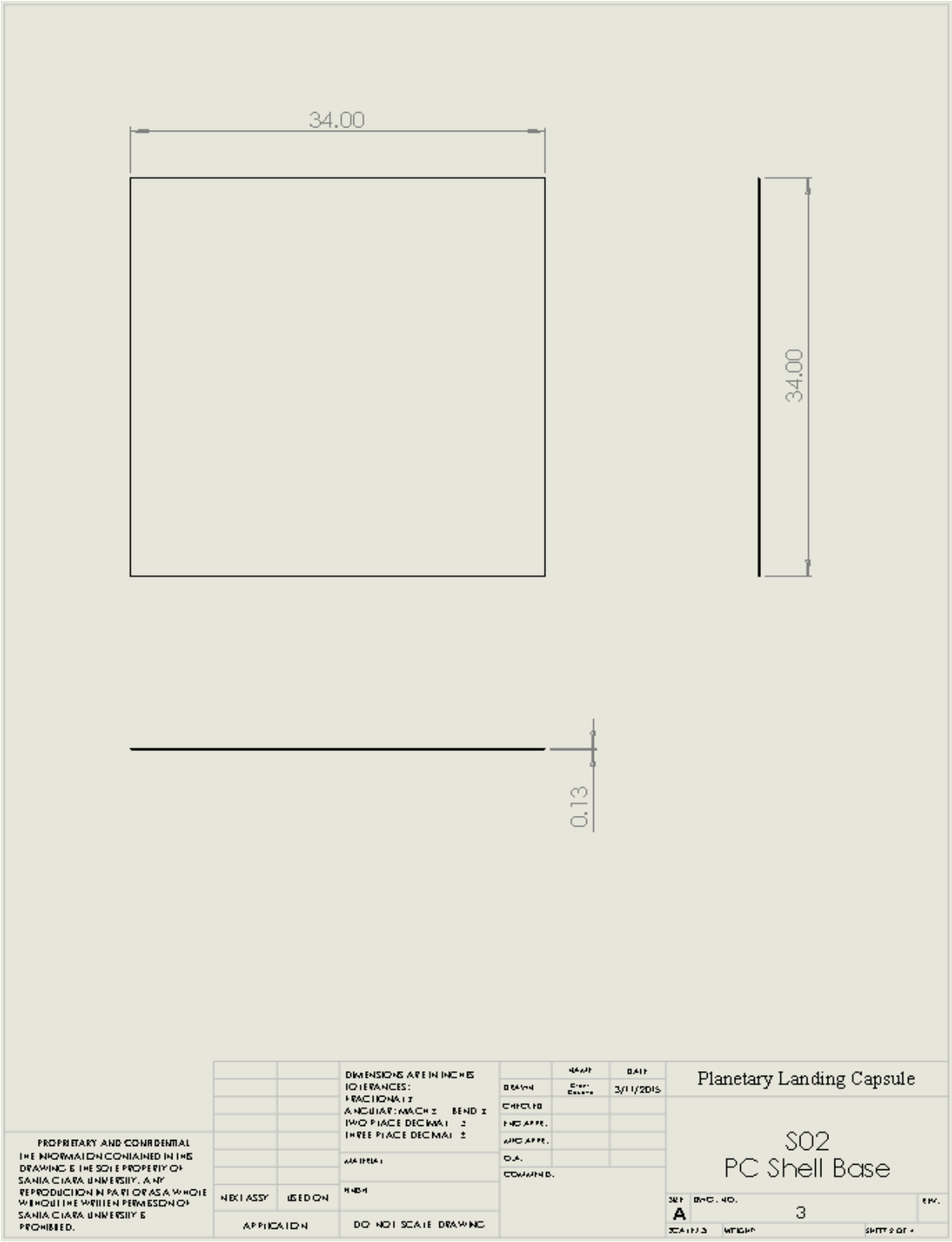
34.00
34.00
0.13
DIMENSIONS ARE IN INCHES
TOLERANCES:
FRACTIONAL ±
ANGULAR: MACH ± BEND ±
TWO PLACE DECIMAL ±
THREE PLACE DECIMAL ±
MATERIAL
FINISH
NEXT ASSY
USED ON
APPLICATION
DO NOT SCALE DRAWING
NAME
DATE
DRAWN
3/11/2015
CHECKED
ENG APPR.
MFG APPR.
Q.A.
COMMENTS:
Planetary Landing Capsule
S02
PC Shell Base
SIZE
A
DWG. NO.
3
REV.
SCALE: 1:3
WEIGHT
SHEET 2 OF 4
PROPRIETARY AND CONFIDENTIAL
THE INFORMATION CONTAINED IN THIS DRAWING IS THE SOLE PROPERTY OF SANTA CLARA UNIVERSITY. ANY REPRODUCTION IN PART OR AS A WHOLE WITHOUT THE WRITTEN PERMISSION OF SANTA CLARA UNIVERSITY IS PROHIBITED.

S03

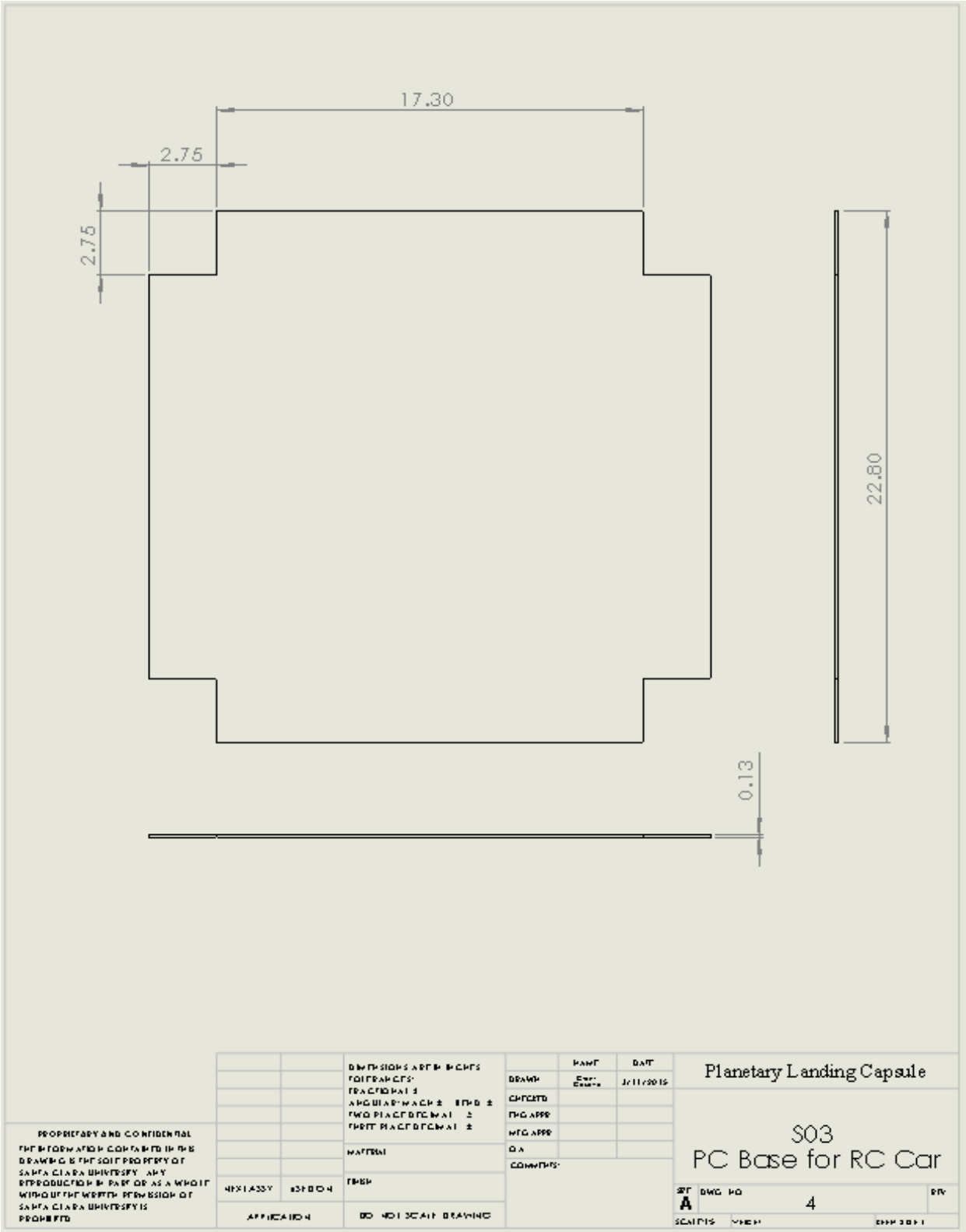
17.30
2.75
2.75
22.80
0.13
Planetary Landing Capsule
S03
PC Base for RC Car
A
4

S04

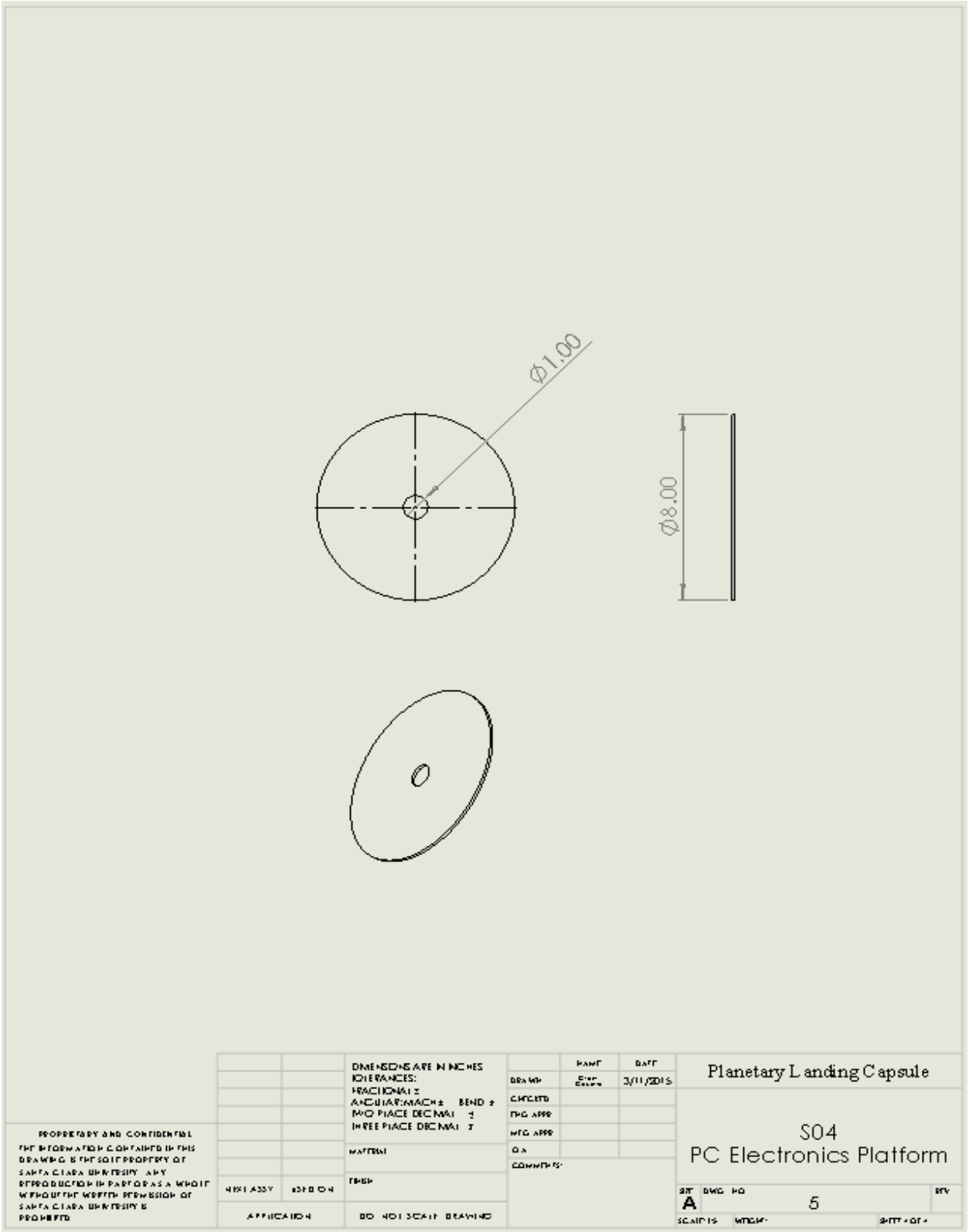
Ø1.00
Ø8.00
DIMENSIONS ARE IN INCHES
TOLERANCES:
FRACTIONAL ±
ANGULAR: MACH ± BEND ±
TWO PLACE DECIMAL ±
THREE PLACE DECIMAL ±
MATERIAL
FINISH
DO NOT SCALE DRAWING
NAME
DATE
DRAWN
3/11/2015
CHECKED
ENG APPR
MFG APPR
Q.A
COMMENTS:
Planetary Landing Capsule
S04
PC Electronics Platform
SIZE
A
DWG NO
5
REV
SCALE: 1:1
WEIGHT:
SHEET 1 OF 1
PROPRIETARY AND CONFIDENTIAL
THE INFORMATION CONTAINED IN THIS DRAWING IS THE SOLE PROPERTY OF SANTA CLARA UNIVERSITY. ANY REPRODUCTION IN PART OR AS A WHOLE WITHOUT THE WRITTEN PERMISSION OF SANTA CLARA UNIVERSITY IS PROHIBITED.
NEXT ASSY
USED ON
APPLICATION

Frame Assembly

F01, F02, F03, F04, F05, F06, F19

Aluminum Pipe for Rail Systems

3/4 Pipe Size

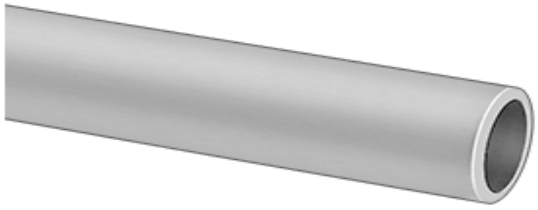

Length, ft.

2	7
3	8
4	9
5	10
6	

Each

ADD TO ORDER

4699T27

Material	Aluminum
Pipe Size	3/4
Actual Diameter	1"
Wall Thickness	0.113"

Make custom railings, guard rails, storage racks, shelving, and framing with ease. Slip rail fittings over the appropriate size pipe and tighten the included set screws for a secure fit.

Pipe is Schedule 40.

Aluminum pipe is lightweight with very good corrosion resistance.

F07

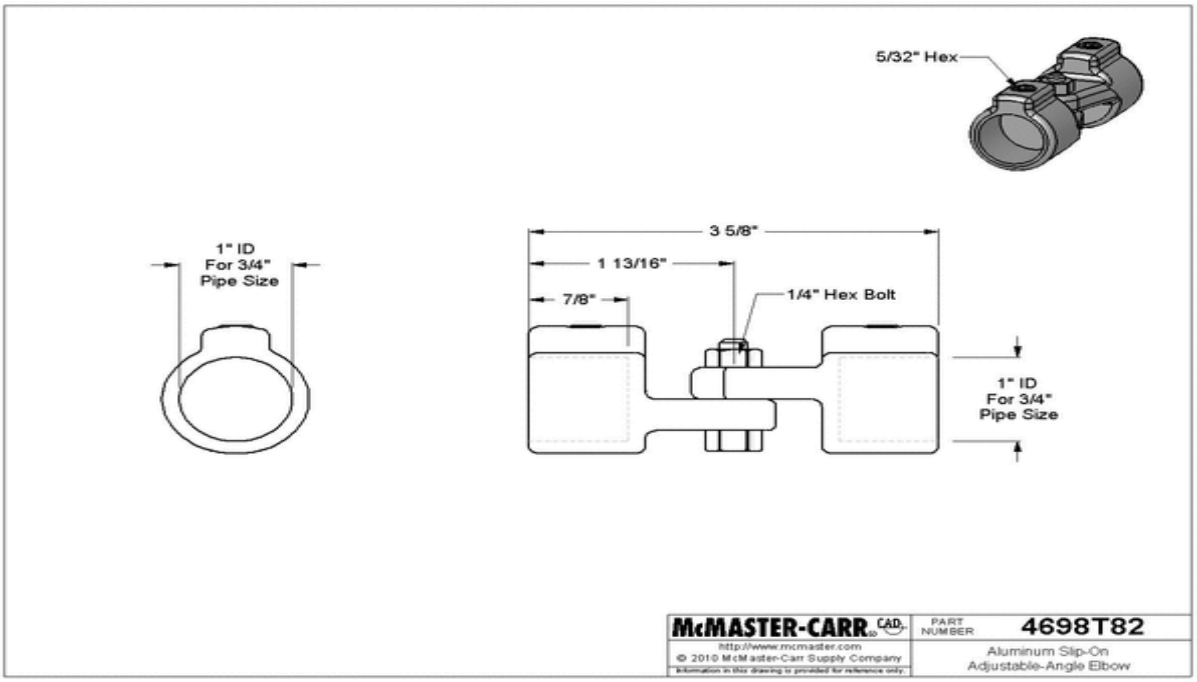

F08

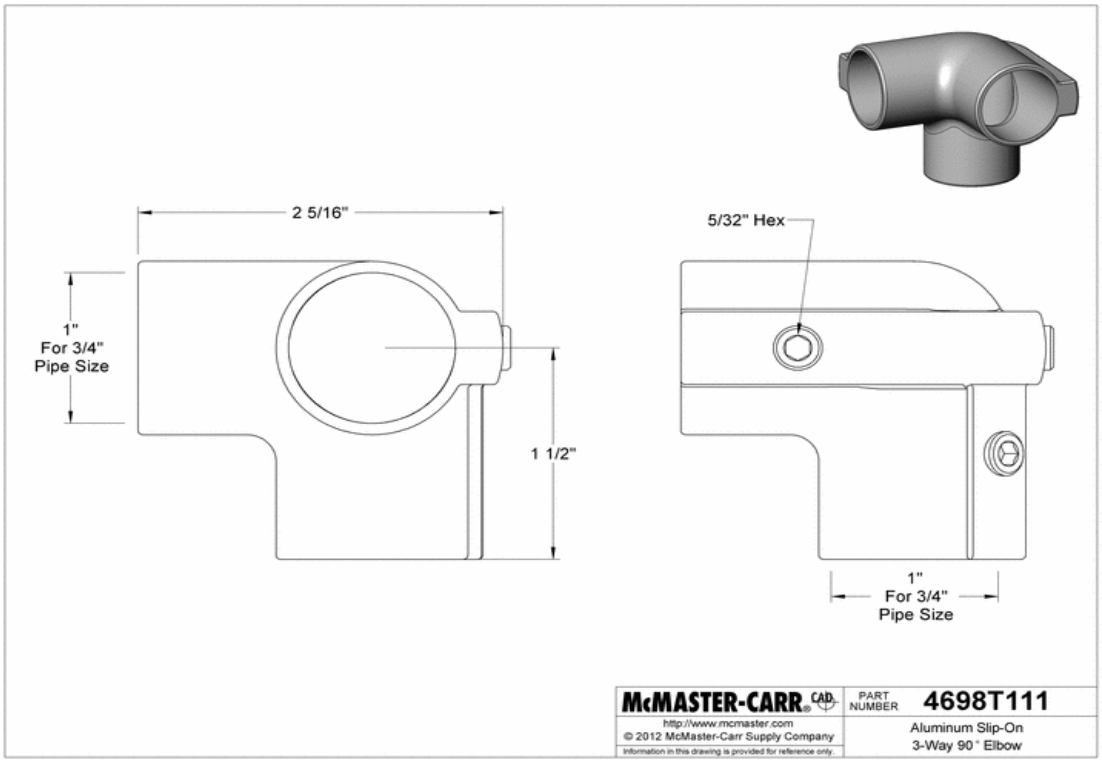
2 5/16"
1"
For 3/4"
Pipe Size
1 1/2"
5/32" Hex
1"
For 3/4"
Pipe Size
McMASTER-CARR
CAD
PART NUMBER
4698T111
http://www.mcmaster.com
© 2012 McMaster-Carr Supply Company
Information in this drawing is provided for reference only.
Aluminum Slip-On
3-Way 90° Elbow

F09

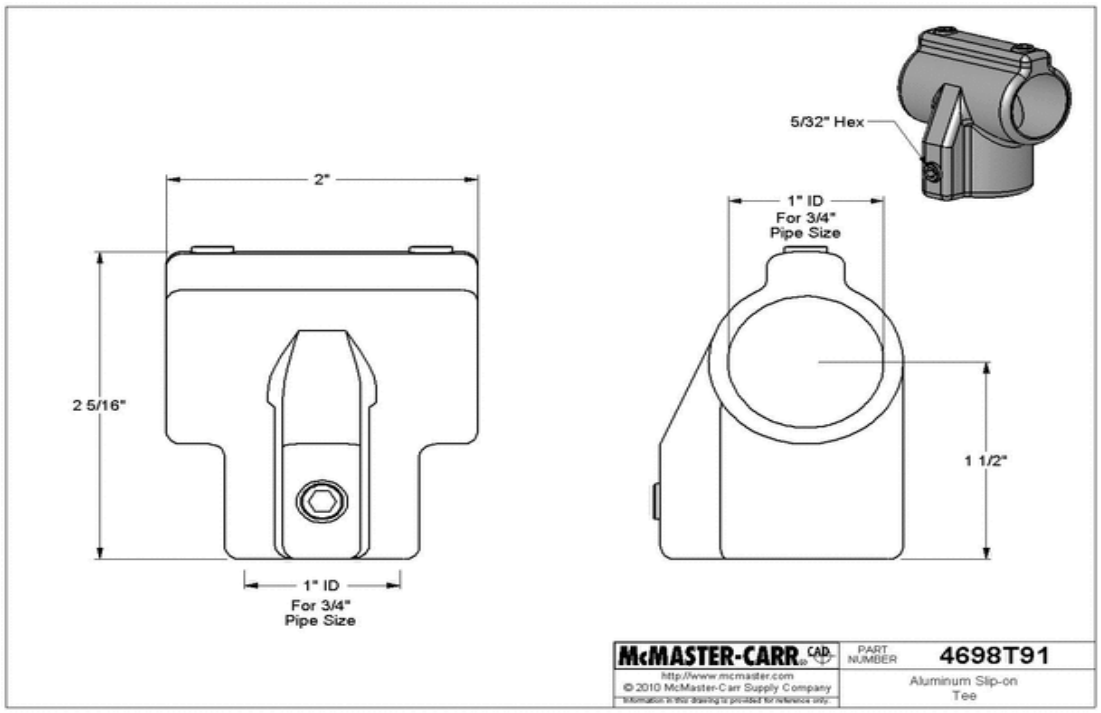
5/32" Hex
2"
2 5/16"
1" ID
For 3/4"
Pipe Size
1" ID
For 3/4"
Pipe Size
1 1/2"
McMASTER-CARR
CAD
PART NUMBER
4698T91
http://www.mcmaster.com
© 2010 McMaster-Carr Supply Company
Aluminum Slip-on
Tee

F10

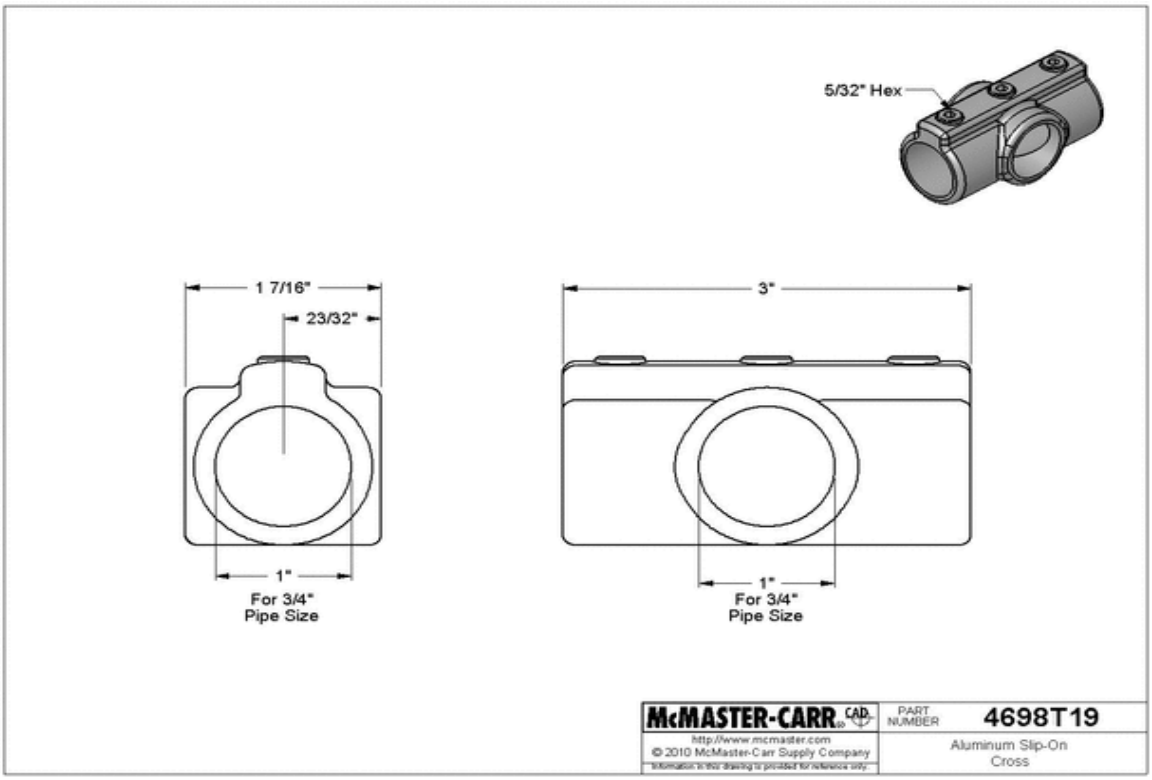
5/32" Hex
1 7/16"
23/32"
1"
For 3/4"
Pipe Size
3"
1"
For 3/4"
Pipe Size
McMASTER-CARR
CAD
PART NUMBER
4698T19
http://www.mcmaster.com
© 2010 McMaster-Carr Supply Company
Information in this drawing is provided for reference only.
Aluminum Slip-On
Cross

F11

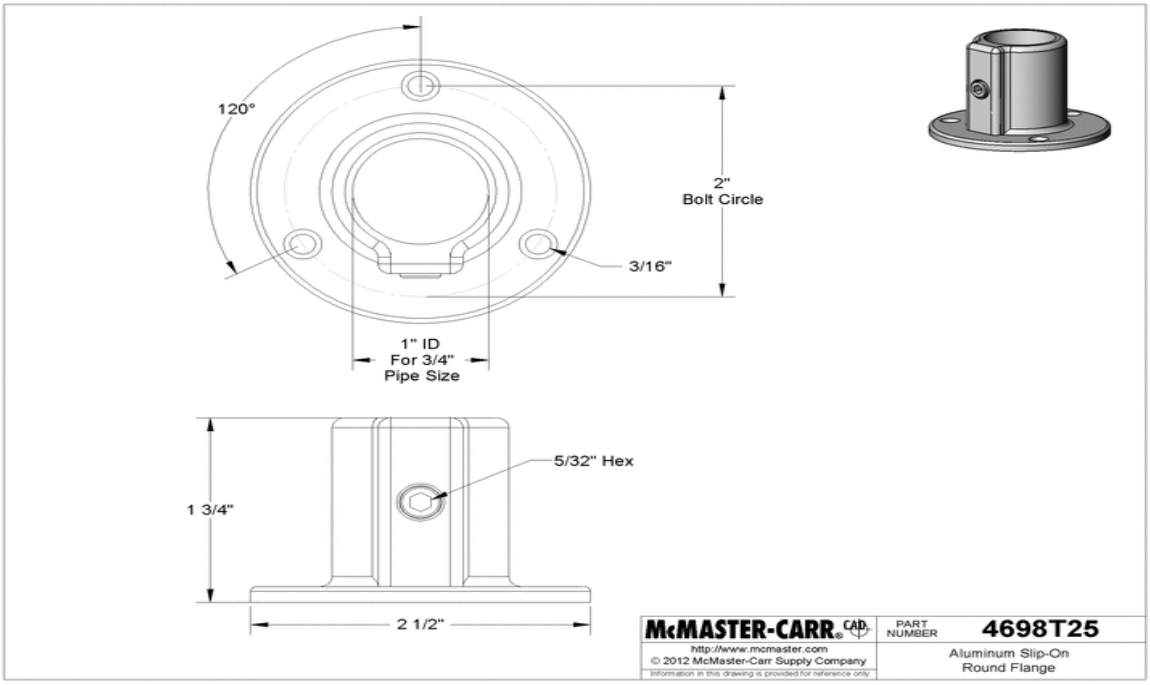
120°
2"
Bolt Circle
3/16"
1" ID
For 3/4"
Pipe Size
5/32" Hex
1 3/4"
2 1/2"
McMASTER-CARR
CAD
PART NUMBER
4698T25
http://www.mcmaster.com
© 2012 McMaster-Carr Supply Company
Information in this drawing is provided for reference only.
Aluminum Slip-On
Round Flange

F12

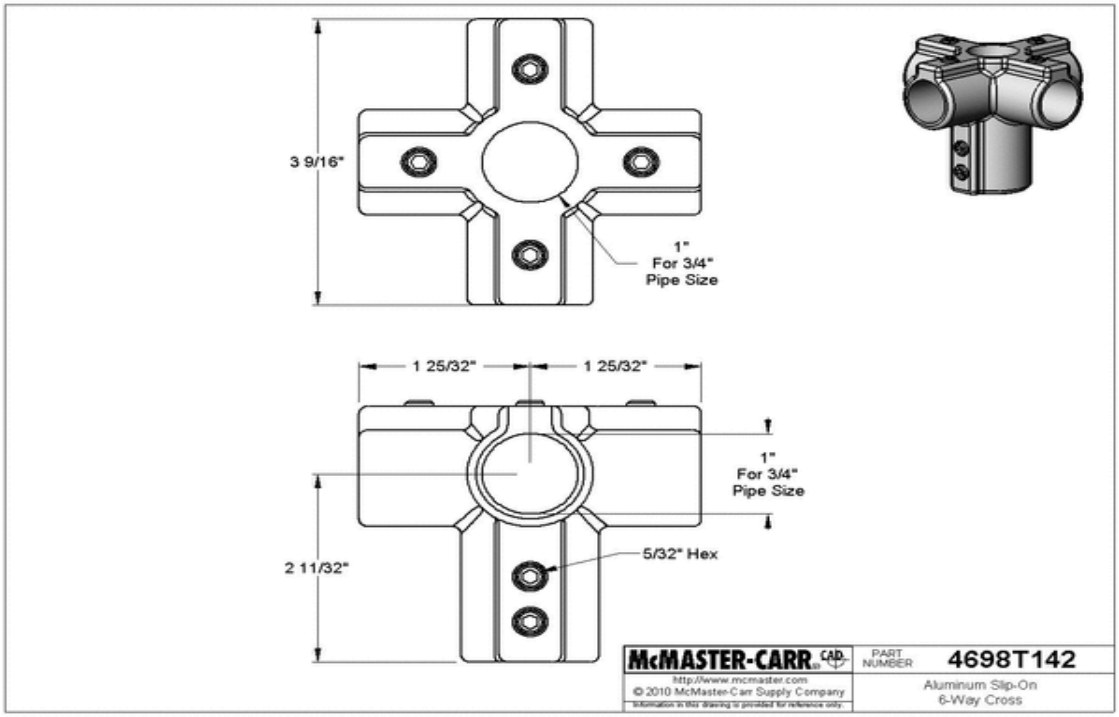
3 9/16"
1"
For 3/4"
Pipe Size
1 25/32"
1 25/32"
1"
For 3/4"
Pipe Size
2 11/32"
5/32" Hex
McMASTER-CARR
PART NUMBER
4698T142
http://www.mcmaster.com
© 2010 McMaster-Carr Supply Company
Aluminum Slip-On
6-Way Cross

F14

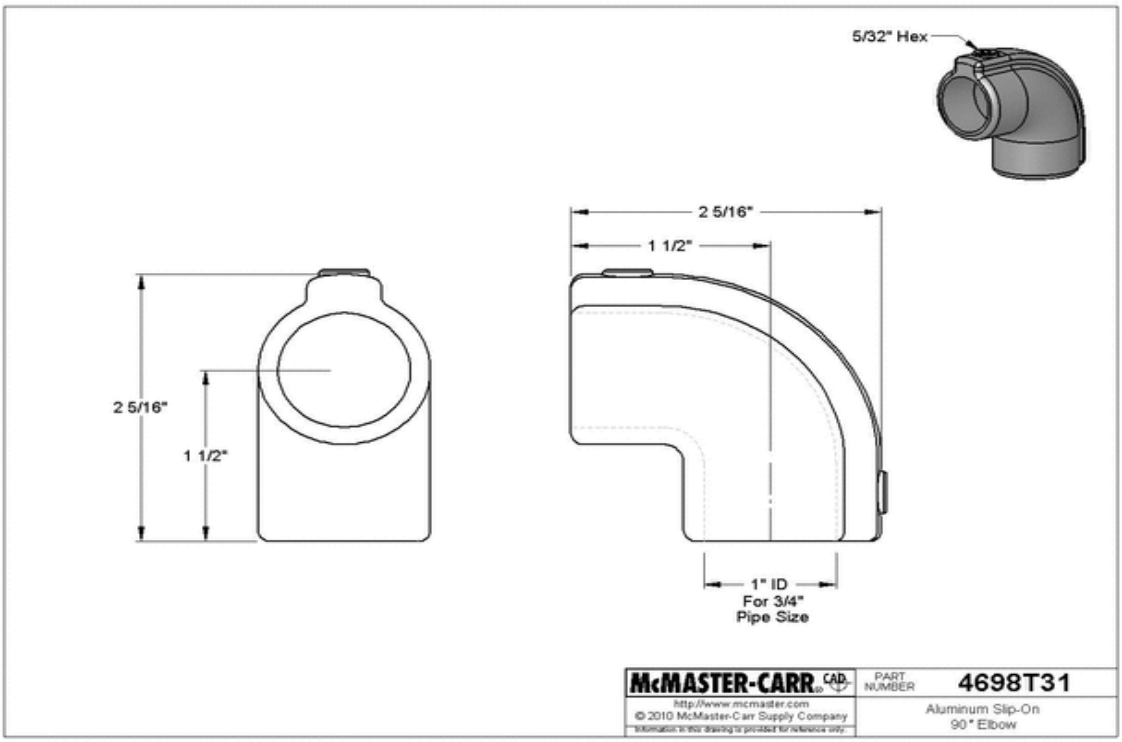
5/32" Hex
2 5/16"
1 1/2"
2 5/16"
1 1/2"
1" ID
For 3/4"
Pipe Size
McMASTER-CARR
PART NUMBER
4698T31
http://www.mcmaster.com
© 2010 McMaster-Carr Supply Company
Aluminum Slip-On
90° Elbow

F15

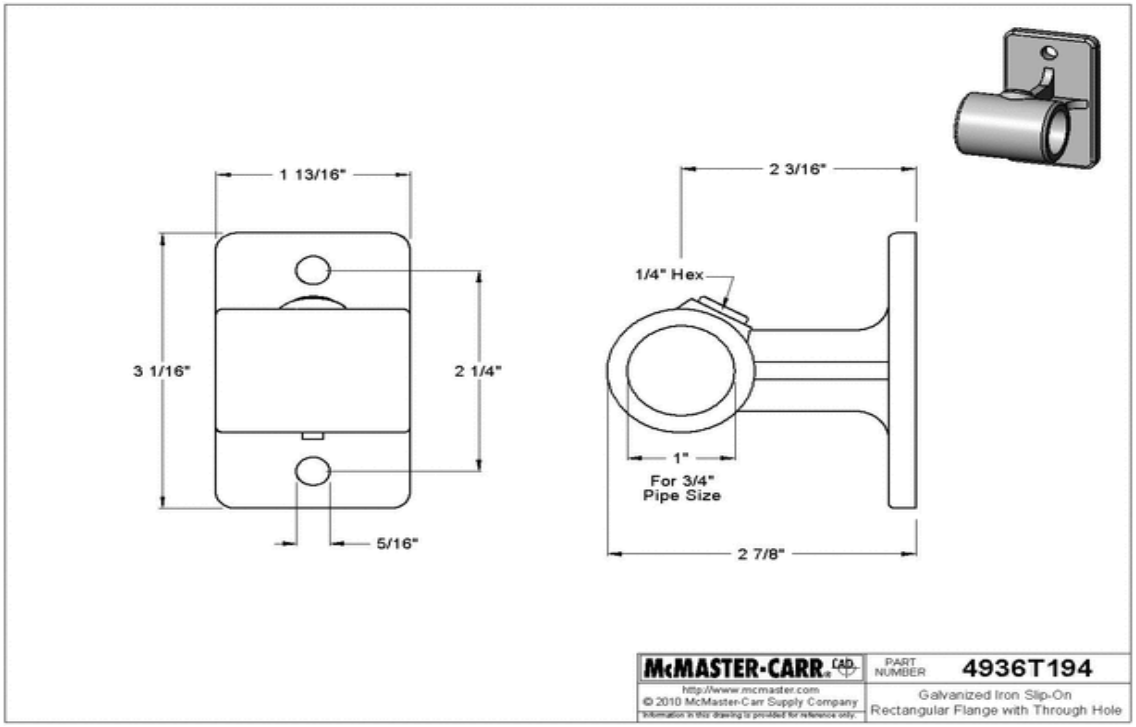
1 13/16"
3 1/16"
2 1/4"
5/16"
2 3/16"
1/4" Hex
1"
For 3/4"
Pipe Size
2 7/8"
McMASTER-CARR
PART NUMBER
4936T194
http://www.mcmaster.com
© 2010 McMaster-Carr Supply Company
Galvanized Iron Slip-On
Rectangular Flange with Through Hole

F16

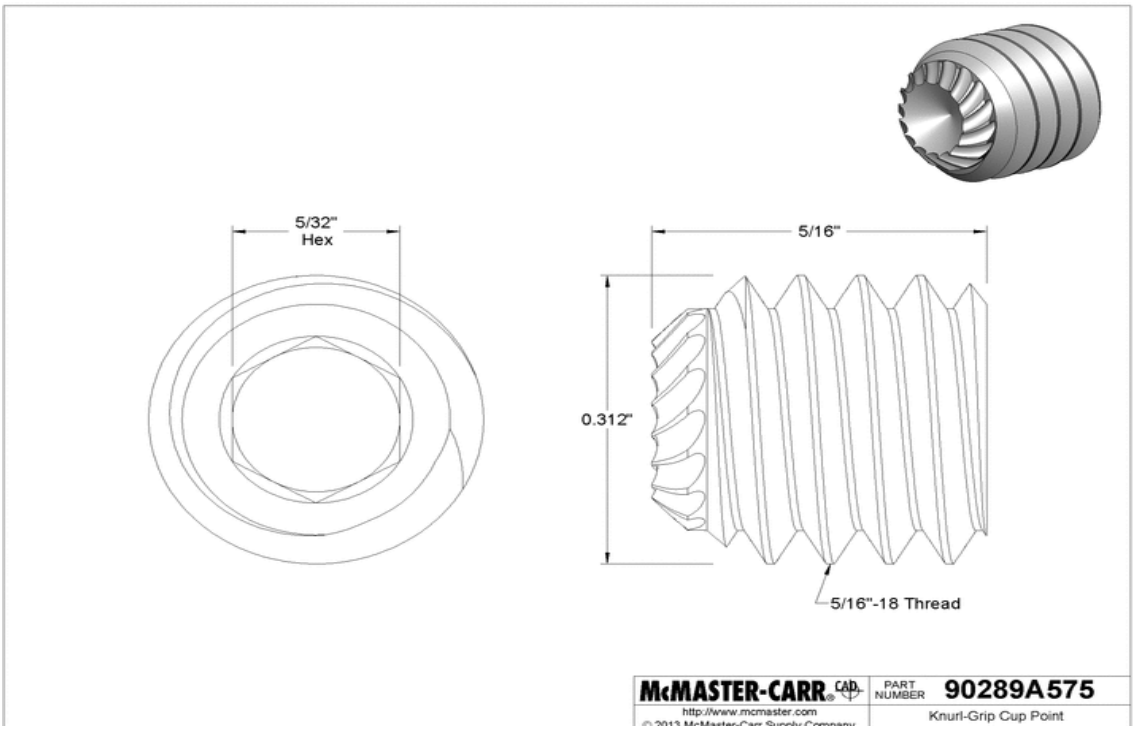
5/32"
Hex
5/16"
0.312"
5/16"-18 Thread
McMASTER-CARR
PART NUMBER
90289A575
http://www.mcmaster.com
Knurl-Grip Cup Point

F18

Set Screw with 1/4" Hex Size for Galvanized Iron Slip-on Rail Fitting

Packs of 10

ADD TO ORDER

In stock
$14.00 per pack of 10
4936T918

Fits Pipe Size	3/4, 1
Fits Actual Diameter	1", 1 1/4"
Hex Size	1/4"

Make custom railings, guard rails, storage racks, shelving, and framing with ease. Slip rail fittings over the appropriate size pipe and tighten the included set screws for a secure fit.

Suspension Assembly

SH00, SH01, SH02, SH03

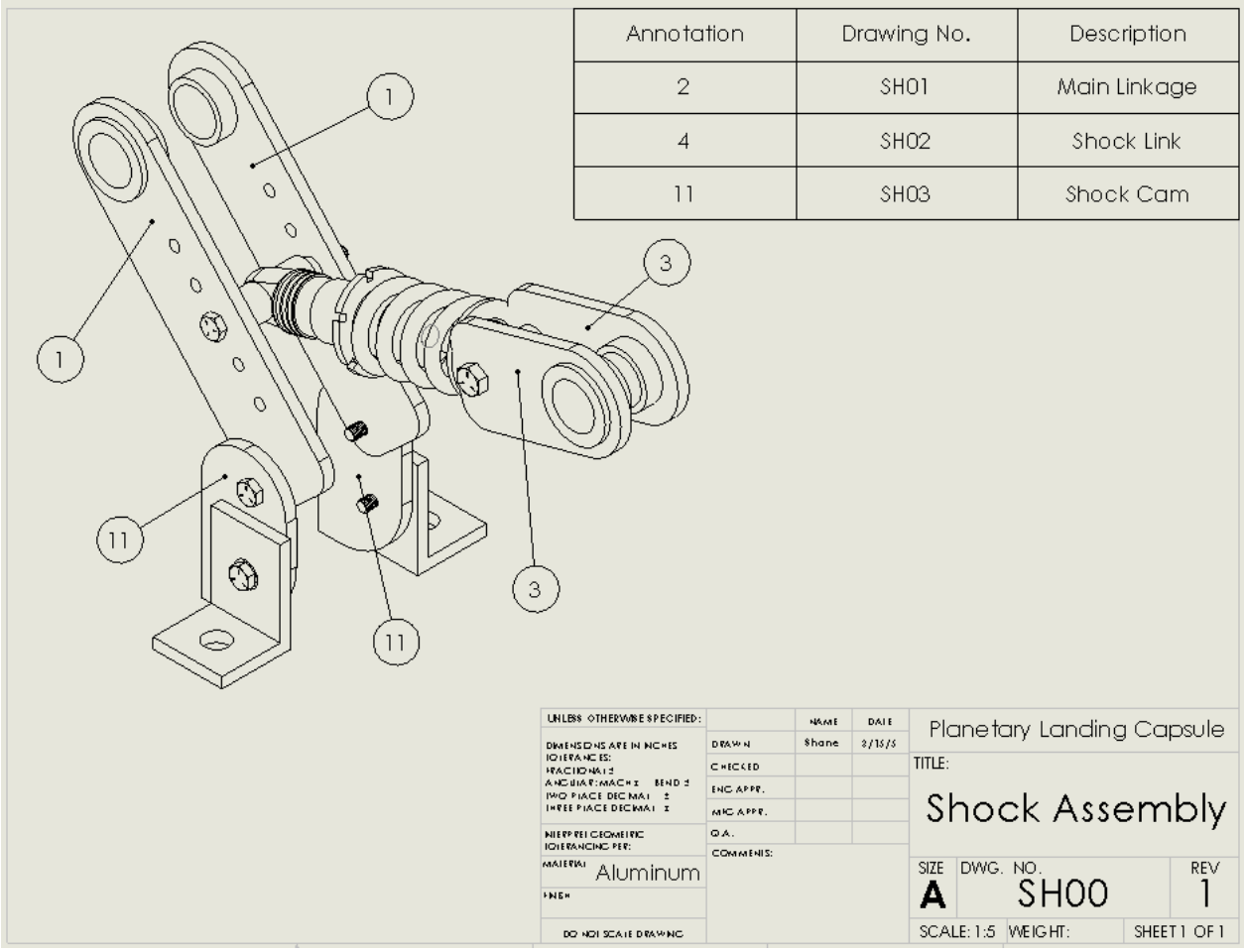

Annotation	Drawing No.	Description
2	SH01	Main Linkage
4	SH02	Shock Link
11	SH03	Shock Cam

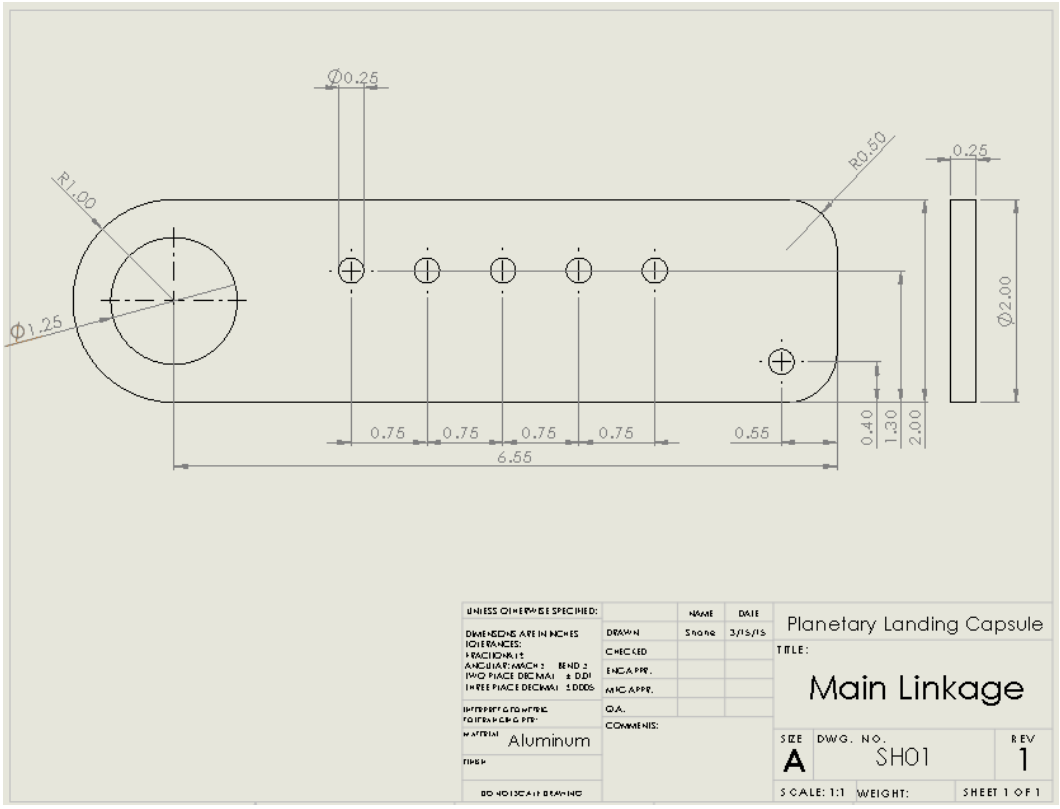
Ø0.25
R1.00
R0.50
0.25
Ø1.25
Ø2.00
0.75
0.75
0.75
0.75
0.55
6.55
0.40
1.30
2.00
UNLESS OTHERWISE SPECIFIED:
NAME
DATE
DRAWN
3/15/15
CHECKED
ENG APPR.
MFG APPR.
Q.A.
COMMENTS:
Aluminum
Planetary Landing Capsule
TITLE:
Main Linkage
SIZE
A
DWG. NO.
SH01
REV
1
SCALE: 1:1
WEIGHT:
SHEET 1 OF 1

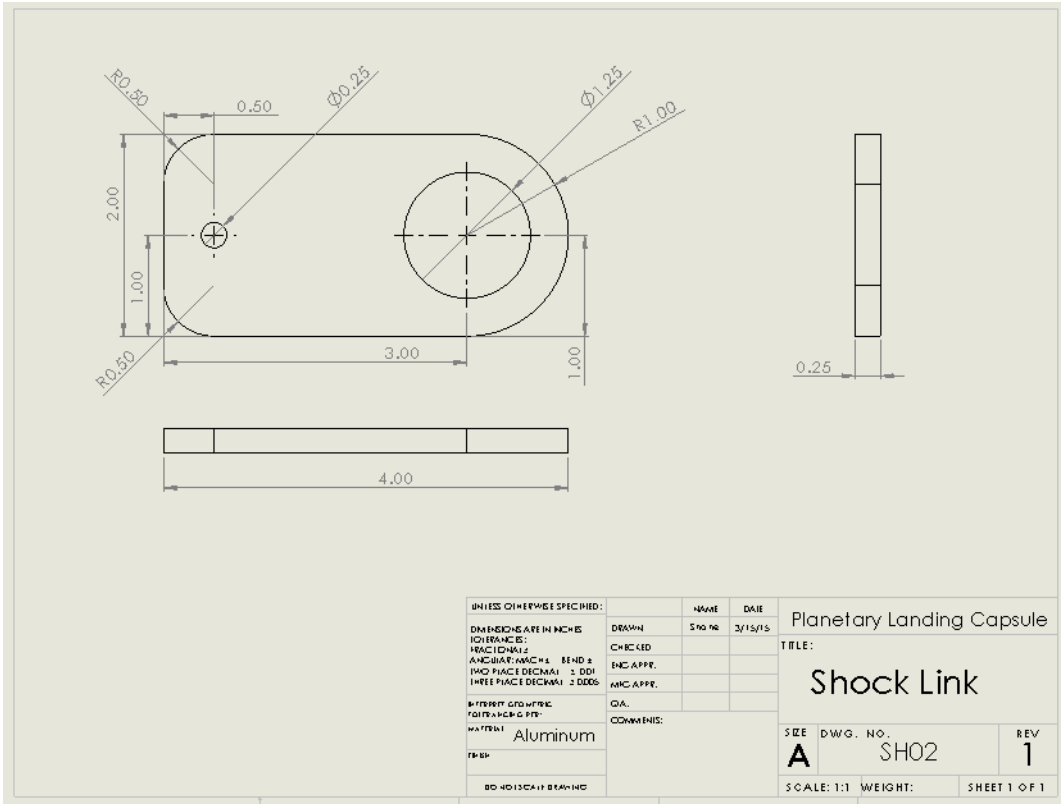
R0.50
0.50
Ø0.25
Ø1.25
R1.00
2.00
1.00
R0.50
3.00
1.00
0.25
4.00
UNLESS OTHERWISE SPECIFIED:
NAME
DATE
DRAWN
3/15/15
CHECKED
ENG APPR.
MFG APPR.
Q.A.
COMMENTS:
Aluminum
Planetary Landing Capsule
TITLE:
Shock Link
SIZE
A
DWG. NO.
SH02
REV
1
SCALE: 1:1
WEIGHT:
SHEET 1 OF 1

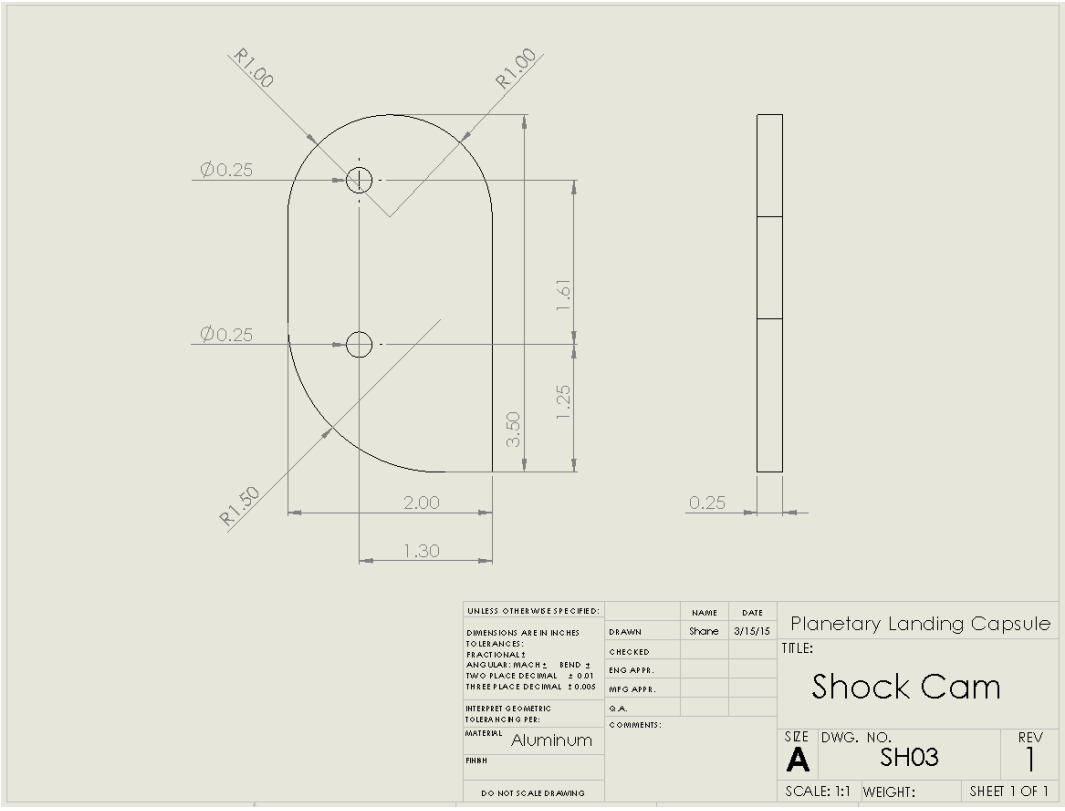
R1.00
R1.00
Ø0.25
Ø0.25
1.61
1.25
3.50
R1.50
2.00
1.30
0.25
UNLESS OTHERWISE SPECIFIED:
DIMENSIONS ARE IN INCHES
TOLERANCES:
FRACTIONAL ±
ANGULAR: MACH ± BEND ±
TWO PLACE DECIMAL ± 0.01
THREE PLACE DECIMAL ± 0.005
INTERPRET GEOMETRIC TOLERANCING PER:
MATERIAL Aluminum
FINISH
DO NOT SCALE DRAWING
NAME
DATE
DRAWN Shane 3/15/15
CHECKED
ENG APPR.
MFG APPR.
Q.A.
COMMENTS:
Planetary Landing Capsule
TITLE:
Shock Cam
SIZE A
DWG. NO. SH03
REV 1
SCALE: 1:1
WEIGHT:
SHEET 1 OF 1

Appendix C: PDS/Requirements

PROJECT DESIGN SPECIFICATION

Design Project: Planetary Landing Capsule

Team: PLC Date: May 18, 2015 Revision: 6

Datum description: Mars Rover Explorer Landing Capsule Page: 1 of 5

ELEMENTS/ REQUIREMENTS		PARAMETERS	
	UNITS	DATUM	TARGET - RANGE
PERFORMANCE			
Max Acceleration	g	8	14
Shock Levels	g	500	200
Size	m^3	4.71	1
Weight	kg	533	43
Deceleration Time	s	150	10
Energy Absorption	J	51,416.4	5141.6
SAFETY			
Functioning Rover	Drivable	Yes	Yes
Sharp Edges	Present	No	No
Shattering Parts	Present	No	No
Unharmed Testing Equipment	Functional	Yes	Yes
Unharmed Sensors	Functional	Yes	Yes
Pinch Points	Present	No	No
Exposed Gears	Present	No	No
PRODUCT COST			
Components	US Dollars		2500

PROJECT DESIGN SPECIFICATION

Design Project: Planetary Landing Capsule

Team: PLC Date: May 18, 2015 Revision: 6

Datum description: Mars Rover Explorer Landing Capsule Page: 2 of 5

ELEMENTS/ REQUIREMENTS		PARAMETERS	
	UNITS	DATUM	TARGET - RANGE
Outsourcing	US Dollars		500
Sensors	US Dollars		400
Test Equipment	US Dollars		250
TIME SCALE			
Finished Prototype	Months	24	9 Months
CUSTOMER			
NASA	Interest	Yes	Yes
MANUFACTURING PROCESS			
Design for Manufacturability	Makeable	Yes	Yes
Outsource ability	Able	Yes	Yes
SHIPPING			
Cost from Moffett to Kennedy	US Dollars		500
Product Size Constraint	m^3	4.71	1
COMPANY CONSTRAINTS			
Intellectual Property	Sued	No	No
DISPOSAL			
Reuse	Reusable	No	No
Recycle	Recyclable	No	Yes

PROJECT DESIGN SPECIFICATION

Design Project: Planetary Landing Capsule

Team: PLC Date: May 18, 2015 Revision: 6

Datum description: Mars Rover Explorer Landing Capsule Page: 3 of 5

ELEMENTS/ REQUIREMENTS		PARAMETERS	
	UNITS	DATUM	TARGET - RANGE
MANUFACTURING FACILITY			
SCU Machine Shop	Permission	No	Yes
Outsourcer's Facility	Permission	No	Yes
POLITICS			
Campus Safety Approval	Permission	No	Yes
MARKETET CONSTRAINTS			
Competition			
MAINTANANCE			
No Maintenance Required	Need	No	No
COMPETITION			
Price	US Dollars	1 Million	2500
Durability	Durable	Yes	Yes
Dependability	Dependable	Yes	Yes
Compact Ability	m^3	4.71	1
Weight	kg	533	43
PACKING			
Compact	m^3	4.71	1
Rectangular	Rectangle	Yes	Yes

PROJECT DESIGN SPECIFICATION

Design Project: Planetary Landing Capsule

Team: PLC Date: May 18, 2015 Revision: 6

Datum description: Mars Rover Explorer Landing Capsule Page: 4 of 5

ELEMENTS/ REQUIREMENTS		PARAMETERS	
	UNITS	DATUM	TARGET - RANGE
QUALITY AND RELIABILITY			
Usable	Usable	Yes	Yes
Reliable	Reliable	Yes	Yes
SHELF STORAGE			
Product Life Span	Years	2 year	1 year
PATENTS			
Infringement	Sued	No	No
MARS ENVIRONMENT			
Gravity	m/s^2	3.71	3.71
Minimum Surface Temperature	°C	-153	-153
Maximum Surface Temperature	°C	20	20
EARTH ENVIRONMENT			
Gravity	m/s^2	9.81	9.81
Average Surface Temperature	°C	20	20
TESTING			
Equipment	Available	Yes	Yes
Safety	Safe	Yes	Yes
DOCUMENTATION			

PROJECT DESIGN SPECIFICATION

Design Project: Planetary Landing Capsule

Team: PLC Date: May 18, 2015 Revision: 6

Datum description: Mars Rover Explorer Landing Capsule Page: 5 of 5

ELEMENTS/ REQUIREMENTS		PARAMETERS	
	UNITS	DATUM	TARGET - RANGE
Design Notebooks	Notebooks		4
CAD Drawings	Number		12
Sketches	Number		1
Reports	Number		3
QUANTITY			
Proof of Concept Test Article	Number		1
MATERIALS			
Material Cost	US Dollars	400 million	3000
Material Durability	Broken	No	No
STANDARDS/SPECIFICATIONS			
PDS Compliance	PDS Check	Yes	Yes
AESTHETICS			
Funding	US Dollars	Yes	Yes
INSTALLATION			
Rover Fits in Capsule	Fits	Yes	Yes

Appendix D: Timelines

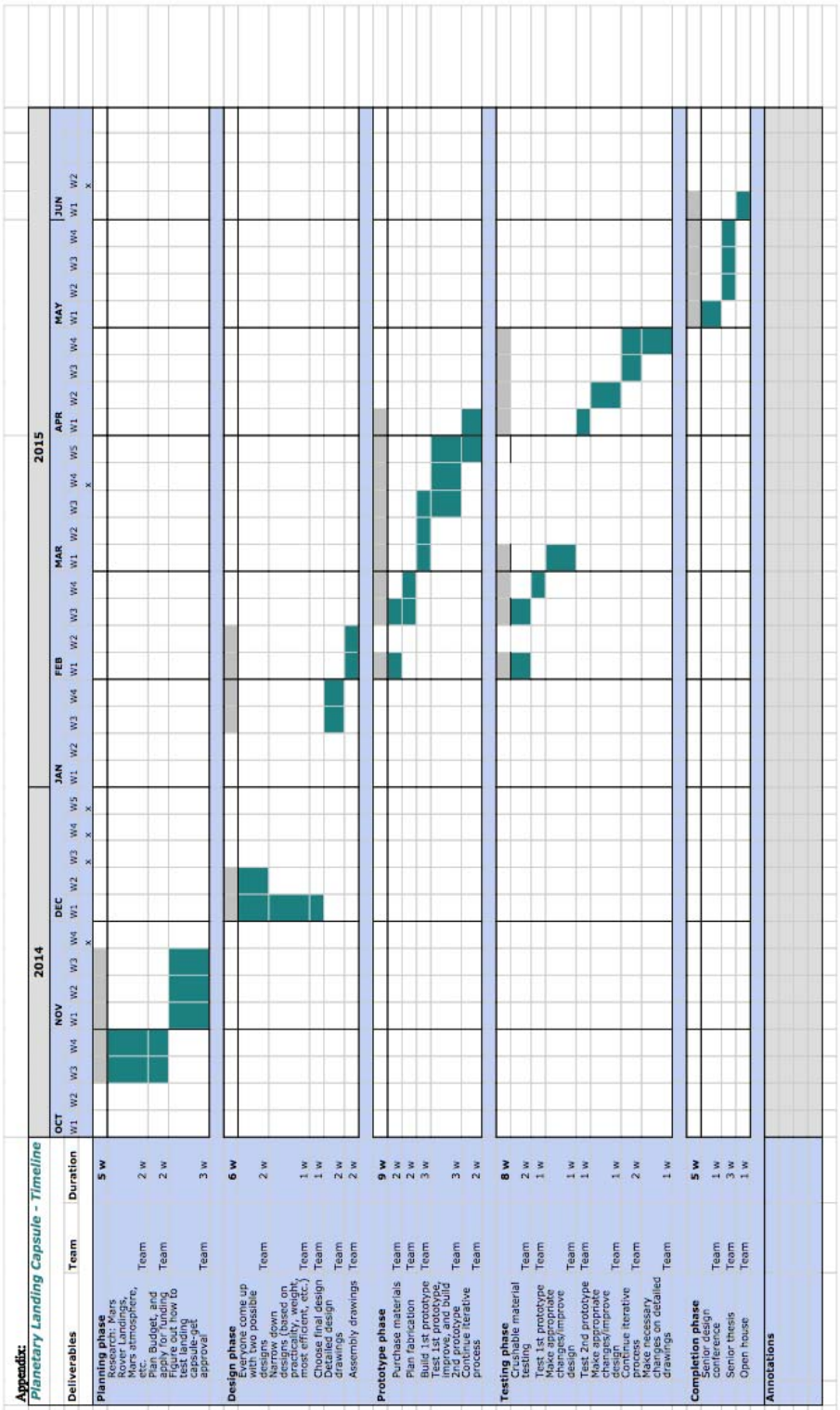

Planetary Landing Capsule - Spring Timeline

Deliverables	Team	Duration	MAR W1	MAR W2	MAR W3	MAR W4	MAR W5	APR W1	APR W2	APR W3	APR W4	MAY W1	MAY W2	MAY W3	MAY W4	JUN W1	JUN W2
			x	x	x	x											x
Testing phase		**10 w**															
Finish Building Final Prototype (Manufacturing and Assembly)	Team	2 w															
Test Final Prototype	Team	2 w															
Make Appropriate Changes/Improve Design	Team	2 w															
Make Necessary Changes on Detailed Drawings	Team	2 w															
Thesis Table of Contents, Introduction (Ch. 1), Attributed Drawings, and Spring Timeline	Team	1 w															
Experimental Protocol, PDS Update	Team	1 w															
Societal/Environmental Impact Presentation	Team	1 w															
Design Conference Practice	Team	2 w															
Patent Search	Team	1 w															
Experimental Results	Team	1 w															
Draft of Final Senior Thesis	Team	1 w															
Completion phase		**4 w**															
Senior Design Conference	Team	1 w															
Final Senior Thesis	Team	3 w															
Open House	Team	1 w															

Appendix E: Decision Matrices

Table 9: Priority matrix based on customer analysis.

	Criterion	1	2	3	4	5	6	7	8	9	SUM	FACTOR
1	Weight		1	1	0	0.5	1	0	0	0	3.5	10
2	Size	0		1	0	0.5	1	0	0	0	2.5	10
3	Aesthetics	0	0		0	0	0	0	0	0	0	1
4	Shock Absorption	1	1	1		1	1	1	1	0	7	75
5	Cost	0.5	0.5	1	0		1	0	0	0	3	10
6	Battery Life	0	0	1	0	0		0	0	0	1	5
7	Accuracy	1	1	1	0	1	1		0	0	5	35
8	Reliability	1	1	1	0	1	1	1		0	6	50
9	Safety	1	1	1	1	1	1	1	1		8	100

Table 10: Design rating matrix used to choose between possible design solutions.

	TARGET or	DESIGN IDEAS											
CRITERIA	FACTOR	Pyramid External Crushable/ Floating Frame Springs		Pyramid External Crushable and Springs		Cylinder Design		Egg Design		Pyramid Bottom Crushable/ Floating Frame Springs		Pyramid Bottom Crushable/ Floating Frame Foam	
Time – Design	1	1		4		2		1		4		5	
Time – Build	1	1		4		2		1		4		5	
Time – Test	1	1		3		3		3		3		3	
Time Score	10		10		36.67		23.33		16.67		36.67		43.33
Weight	10	3	30	2	20	4	40	2	20	4	40	4	40
Size	10	3	30	2	20	4	40	2	20	4	40	4	40
Aesthetics	1	3	3	2	2	4	4	5	5	4	4	4	4
Shock Absorption	75	3	225	3	225	4	300	4	300	3	225	3	225
Cost	10	3	30	3	30	2	20	1	10	3	30	3	30
Battery Life	5	3	15	3	15	3	15	3	15	3	15	3	15
Accuracy	35	3	105	2	70	4	140	2	70	3	105	4	140
Reliability	50	3	150	3	150	2	100	3	150	3	150	4	200
Safety	100	3	300	2	200	3	300	3	300	3	300	3	300
	TOTAL		888.0		732.0		959.0		890.0		909.0		994.0
	RANK												
	% MAX		89.3%		73.6%		96.5%		89.5%		91.4%		100.0%

Appendix F: Detailed Parts List

Subsystem	Part #	Component	Quanitity	Vendor Part Number	B/M/O	Vendor	Price/part	Price Total	Responsible Person	Design Time (hrs)	Build Time (hrs)	Assemble Time	Order/Start Date	Recieve/Finish Date
Frame (F)		Frame Assembly												
Aluminum Pipe 1" OD	F01	1.8' Aluminum Pipe 1" OD	5	4699T27	B	McMaster Carr	See Col A		Grant/Heather	0.25	0.25	0.25	1/30/2015	
2 @ 10 ft - $36.89ea	F02	0.585' Aluminum Pipe 1" OD	4	4699T27	B	McMaster Carr	See Col A		Grant/Heather	0.25	0.25	0.25	1/30/2015	
1 @ 4 ft - $14.75ea	F03	0.242' Aluminum Pipe 1" OD	8	4699T27	B	McMaster Carr	See Col A		Grant/Heather	0.25	0.25	0.25	1/30/2015	
to cut all pipe parts	F04	0.917' Aluminum Pipe 1" OD	1	4699T27	B	McMaster Carr	See Col A		Grant/Heather	0.25	0.25	0.25	1/30/2015	
	F05	1.33' Aluminum Pipe 1" OD	4	4699T27	B	McMaster Carr	See Col A		Grant/Heather	0.25	0.25	0.25	1/30/2015	
	F06	.792' Aluminum Pipe 1" OD	2	4699T27	B	McMaster Carr	See Col A	$73.78	Grant/Heather	0.25	0.25	0.25	1/30/2015	
	F07	Al Adjustable Angle Elbow 1" OD	8	4698T82	B	McMaster Carr	$15.30	$122.40	Grant/Heather	0.25	0	0.5	1/30/2015	
	F08	Al 3 Way 90 deg Elbow 1" OD	4	4698T111	B	McMaster Carr	$11.18	$44.72	Grant/Heather	0.25	0	0.5	1/30/2015	
	F09	Al Tee 1" OD	4	4698T91	B	McMaster Carr	$8.59	$34.36	Grant/Heather	0.25	0	0.5	1/30/2015	
	F10	Al Cross 1" OD	5	4698T19	B	McMaster Carr	$9.15	$45.75	Grant/Heather	0.25	0	0.5	1/30/2015	
	F11	Al Round Flange 1" OD	2	4698T25	B	McMaster Carr	$8.93	$17.86	Grant/Heather	0.25	0	0.5	1/30/2015	
	F12	Al 6 Way Cross 1" OD	1	4698T142	B	McMaster Carr	$18.87	$18.87	Grant/Heather	0.25	0	0.5	1/30/2015	
	F14	Al 90 deg Elbow 1" OD	4	4698T31	B	McMaster Carr	$8.13	$32.52	Grant/Heather	0.25	0	0.5	1/30/2015	
	F15	Galv Iron Flange 1" OD	4	4936T194	B	McMaster Carr	$9.67	$38.68	Grant/Heather	0.25	0	0.5	1/30/2015	
	F16	5/32" Hex Set Screws (50 pkg)	2	90289A575	B	McMaster Carr	$8.21	$16.42	Grant/Heather	0.25	0	0.25	1/30/2015	
	F18	1/4" Hex Set Screws (10 pkg)	1	4936T918	B	McMaster Carr	$14.00	$14.00	Grant/Heather	0.25	0	0.25	1/30/2015	
	F19	.1566' Aluminum Pipe 1" OD	4	4699T27	B	McMaster Carr	See Col A	$14.75						
		Tax						$70.68						
		Shipping (Shell and Frame Parts)						$287.46						
	FA01	Frame Assembly			M			$832.25	Team					2/13/2015
Subtotal Price		$832.25									*Subtotal Man Hours*	11.5		
Shell (S)		Shell Assembly												
	S01	1/8" Polycarbonate Sheet 3x3'	4	8574K266	B	McMaster Carr	$49.06	$196.24	Shane	0.5	1.5	0.5	1/30/2015	
	S02	1/8" Polycarbonate Sheet 3x3'	1	8574K266										
	S03	1/8" Polycarbonate Sheet 2x2'	1	8574K53	B	McMaster Carr	$26.98	$26.98	Shane	0.5	1	0.5	1/30/2015	
	S04	1/8" Polycarbonate Sheet 1x1'	1	8574K26	B	McMaster Carr	$9.16	$9.16	Shane	0.5	1	0.5	1/30/2015	
	S05	Spring Butt Hinges, Square Corner 4.5" x 4.5	8	892056	B	Hardware Source	$10.97	$87.76	Shane	0.5	0.5	0.5	1/30/2015	
	S06	Velvet Fabric 10' length 48" width	1	88015K1	B	McMaster Carr	$39.40	$39.40	Shane	0.5	0.5	0.5		
	S07	Magnet 5' L x 1/32" Thick x 1" Wd	1	4774K34	B	McMaster Carr	$5.10	$5.10	Grant		0.5	0.5		
	S08	Adhesive Magnet 5' L x 1/32" Thick x 1" Wd	1	5759K46	B	McMaster Carr	$7.65	$7.65	Grant		0.5	0.5		
	SA01	Shell Assembly			M			$372.29	Team					2/13/2015
Subtotal Price		$372.29									*Subtotal Man Hours*	11.5		
Mock-up (M)		Mockup												
3/4"X10' PVC Pipe	M01	3/4" x 20" PVC pipe	8		B	Home Depot	See Col A		Shane	0.5	0.25	0.25	1/20/2015	
2 @ $1.37ea	M02	3/4" x 6" PVC Pipe	4		B	Home Depot	See Col A		Shane	0.5	0.25	0.25	1/20/2015	
to cut PVC to length	M03	3/4" x 4" PVC Pipe	4		B	Home Depot	See Col A	$2.74	Shane	0.5	0.25	0.25	1/20/2015	
	M04	4' x 4' TriPly Wood Panel	5		B	Home Depot	$7.97	$39.85	Shane	0.5	0.25	0.25	1/20/2015	
	M05	1.5" x 2' x 4' Polystyrene	1		B	Home Depot	$5.25	$5.25	Shane	0	0.25	0.25	1/20/2015	
	M05	3" Hindge (w/ Screws)	4		B	Home Depot	$2.58	$10.32	Shane	0	0	0.25	1/20/2015	1/30/2015
		Sales Tax						$5.44						
Subtotal Price		$63.60							Team		*Subtotal Man Hours*	4.75		
Suspension (S)		Suspension												
	S01	Low-Carbon Steel Bar .25"x2"x6'	1	8910K557	B	McMaster Carr	$37.51	$37.51	Shane	2	1	1	3/3/2015	
	S02	Low-Carbon Steel Bar .25"x2"x2'	1	8910K557	B	McMaster Carr	$16.88	$16.88	Shane	2	1	1	3/3/2015	
	S03	SAE 863 Brass Bearing, Flanged	16	2938T25	B	McMaster Carr	$1.79	$28.64	Shane	0.5	1	1	3/3/2015	
	S04	Hex Bolt 3", 1/4"-28 full thread	10	92865A020	B	McMaster Carr	$2.08	$20.82	Shane	0.5	1	1	3/3/2015	
	S05	Hex Bolt 3/4", 1/4"-28 full thread	100	92865A006	B	McMaster Carr	$0.09	$9.68	Shane	0.5	1	1	3/3/2015	
	S06	Spacer Stock .252"ID, .508"OD	1	92377A120	B	McMaster Carr	$4.69	$4.69	Shane	0.5	1	1	3/3/2015	
	S07	Hex Nut 1/4"-28 thread	100	90490A205	B	McMaster Carr	$0.02	$2.63	Shane	0.5	1	1	3/3/2015	
	S08	18-8 Stainless Washer 1/4" Screw	100	92141A029	B	McMaster Carr	$0.03	$3.37	Shane	0.5	1	1	3/3/2015	
	S10	304 Steel L Bracket	8	33125T11	B	McMaster Carr	$5.63	$45.04	Shane	0.5	1	1	3/3/2015	
	S11	PTFE Washer 1/4" Screw	10	95630A217	B	McMaster Carr	$0.32	$3.23	Shane	0.5	1	1	3/3/2015	3/20/2015
	S12	DNM Bike Shock 750lb x 150mm	4		B	Amazon	$30.00	$120.00						
		Shipping + Tax (Amazon)						$10.80						
		Shipping + Tax (McMaster Carr)						$46.07						

Subtotal		$349.36									*Subtotal Man Hours*	17.5		
Accelerometer (A)		Accelerometer												
	A01	YEI Tech 3-Space Sensor, Bluetooth	1		B	YEI Technology	$355.00	$355.00						
		Shipping						$13.70						
Subtotal Price		$368.70												
Payload (P)		Payload												
	P01	RC Car	1		B	Radio Shack	$25.00	$25.00	Shane	0.5	1		1/30/2015	
	P02	RC Car Mount	1		B	McMaster Carr	$10.00	$10.00	Shane	0.5	1			
Subtotal Price		$35.00									*Subtotal Man Hours*	1.5		
Total Price		$2,021.20									Total Man Hours	46.75		
		(not including payload atm)	B/M/O											
			Buy, Made,											
			Oursourced											

Appendix G: Simulink Block Diagram

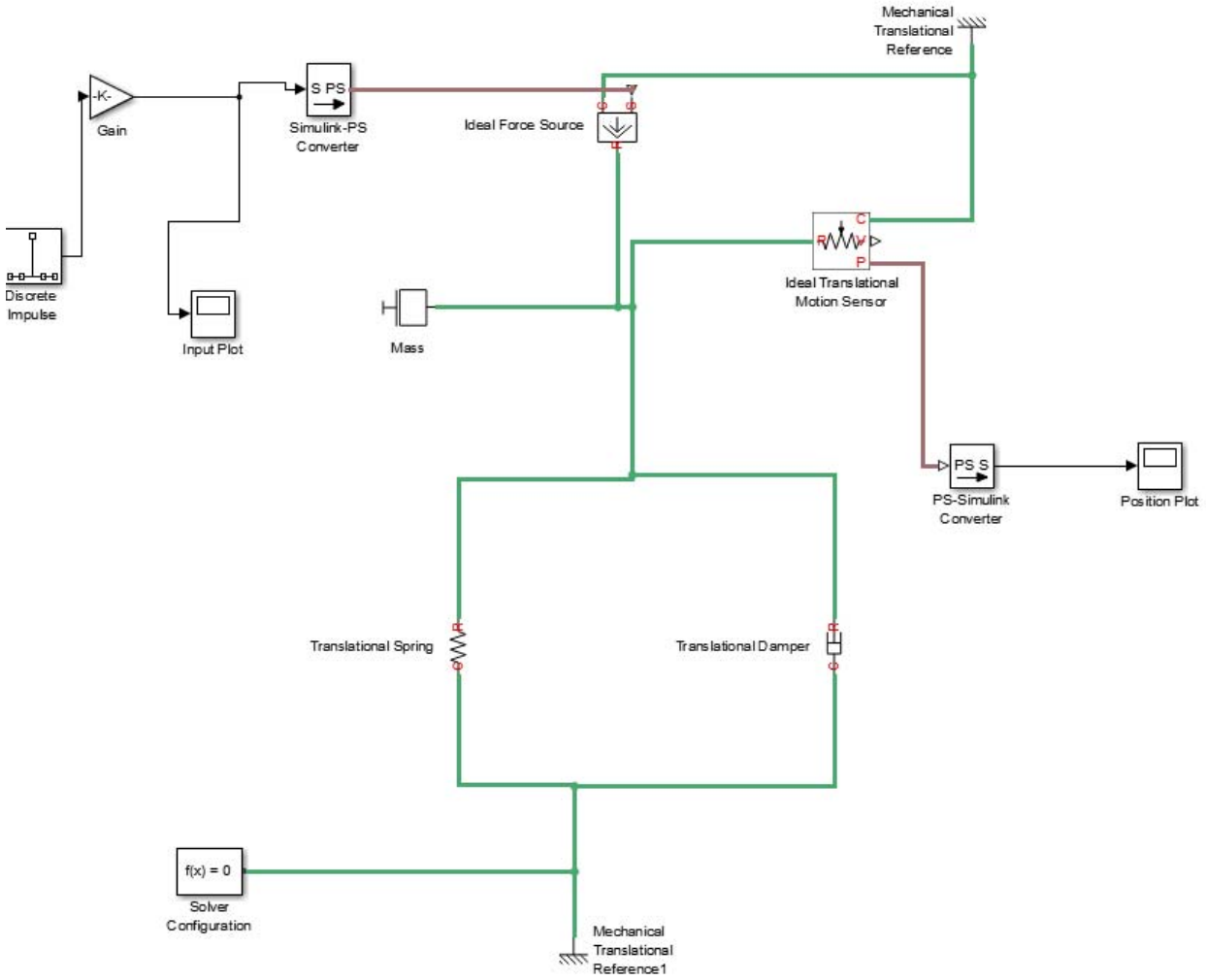

Appendix H: Copies of Important Patents

United States Patent

Paine et al.

[15] **3,637,051**

[45] **Jan. 25, 1972**

[54] **IMPACT ENERGY ABSORBING SYSTEM UTILIZING FRACTURABLE MATERIAL**

[72] Inventors: **T. O. Paine**, Administrator of the National Aeronautics and Space Administration with respect to an invention of; **Earl R. Collins, Jr.**, LaCanada, Calif.

[22] Filed: **Sept. 15, 1969**

[21] Appl. No.: **857,967**

[52] **U.S. Cl.** .....**188/1 B**, 188/1 C, 188/268
[51] **Int. Cl.** **F16d 63/00**
[58] **Field of Search** .....188/1 B, 1 C, 268

[56] **References Cited**

UNITED STATES PATENTS

3,010,540 11/1961 Dahlen .....188/1 C
3,110,262 11/1963 West .....188/101 X
3,265,163 8/1966 Gilbert et al. .....188/1 C X

Primary Examiner—George E. A. Halvosa
Attorney—G. T. McCoy, J. H. Warden and Monte F. Mott

[57] **ABSTRACT**

A shock absorber particularly suited for use as a protective barrier in an impact energy absorbing system, characterized by the utilization of a myriad of contiguous spheres arranged in multiple strata for absorbing forces developed on impact, a feature of the shock absorber being the employment of a brittle material in the fabrication of the spheres, whereby payload rebound is inhibited and impact force dissipation is enhanced through a sequential fracture and collapse of successive strata of spheres.

8 Claims, 4 Drawing Figures

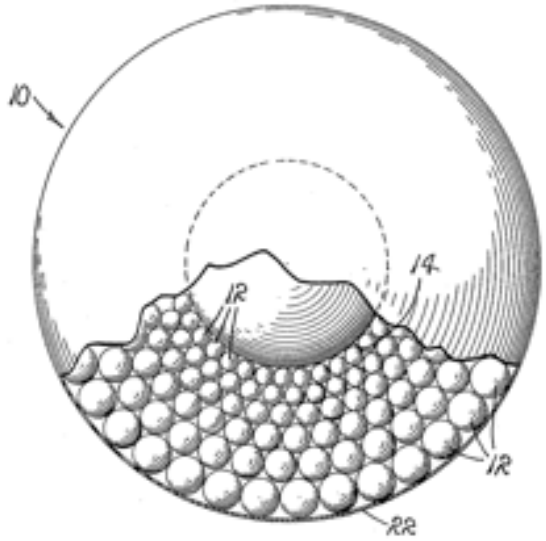

PATENTED JAN 25 1972

3,637,051

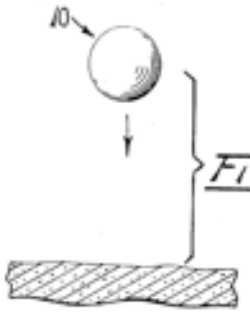

FIG. 1.

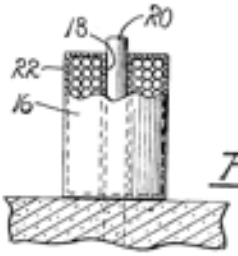

FIG. 3.

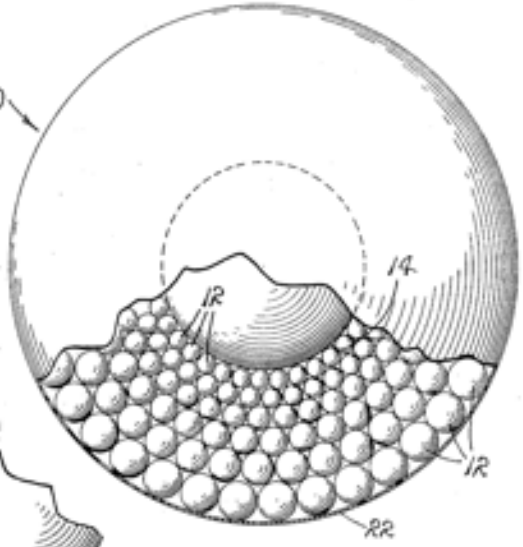

FIG. 2.

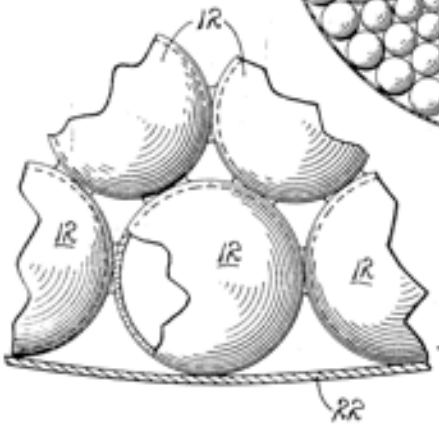

FIG. 4.

INVENTOR
EARL R. COLLINS JR.

ATTORNEYS

IMPACT ENERGY ABSORBING SYSTEM UTILIZING FRACTURABLE MATERIAL

ORIGIN OF INVENTION

The invention described herein was made in the performance of work under a NASA contract and is subject to the provisions of Section 305 of the National Aeronautics and Space Act of 1958, Public Law 85-568 (72 Stat. 435; 42 USC 2457).

BACKGROUND OF THE INVENTION

1. Field of the Invention

The invention relates to shock absorbers and more particularly to a self-destructing shock absorber wherein impact energy is dissipated through a destruction of the device.

2. Description of the Prior Art

Shock absorbers designed for repetitive employment normally utilize various types of energy dissipating devices, including resilient devices such as springs, air-filled bags, foam and plastic pads, as well as hydraulic or oleo absorbers, or the like, which dissipate energy by forcing a fluid through a restricted orifice. Attempts have been made to utilize crushable structures such as metallic bodies and natural balsa wood for dissipating energy on a one-shot basis wherein energy is dissipated through the destruction of the device. In most instances, where resilient material is employed in dissipating energy, it is difficult to avoid the tendency of an impacting object to rebound, due to the resiliency of the material employed in such systems. In instances where the absorber is to be employed under conditions of extreme temperatures, such as may be encountered on celestial bodies, difficulty is encountered in using devices which employ fluids forced through restrictive orifices, since the viscosity of the fluid normally will undergo significant change as a heat transfer occurs. In those instances where a natural substance such as balsa wood has been utilized, in one-shot absorbers, difficulty has been experienced in selecting the proper wood to achieve the desired dissipation of forces under varying operative conditions and where metallic containers have been employed, rebound has not been entirely eliminated due to the inherent resiliency of the metal employed. For all of the aforementioned devices, the weight of systems capable of effectively employing them frequently prohibits their use in practical applications. This is particularly true where the system is to be employed in protecting landing capsules for payloads delivered to the surface of a celestial body or delivered by aircraft to an impacting surface.

OBJECTS AND SUMMARY OF THE INVENTION

This invention overcomes many of the aforementioned difficulties by providing a lightweight, simplified absorber which utilizes a novel arrangement of a myriad of contiguous, brittle spheres interposed as a barrier member between impacting surfaces.

Accordingly, an object of the instant invention is to provide an improved shock absorber.

Another object is to provide an improved shock absorber particularly adapted for use in mechanical energy absorbing systems.

Another object is to provide a lightweight, highly effective, shock absorber particularly adapted for use in delivering payloads to the surfaces of celestial bodies.

Another object is to provide a highly efficient, self-destructing, economical shock absorber adapted to be employed in dissipating impact energy by fracturing brittle materials.

Another object is to provide an improved shock absorber, including a myriad of contiguous glass spheres arranged in contiguous strata surrounding a payload in a manner such that as the payload is delivered to an impacting surface of a given body the force of impact is controllably dissipated through a fracture and a collapse of successive strata of spheres.

These together with other objects and advantages of the present invention will subsequently become more clearly apparent upon reference to the following description in the specification and accompanying drawing.

DESCRIPTION OF THE DRAWING

FIG. 1 is a pictorial view of a payload being delivered employing a shock absorber embodying the principles of the present invention.

FIG. 2 is a partially sectioned view of the shock absorber of FIG. 1, illustrating the strata of spheres employed in the present invention.

FIG. 3 is a partially sectioned view of a modified form of the shock absorber illustrated in FIGS. 1 and 2.

FIG. 4 is a fragmentary view, on somewhat an enlarged scale, of the hollow spheres employed in the shock absorber embodying the principles of the present invention.

DESCRIPTION OF THE PREFERRED EMBODIMENT

Turning now to FIG. 1, therein is pictorially illustrated a payload employing a shock absorber 10 of a type which embodies the principles of the present invention. As best illustrated in FIG. 2, the shock absorber is made up of a myriad of individual spheres 12 arranged in a multiplicity of superimposed spherical layers or strata arranged in supporting engagement with a selected payload 14. While the payload 14 is illustrated as being of a spherical configuration, it is to be understood that the payload may assume any convenient configuration.

In practice, the spheres are formed from any extremely brittle material which is both hard and inelastic. A high grade of silicon glass serves as a convenient material from which the spheres may be fabricated whereby, prior to fracture and collapse of the individual spheres, deformation is minimized so that the impact force may be resisted and then dissipated as a fracture followed by a collapse of the spheres. The sudden fracture and collapse of each of the individual spheres substantially eliminates any tendency of the payload to experience rebound.

As a practical matter, the capability of the individual spheres to withstand impact loads is determined principally by a T/D ratio where T is the thickness of the wall and D is the diameter of the sphere. The maximum stress which a sphere will withstand is a readily determinable value. For purposes of calculating maximum stress, the formula $S=B\,P/t^2$ may be employed, where:

B is a numerical coefficient that depends on

$$\mu=\sqrt[4]{12(1-\nu^2)}\frac{(ro)}{\sqrt{R_s t}}$$

t is the thickness of the wall of the sphere;

R is the radius of the sphere;

v is Poisson's ratio; and

ro is the radius of the area to which the load is applied. In practice, B is a value provided by various tables, such as those found at page 273, Case 17 of "Formulas For Stress And Strain," third edition, 1954, by Raymond J. Roark and published by McGraw-Hill Book Company of New York, Toronto and London. Having solved for the stress, a material having the required stress level may be selected. Conversely, should a particular material be selected, the formula may be employed in solving for the required thickness of the walls of the spheres. By disposing in the outermost strata spheres having a larger diameter and greater wall thickness to sphere diameter ratios, greater amounts of impact force can be absorbed as the shock absorber engages or impacts the impacting surface, since the maximum stress is greater for those spheres.

Furthermore, by successively reducing the T/D ratio of the spheres in succeeding strata, progressing inwardly, the ability to withstand impact is reduced. Consequently, upon impact, the larger quantities of force are dissipated through the fracture and collapse of the spheres near the external surface of

the shock absorber and smaller and smaller quantities of force are dissipated by the progressively smaller spheres. Hence, it should be appreciated that the outer strata serve to dissipate the largest quantities of force, while the innermost stratum serves to dissipate the smallest quantities of force, so that the kinetic energy of the payload **14** is dissipated at a selected rate which is proportional to the negative acceleration of the payload as it comes to rest.

While the shock absorber has been disclosed as being particularly useful in delivering "hard-landed" payloads to the surfaces of celestial bodies, as well as in delivering payloads employing airdrop techniques, it is to be understood that the shock absorber has utility separate and apart from either of these uses. For example, a shock absorber embodying the principles of the present invention may be formed to assume a configuration of a cylindrical shock absorber **16**, FIG. **3**. The shock absorber **16** includes an opening **18** into which is inserted an elongated member **20**, and, as a practical matter, may comprise a vertical post such as a lamp post, a bridge abutment, a support for a guardrail, or the like, as frequently found along automobile roadways.

Where desired, the shock absorbers **10** and **16** preferably are enclosed in a flexible cover **22** formed of any convenient material such as Plexiglass or the like which serves to contain the fractured glass as impact occurs. However, should the shock absorber be employed in delivering payload to celestial bodies wherein it is desired that the payload be broken-out, the cover **22** can be eliminated so that the payload **14** is caused to be released from the shock absorber once the spheres of the strata are crushed.

Depending upon the intended employment of the shock absorber, various types of adhesive material or bonding agents may be employed in securing the spheres into a unitary structure. Preferably, the bonding agent is a brittle substance, such as epoxy, which accommodates assembly of the spheres into a cohesive structure, while accommodating fracture of the multiple spheres.

Assembly of the shock absorber is achieved by employing numerous techniques. For example, the individual spheres may be treated with adhesive and then deposited about the surface of the payload, or adhesive may be applied to the individual spheres as they are deposited in the various strata. In any event, the resulting shock absorber is provided with an internal and external wall having therebetween a multiplicity of strata formed of individual hollow spheres disposed in a contiguous relationship. Each of the spheres has a T/D ratio such that the spheres may be fractured for absorbing a predetermined quantity of impact energy as the external surface of the

shock absorber engages an impacting surface.

Although the invention has been herein shown and described in what is conceived to be the most practical and preferred embodiment, it is recognized that departures may be made therefrom within the scope of the invention.

What is claimed is:

1. A shock absorber adapted for use in a mechanical impact energy absorbing system comprising:

A. a spherical payload compartment;

B. a plurality of contiguous, thin walled, hollow bodies of a substantially spherical configuration formed of a brittle material and arranged in spherical strata surrounding said payload compartment, said bodies being so dimensioned that the diameter of the bodies of the outermost stratum is greater than the diameter of the bodies of the innermost stratum; and

C. a bonding agent impregnating said shock absorber and uniting said bodies into a unitary mass

2. A destructible shock absorber comprising a labyrinth of brittle thin walls defining a multiplicity of isolated substantially spherical compartments, said labyrinth of brittle thin walls being disposed between an object to be protected and a potential source of impact force, the compartments being arranged in contiguous strata and the compartments being of increased size outwardly from the object to be protected for successive collapse inwardly toward said object upon impingement of a destructive impact force thereagainst.

3. A shock absorber for absorbing impact energy comprising a unitary barrier including a plurality of contiguous, thin walled, hollow bodies of a substantially spherical configuration formed of a brittle material and adapted to fracture on impact.

4. A shock absorber according to claim **3** further comprising bonding means fixedly securing said contiguous bodies into a unitary mass with voids being established therebetween.

5. The shock absorber according to claim **3** wherein the bodies are arranged in strata with each stratum containing a plurality of bodies of a common diameter.

6. The shock absorber according to claim **5** wherein the diameter of the bodies of each stratum varies with respect to the diameter of the bodies of the adjacent strata.

7. The shock absorber according to claim **6** wherein the strata are so arranged that the barrier is of a substantially cylindrical configuration.

8. The shock absorber according to claim **6** wherein the strata are so arranged that the barrier is of a spherical configuration and defines a payload cavity therein.

* * * * *

May 4, 1965 JAMES E. WEBB 3,181,821

ADMINISTRATOR OF THE NATIONAL AERONAUTICS AND SPACE ADMINISTRATION

SPACE CRAFT SOFT LANDING SYSTEM

Filed June 4, 1964 2 Sheets-Sheet 1

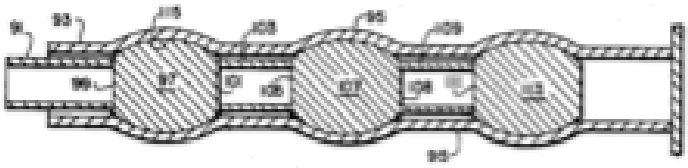

FIG. 4

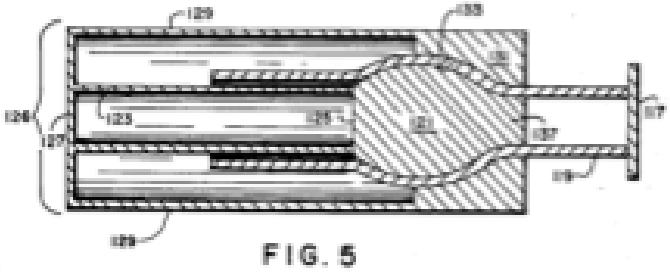

FIG. 5

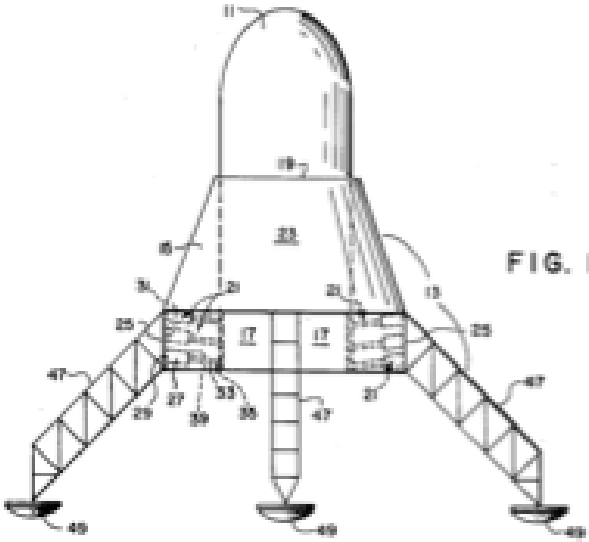

FIG. 1

INVENTOR,
TIMOTHY O. EDGINS
BY G. T. McCoy
B. R. Smallwood
ATTORNEYS

May 4, 1965 JAMES E. WEBB 3,181,821

ADMINISTRATOR OF THE NATIONAL AERONAUTICS AND SPACE ADMINISTRATION

SPACE CRAFT SOFT LANDING SYSTEM

Filed June 4, 1964 2 Sheets-Sheet 2

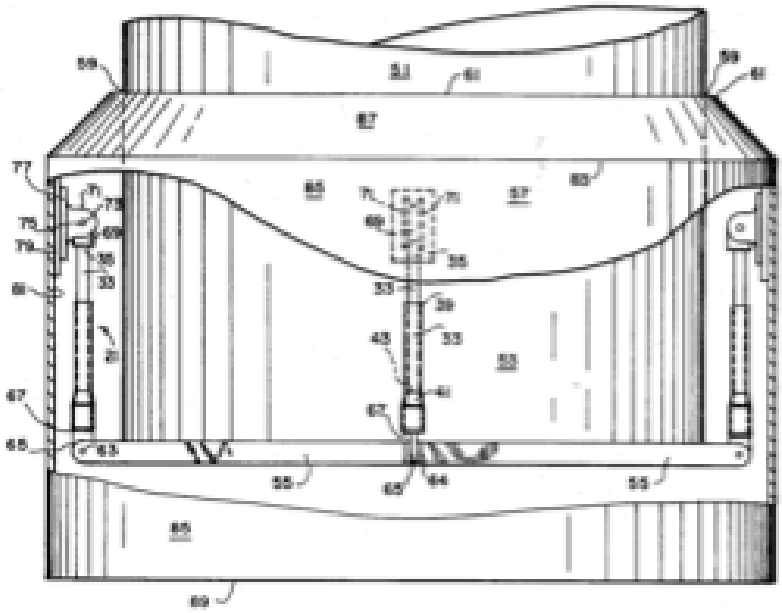

FIG. 3

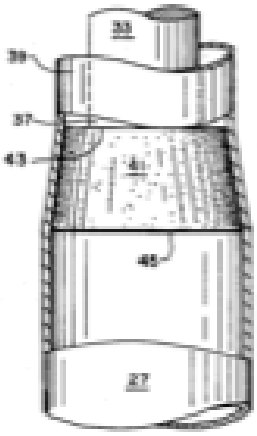

FIG. 2

INVENTOR.
TIMOTHY G. EDDINS
BY G. T. McCoy
S. E. Smallwood
ATTORNEYS

United States Patent Office

3,181,821

Patented May 4, 1965

1

3,181,821

SPACE CRAFT SOFT LANDING SYSTEM

James E. Webb, Administrator of the National Aeronautics and Space Administration, with respect to an invention of Timothy O. Eddins

Filed June 4, 1964, Ser. No. 373,727

13 Claims. (Cl. 244—100)

The invention described herein may be manufactured and used by or for the Government of the United States of America for governmental purposes without the payment of any royalties thereon or therefor.

This invention relates generally to energy absorbing systems for missile or spacecraft soft landings on the earth, moon or other terrestrial surfaces. More particularly, the invention relates to spacecraft energy absorbing systems of the shock impact type capable of absorbing large quantities of kinetic energy at a substantially constant rate of deceleration force applied per unit of stroke distance.

With the advent of reaction engines of greater thrust and the corresponding development of spacecraft structures and other missile systems, the possibility of effecting a landing on the moon (and other terrestrial surfaces) with a manned spacecraft capable of returning to the earth has become more realistic. There are however many problems connected with such a venture. One of these problems to which a solution had to be found was a way to deposit the spacecraft, its personnel and equipment on the lunar surface without injury to the personnel, and without excessive damage to the spacecraft and equipment needed for exploration and subsequently return to the earth. Thus, the problem of absorbing the initial landing impact shock had to be formulated, analyzed and solved. As was stated by Mr. Robert E. Lavender in a National Aeronautics and Space Administration publication entitled, Touchdown Dynamics Analysis of Spacecraft for Soft Lunar Landing: "It would indeed be a pity for the vehicle system to perform successfully all phases of flight to the moon only to result in a failure during the few seconds of motion remaining after initial touchdown." NASA TN D-2001, January 1964.

This specific area or problem of space flight is not to be approached as an absolute, but it is correlative with other parameters including the motion of the spacecraft from its initial position above the surface of the moon after descent from a moon orbit until the spacecraft comes to rest on the surface. Among the many parameters involved in this general problem are, for example, local "touchdown area" lunar slope, coefficient of friction, initial touchdown vertical and horizontal velocity components, vehicle weight and radius of gyration, landing gear diameter, characteristics of the impact energy absorbing devices in the landing gear, and the number of legs in the landing gear arrangement. These and other parameters are considered when the requirements of the various systems operative during this critical phase of the mission are specified. Thus, for a lunar landing, the coefficient of friction of the surface with respect to the landing gear feet, the local touchdown area slope (and degree of roughness), whether stabilization rockets will be used just before landing impact, and, of course, others are predetermined based on unmanned lunar explorations and used to calculate the design requirements of the systems to be used. For our purposes, the critical parameters in the design of an impact energy absorbing system is concerned mainly with the various force component requirements placed on the system resulting from an analysis of these other areas of investigation and the formulation of a cybernetic model of the landing problem. Therefore the present invention is directed primarily to energy absorbing devices and a spacecraft landing gear system in which they may be used.

2

Consistent with the other parameters involved, and based on the physical environment expected and the particular missions to be performed, various approaches to the general problem indicated above have been studied. Each of the approaches has advantages and disadvantages attendant with its implementation, and, for that reason, various combinations of approaches have been considered to offer the best solution to particular mission requirements. The following are some of the approaches which have been studied: Braking retrorockets, gas filled bags, frangible metal tubing, collapsible plastic or metal shells or cylinders, strain straps, burrowing or spike penetration, crushable materials including metal honeycomb, balsa wood or plastic foam, and structural deformation.

In addition to the above enumerated systems for braking the descent of a spacecraft, it is obvious that there are several means of effecting a recovery of a spacecraft on earth which are not available for such landings on the moon. Among these would be systems requiring a supporting atmosphere such as, for example, aerial snatch or the use of parachutes. Water landings require special environmental conditions, and skidding has been found to require a prepared landing area. However, regardless of whether the landing is to occur on a lunar or earth like surface, it is foreseeable that braking retro rockets will be used as a basic means to dissipate the kinetic energy of a spacecraft preparatory to making the soft landing with one or more other devices or methods being employed to help absorb the shock energy released on and immediately after the initial touchdown.

It is generally felt that the retro rockets would place the spacecraft approximately 15 to 60 feet above the lunar surface in a zero velocity hovering configuration. The exact altitude will depend on the results of unmanned lunar explorations indicative of the composition of the lunar surface. If there is a large quantity of loose rock and dust, as is expected, the rocket exhaust gases may make visibility difficult and may even change the local terrain features if the hovering altitude is too low. But given this hovering altitude, the spacecraft will attain a zero velocity position above the desired landing site and the rocket engines will be shut down. The spacecraft, under the influence of the local gravitational field of the moon, will accelerate toward the lunar surface and will impact with little or no attitude correction until the landing gear makes first contact with the surface. It is at this point that desirable deceleration characteristics of the landing gear configuration can mean success or failure of the mission. It is, of course, desirable that the rate of build up of the deceleration force be moderate and preferably constant until optimum deceleration force has been reached and then to remain zero (i.e. constant deceleration force) until the spacecraft has come to rest. It is necessary that there be an adequate stroke distance capacity inherent in the energy absorbing system since the longer the stroke the smaller the average deceleration forces that need be developed to absorb a given quantity of energy. The stroke must be adequate even though the exact amount of energy to be absorbed may not be precisely known in advance. The energy in this discussion has been termed kinetic energy since it can be seen that, at impact, the potential energy of the spacecraft in its zero velocity hovering position has almost all been converted to kinetic energy.

It is very desirable that the energy absorbing system exhibit to the spacecraft a constant deceleration force regardless of the total energy to be absorbed. It is also very desirable that the energy absorbing system be capable of withstanding moderate horizontal velocity components at touchdown. Among other desirable features are favor-

United States Patent [19]

Rogers

[11] **Patent Number: 5,039,036**

[45] **Date of Patent: Aug. 13, 1991**

[54] **ENERGY ABSORBING AIR DROP PALLET**

[76] Inventor: **Roy K. Rogers**, 26575 Barns, Roseville, Mich. 48066

[21] Appl. No.: **580,690**

[22] Filed: **Sep. 11, 1990**

[51] **Int. Cl.**[5] **B64D 1/14**

[52] **U.S. Cl.** ..... **244/138 R**; 244/137.3

[58] **Field of Search** ..... 244/137.3, 138 R, 142; 188/129, 166, 268, 271; 54/62

[56] **References Cited**

U.S. PATENT DOCUMENTS

2,587,448	2/1952	Eakin	244/138 R
3,010,540	11/1961	Dahlin	244/138 R
3,117,752	1/1964	Gillmore	244/138 R
3,181,821	5/1965	Webb	244/138 R
3,195,686	7/1965	Johnson	244/138 R
3,387,805	6/1968	Barnett et al.	244/138 R
4,779,824	10/1988	Leger	244/137.3

FOREIGN PATENT DOCUMENTS

467259	8/1950	Canada	244/138 R
2373392	8/1978	France	244/138 R

Primary Examiner—Joseph F. Peters, Jr.
Assistant Examiner—Carla Mattix
Attorney, Agent, or Firm—Peter A. Taucher; David L. Kuhn

[57] **ABSTRACT**

The invention is a carrier for use in air dropping cargo from an aircraft, the carrier comprising a pallet suspended from a parachute. The pallet has struts which absorb shock and prevent cargo roll over when the pallet lands, the struts being deployed into a shock absorbing, anti-roll-over position by the drag of the parachute when it opens. The pallet includes shock absorbing supports between its upper and lower surfaces to further protect air dropped cargo upon landing.

3 Claims, 2 Drawing Sheets

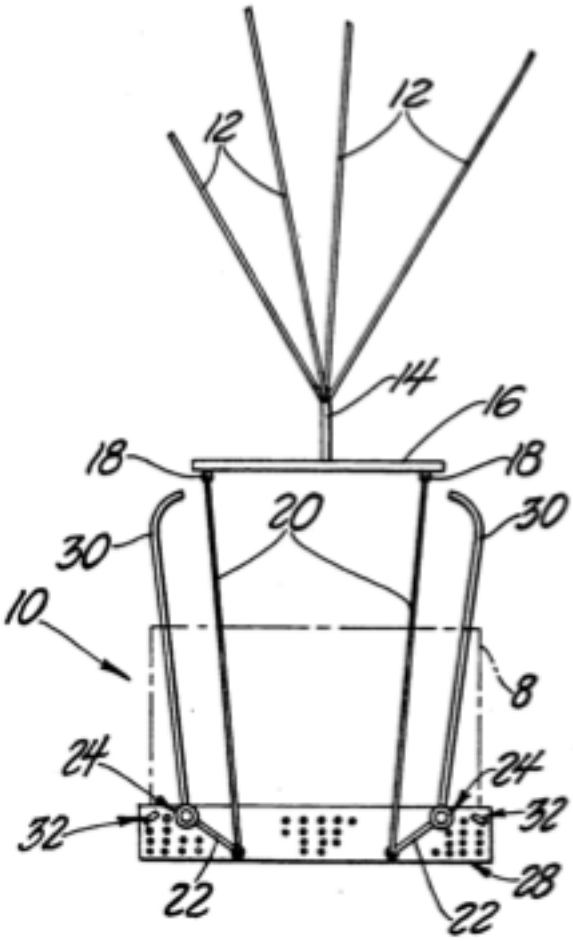

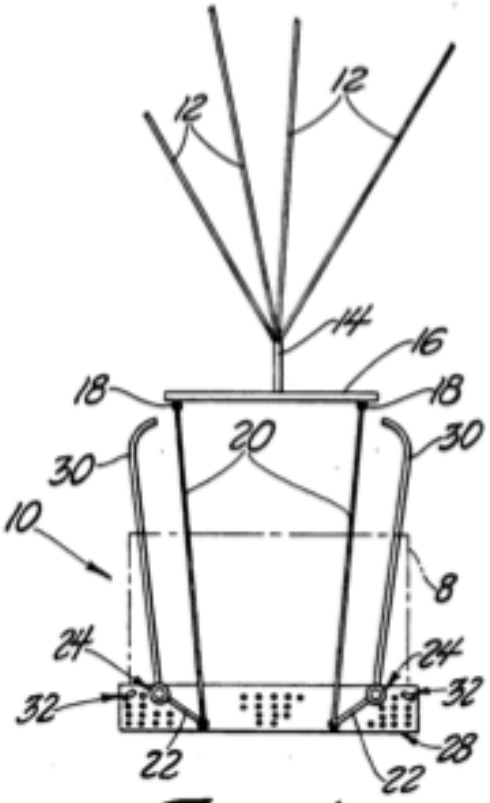

Fig. 1

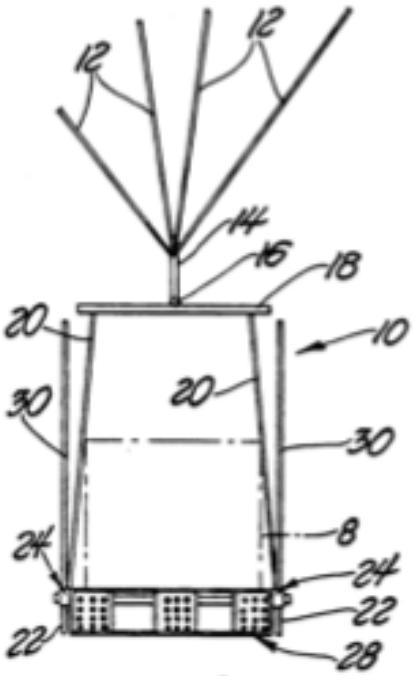

Fig. 2

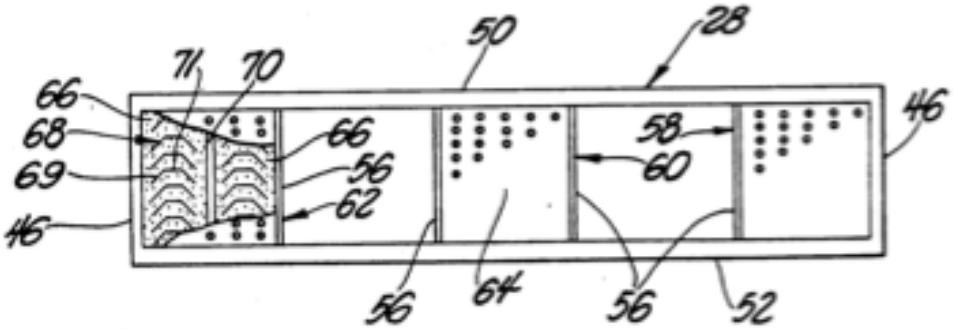

Fig. 3

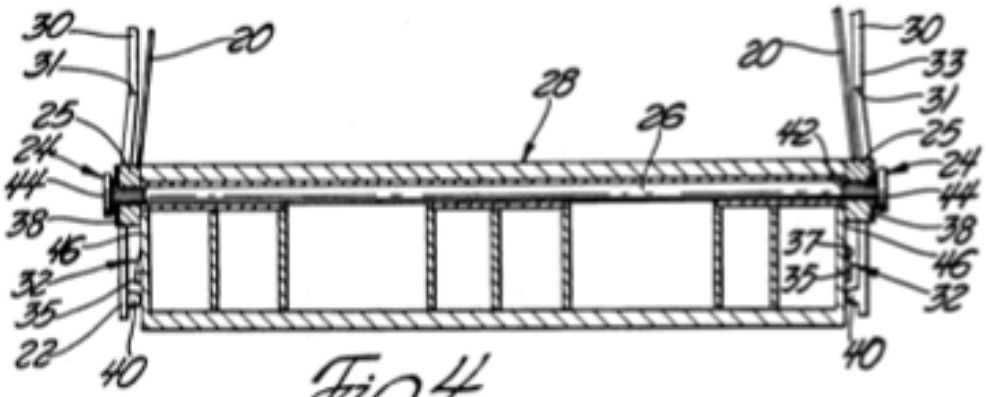

Fig.4

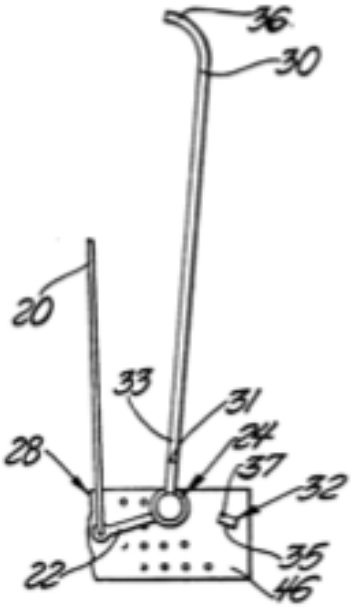

Fig.5

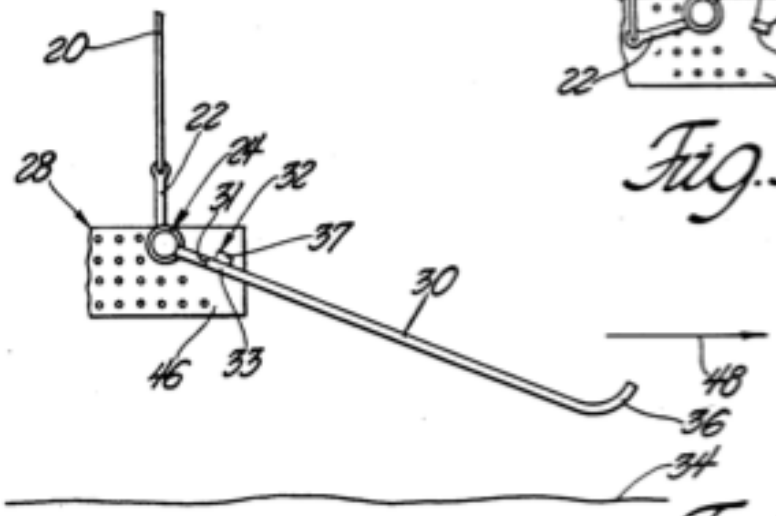

Fig.6

ENERGY ABSORBING AIR DROP PALLET

GOVERMENT INTEREST

The invention described herein may be manufactured, used, and licensed by or for the U.S. Government for governmental purposes without payment to me of any royalty thereon.

BACKGROUND AND SUMMARY

One of the problems encountered when parachuting or air dropping supplies is impact damage to the air dropped material when it hits the ground. A particular problem experienced by the U.S. Army during air drop operations is the rolling over of palletized cargoes such as artillery guns or vehicles once these cargos strike the ground.

My invention is an air-drop cargo carrier having a pallet whose design enhances its ability to absorb impact shock and deter rolling over of palletized loads. The components of my carrier which enhance these abilities take virtually no cargo space of an aircraft and the weight of these components is negligible compared to the weight capacity of the pallet.

The pallet has struts which deploy outward and downward from the pallet to absorb impact shock and inhibit cargo roll over. The carrier also has a mechanism for using the upward force on the parachute lines to effect strut deployment when the parachute opens. The pallet has elongate supports of reinforced elastomeric material, which deform in a controlled manner to absorb impact shock when the pallet lands.

BRIEF DESCRIPTION OF THE DRAWINGS

FIG. 1 is a side elevational view of an air drop carrier, the parachute being omitted for convenience.

FIG. 2 is an end elevational view of the air drop carrier, the parachute again being omitted for convenience.

FIG. 3 is an end elevational view of the pallet of the air drop carrier, a part of the pallet being removed to show the interior structure of a pallet support.

FIG. 4 is sectional end view of the pallet showing further internal structure of the pallet and showing elements of the strut deployment mechanism.

FIGS. 5 and 6 show the undeployed and deployed positions, respectively, of the strut.

DETAILED DISCLOSURE

Shown in FIGS. 1 and 2 is an improved carrier 10 for an air-dropped cargo or load 8, the carrier being suspended from lines 12 of a set of parachutes (not shown). Lines 12 attach at their lower ends to a short vertical post 14 fixed normally to spacer bar 16, there being two cross bars 18 perpendicularly attached at the ends of the spacer bar to form an H-like spider frame therewith. At the ends of cross bars 18 are attached the upper ends of cables 20, the cables being secured at their lower ends to levers 22, which in turn are fixed to axle head assemblies 24. Assemblies 24 are fixed to the ends of shafts or axles 26 (FIG. 4) rotatably mounted in pallet 28. Axles 26 will rotate about their longitudinal axes, so that head assemblies 24 and levers 22 will also rotate about these axes when cables 20 pull upward on levers 22. Fixed to head assemblies 24 and forming obtuse angles with levers 22 are deployable struts 30, which rotate in concert with the levers. The struts and levers preferably define an

angle of between 90 degrees and 180 degrees with one another.

Struts 30 can be rotated from their essentially vertical undeployed position of FIG. 1 to a deployed position where the struts extend outward and downward from pallet 28, as demonstrated in FIG. 6. Once strut 30 reaches the FIG. 6 position, it is prevented from rotating upward by a suitable means such as keeper 32, whereby strut 30 absorbs shock when carrier 10 arrives at landing surface 34. It is contemplated that the strut will strike surface 34 with its curved foot 36, which is the portion of the strut most distal from pallet 28. It is preferred that strut 30 be made of flexible material so that the strut will act as a cantilever spring once foot 36 strikes the ground.

When carrier 10 is descending toward surface 34, it may also have a horizontal component of motion 48 because of wind conditions at the time of the air drop. This horizontal component of motion results in a tendency of the carrier and its load to tilt in the direction of the horizontal component when the carrier strikes surface 34. Because of the shock absorbing qualities of pallet 28, which are discussed later, it is preferred that pallet be tilted as little as possible relative to surface 34 when carrier 10 strikes this surface. The curved feet 36 alleviate this problem by causing strut 30 to act similar to a runner on a sled, so that the leading edge of carrier 34 does not dig into surface and instead the carrier 10 slides horizontally over the surface. The strut's contact with the ground also tends to return the pallet to a level position, thereby inhibiting roll over of the pallet and cargo upon landing.

Further details of head assembly 24 are shown in FIG. 4. Disposed on axle 26 between internally toothed hub 25 and axle end 44 is an annular spring 38, which can be a bellville washer. Splines 42 at the ends of axle 26 are complimentary with the internal teeth of the hubs 25, whereby the hubs can translate along the ends of the axle. When strut 30 rotates from its FIG. 5 position to its FIG. 6 position, an engagement zone 33 adjacent elbow 31 of the strut follows a rotational path. As zone 33 travels along this path, it engages camming surface 37 on the outboard side of keeper 32. Zone 33 slides against the camming surface so that strut 30 and hub 25 translate outboard from the pallet, whereby spring 38 is compressed. After engagement zone 33 passes keeper 32, spring 38 snaps hub 25 and strut 30 inboard so that engagement zone 33 translates inboard along blocking surface 35 of keeper 32. Engagement zone 33 arrives at a position immediately below and abutting surface 35 and immediately adjacent outboard side 46 of the pallet. As seen in FIG. 6, keeper 32 then prevents strut 30 from rotating counterclockwise and tension on cable 20 will prevent clockwise rotation of the strut until pallet 28 impacts surface 34. To keep strut 30 and head assembly 24 in their FIG. 5 positions until the parachute is deployed, a flexible contact boss 40 frictionally engages the outboard sidewall 46 of the pallet during the FIG. 5 position.

FIG. 3 is a partial sectional end view of pallet 28 showing the structural details thereof. Pallet 28 has a top or upper surface 50, a bottom or lower surface 52 and flexible sidewalls 46. Between the top and bottom of pallet 28 and extending along the length thereof are elongate supports 58, 60 and 62, each support having a perforated end panel as at 64 which allow passage of air. Although omitted for convenience from FIG. 3, there are air passing perforations in sidewalls 46 and flexible

United States Patent [19]

Auth

[11] **4,078,837**

[45] **Mar. 14, 1978**

[54] **ENERGY ABSORBING BUMPER**

[75] Inventor: **Paul Auth**, Bricktown, N.J.

[73] Assignee: **Action Research Development Corporation**, Bricktown, N.J.

[21] Appl. No.: **638,501**

[22] Filed: **Dec. 8, 1975**

Related U.S. Application Data

[63] Continuation-in-part of Ser. No. 523,319, Nov. 13, 1974, abandoned.

[51] **Int. Cl.**[2] **B61F 19/04**

[52] **U.S. Cl.** ..... **293/71 R**; 213/1 A

[58] **Field of Search** ..... 293/1, 60, 70, 71 R, 293/85, 88, 89, 62, 63, DIG. 3; 188/1 C; 213/1 A

[56] **References Cited**

U.S. PATENT DOCUMENTS

2,732,040	1/1956	DeVost et al.	293/85
3,284,122	11/1966	Rich	213/1 A X
3,494,607	2/1970	Rusch	293/71 R X
3,610,609	10/1971	Sobel	293/63 X
3,724,833	3/1971	Sergay	293/88 X
3,752,462	8/1973	Wight, Jr.	293/88 X

Primary Examiner—Joseph F. Peters, Jr.
Assistant Examiner—Norman L. Stack, Jr.
Attorney, Agent, or Firm—Lerner, David, Littenberg & Samuel

[57] **ABSTRACT**

An energy absorbing bumper for attachment to vehicles, such as automobiles, is disclosed. The energy absorbing bumper includes a low density foamed plastic having a semi-rigid cellular structure, so that upon impact greater than a pre-determined minimum impact the energy absorbing material collapses, and absorbs substantially the entire impact, without any increase in its density. In particular, low density foamed plastics, such as urethane, are empolyed, having a density of less than 7 pounds per cubic foot. The bumper disclosed includes means for permitting collapse of the foamed plastic without any substantial increase in its density, so that the plastic itself absorbs substantially the entire force of impact upon the bumper.

7 Claims, 10 Drawing Figures

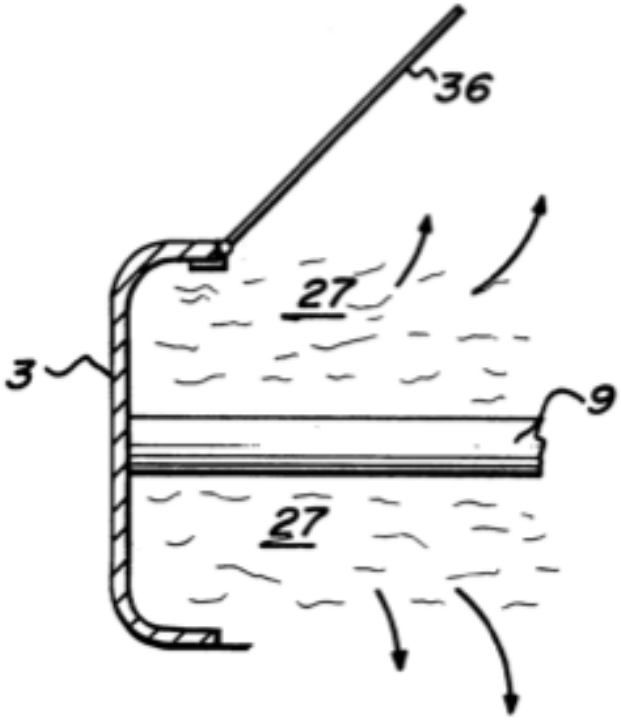

FIG. 1

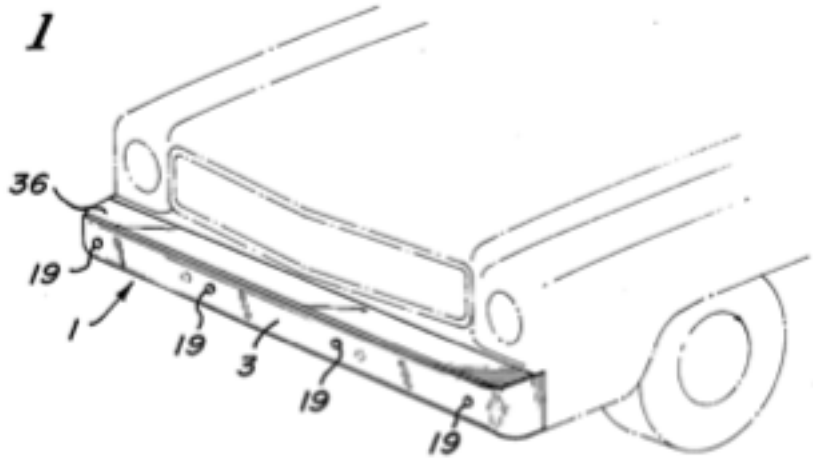

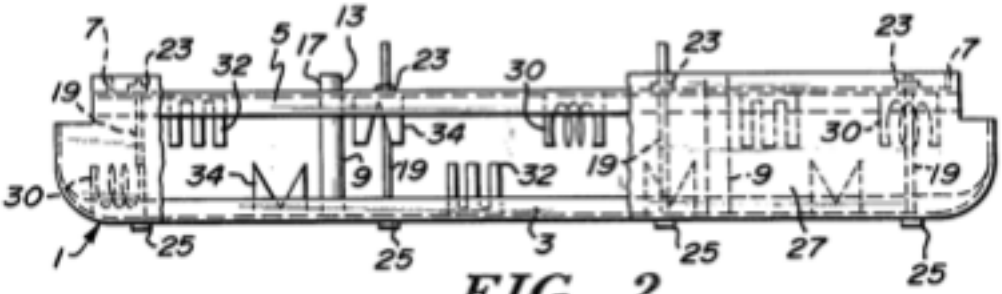

FIG. 2

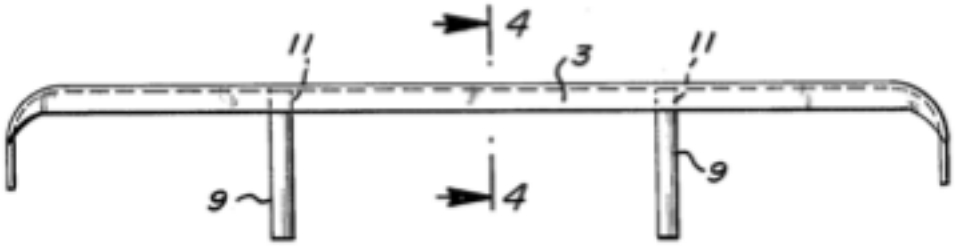

FIG. 3

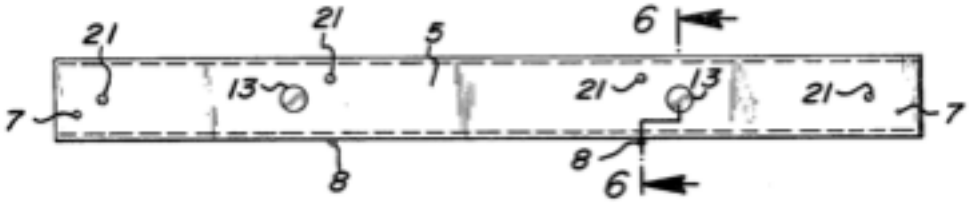

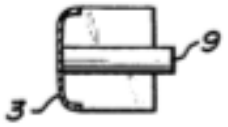

FIG. 4

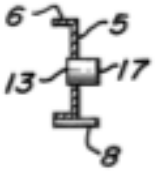

FIG. 6

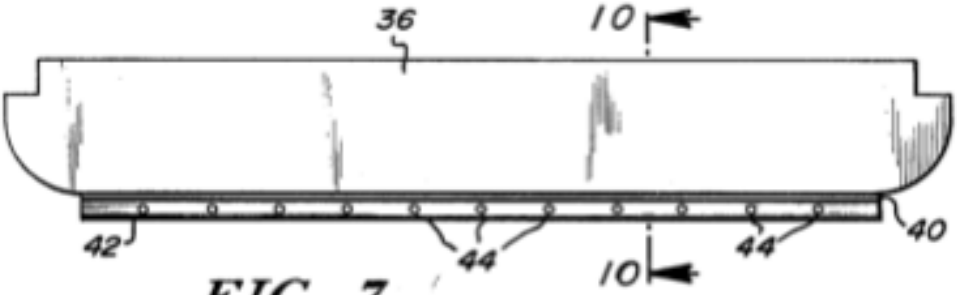

FIG. 7

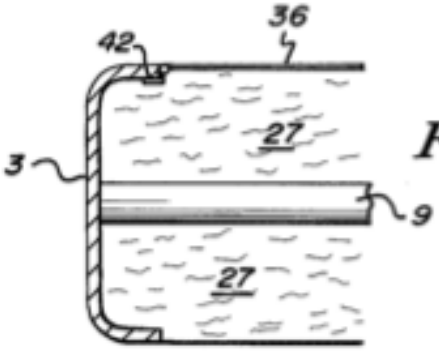

FIG. 8

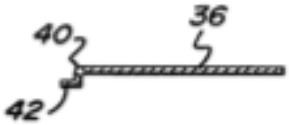

FIG. 10

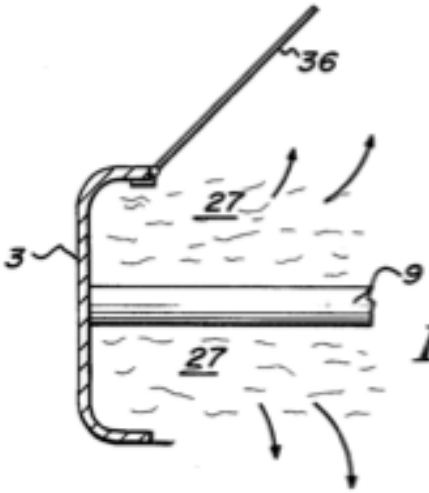

FIG. 9

ENERGY ABSORBING BUMPER

CROSS REFERENCES TO RELATED APPLICATIONS

This application is a continuation-in-part of application Ser. No. 523,319, filed on Nov. 13, 1974, now abandoned.

FIELD OF THE INVENTION

The present invention relates to energy absorbing bumpers for attachment to vehicles, such as automobiles.

More particularly, the present invention relates to such energy absorbing bumpers which are capable of withstanding severe impact without consequent damage to the vehicles to which they are attached.

Still more particularly, the present invention is concerned with energy absorbing bumpers containing energy absorbing materials which can absorb large amounts of energy.

BACKGROUND OF THE INVENTION

With the continued development of vehicles capable of traveling at greater and greater speeds, there has been a continuing attempt to develop bumpers and other means to protect the vehicle body from damage upon impact. Many such bumpers have been developed in the past, but each is capable of only withstanding limited amounts of impact pressure without imparting substantial damage to the vehicle body.

For example, devices such as that disclosed in U.S. Pat. No. 1,438,177 to Hatashita have employed springs and other means for the temporary absorption of shocks imparted to the outer surface of bumpers, such that the spring then immediately returns to its initial position subsequent thereto. For this reason, as soon as the impact is greater than the tension on the spring, damage is caused to the front part of the automobile, as shown therein.

Furthermore, other such bumpers, including water-filled bumpers and hydraulic shock absorbers, of relatively high cost, have also been developed. Such bumpers, which normally cannot withstand impacts of greater than about 5 miles per hour, have thus led to the need for further developments. U.S. Pat. No. 3,694,019 to Carter discloses an energy absorbing bumper which can allegedly withstand low speed collision damage (approximately 5 miles per hour) and which relies upon the realignment of the molecules in certain synthetic thermoplastic materials during elongation to do so. These materials thus must be capable of being permanently elongated. Thus, when employing such a device, not only is a complex structure required, but after a single such impact complex methods for readjusting the device and removing the stretched material and replacing it with new material is required.

For these and other reasons there have been various attempts to employ new materials, and particularly various foamed plastic materials, for such purposes. Thus, U.S. Pat. No. 3,610,609 to Sobel discloses a deformable shock-absorbing bumper guard. The specific device of this patent includes both an encased rigid crushable cellular material and a flexible compressible material which returns to its normal position after impact. The encased crushable material of Sobel is " . . . totally encased . . . " in a housing, thus " . . . assuring density buildup upon impact of collision." Furthermore, the resilient material, or rubber, of this patent is intended to return to its normal dimensions when the colliding vehicle or body is removed.

Furthermore, U.S. Pat. No. 3,493,257 to Fitzgerald, et al, teaches an encased micro-cellular foam bumper including an inner high density foam material and an outer elastomeric coating thereon. This bumper is again intended to ". . . return to its original configuration . . . " after impact. Furthermore, the foamable material is cured to produce a tough elastomeric micro-cellular foam having a density of from 25 to 60 pounds per cubic foot, and which is integrally bonded to the elastomeric film thereabout.

In addition, U.S. Pat. No. 3,666,310 to Burgess, et al. is another shock absorbing bumper which includes a foamed plastic material therewithin. The patentee therein again teaches the necessity of employing high density foams, and particularly such foams which are "tight" foams having ". . . between about 90 and about 99% of the cells being of the open type . . . " The specific polyurethane foam employed by Burgess, et al. has a material density of over 7 pounds per cubic foot and preferably between 10 and 20 pounds per cubic foot, and is again encased within a rigid bumper assembly, or in certain embodiments by a high density skin, as in the prior Fitzgerald et al. patent. Again, therefore, the increase in density of the foam material during impact is also contemplated by this patentee.

Finally, U.S. Pat. No. 3,721,433 also to Sobel, teaches another deformable shock-absorbing guard for attachment to automobiles, this particular guard including an encased foamed plastic material, and preferably including different density components allegedly further aiding in accomplishing safe deceleration. The patentee thus employs various open cell rigid crushable foam-like materials, in addition to an 8 pound per cubic foot fine rigid and crushable closed cell foam-like material therein. The patentee specifically notes that these components are "completely enclosed and sealed in the housing."

It is therefore an object of this invention to provide an energy absorbing bumper which overcomes all of these deficiencies on such prior art bumpers.

SUMMARY OF THE INVENTION

In accordance with the present invention, it has now been discovered that a highly improved energy absorbing bumper for attachment to motor vehicles, such as automobiles, trucks, etc., can be prepared by including a specific energy absorbing material between the main body of the vehicle and the point of impact in a particular bumper structure, so that upon more than a predetermined minimum amount of impact the energy absorbing material collapses and the main vehicle body is thereby protected. Specifically, a low density plastic foam material which includes void spaces is employed, so that upon an impact of greater than a predetermined minimum impact this specific energy absorbing material collapses. This is accomplished by permitting the foamed plastic material to be free to escape, so that there is substantially no density increase in the foamed plastic material during its collapse. This results in the absorption by this material of substantially all of the energy so imparted, and without the subsequent transfer or release of that energy.

In one embodiment, the low density foamed plastic material has a semi-rigid cellular structure, and is preferably relatively inelastic, particularly as compared to

US 20140239684A1

(19) United States

(12) Patent Application Publication

Mindel et al.

(10) Pub. No.: US 2014/0239684 A1

(43) Pub. Date: Aug. 28, 2014

(54) **SAFETY SEAT**

(71) Applicant: **MOBIUS PROTECTION SYSTEMS LTD.**, Holon (IL)

(72) Inventors: **Shy Mindel**, Kibutz Bahan (IL.); **Anan Hassan**, Julis (IL.); **David Engel**, Yavne (IL.)

(21) Appl. No.: **14/347,877**

(22) PCT Filed: **Sep. 27, 2012**

(86) PCT No.: **PCT/IL2012/000351**

§ 371 (c)(1), (2), (4) Date: **Mar. 27, 2014**

Related U.S. Application Data

(60) Provisional application No. 61/539,520, filed on Sep. 27, 2011.

Publication Classification

(51) **Int. Cl.**

B60N 2/427 (2006.01)

B60N 2/42 (2006.01)

(52) **U.S. Cl.**

CPC ***B60N 2/42736*** (2013.01); ***B60N 2/4214*** (2013.01)

USPC **297/216.18**; 248/636

(57) **ABSTRACT**

An energy absorbing device for carrying a passenger seat; the device comprises a base fixed to a vehicle; a member displaceable from base; at least one energy-absorbing arrangement interconnecting base and displaceable member. The energy-absorbing arrangement comprises a plastically deformable absorbing element in response to stresses greater than a predetermined threshold stress. In some embodiments the plastically deformable absorbing element is a helically configured ribbon having spaced-apart ribbon laps. In other embodiments the plastically deformable absorbing element is compressible, and/or extendable. A method of attenuating the acceleration applied to a passenger due to impact is disclosed; the method comprises steps of: providing an energy absorbing device fixedly attaching the base to the vehicle; fixedly attaching the passenger seat to the base; accidently applying the impact to the vehicle; displacing the displaceable member relative to the base; attenuating the effect of the impact on the passenger.

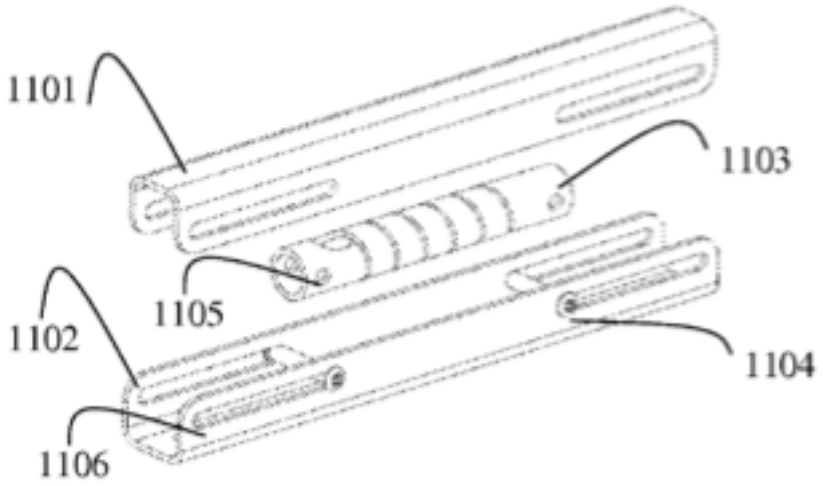

SAFETY SEAT

FIELD OF THE INVENTION

[0001] The present invention relates to a passenger safety seat for use in vehicles or other mobile applications, designed to limit horizontal occupant accelerations.

BACKGROUND OF THE INVENTION

[0002] In vehicle collisions a chief cause of injury is the extreme impulses experienced; the human body has a limited ability to cope with accelerations experienced over given durations of time. For example, the US Federal Motor Vehicle Safety Standards specify maximum allowable measures listed in FIGS. **1***a* and **1***b*.

[0003] To lower the maximum impulse experienced, the distance through which the body travels when changing its initial to final velocity must be increased, or equivalently, the time during which the acceleration is experienced must be increased. For example, in a head-on collision of a vehicle with a rigid wall, the occupant's body will undergo a change from the vehicle's initial speed to zero speed within a certain distance. The acceleration undergone is determined by the initial velocity and this distance. If this distance can be increased, the acceleration will be decreased. Care must be taken that the passengers will experience the maximum possible acceptable impulse or less, which can be accomplished by use of energy-absorbing elements of suitable design, devices to increase the travel available to the occupant, or both. The ideal energy absorber connecting a passenger to the rest of a vehicle transmits the maximum acceptable stress to the occupant or less, reaching this level after a minimum of travel. It would transmit this level of stress and no more, no matter the level of stress imparted to it.

[0004] Solutions known from the prior art provide shock absorbing seats based on different types of elastic or plastic deformation or breakage of metallic components, collapsible bar mounts or columns made of metals and/or composite materials, crushable honeycomb, etc. Some available solutions present a full system including both an original seat and a built-in integrated absorbing mechanism.

[0005] U.S. Pat. No. 5,685,603 discloses an apparatus for a vehicle includes a child seat for holding a child. A support device supports the child seat on a seat of the vehicle for movement relative to the seat during a collision in which at least one condition exceeds a predetermined threshold. An energy absorbing device absorbs kinetic energy of the child and the child seat during such relative movement. The support device may include support bars that permit sliding movement of the child seat relative to the support bars and the vehicle seat. Several types of energy absorbing devices may be used, including compressible bellows, cut able strips of sacrificial material, crushable pieces of sacrificial material, deformable projections, a payout device with webbing, compressible shock absorber assemblies, and slid able frictionally engaging portions.

[0006] U.S. Pat. No. 5,152,578 a front leg is formed by an upright support rod extending vertically above a fixing stud, a rear leg is formed by both a lower support rod extending on a diagonal line joining the upper end of the front leg and the lower end of the rear leg and an upper support rod contiguous to the lower support rod in an upper position relative to the lower support rod, the upper support rod being curved accurately and inclined rearward and upwards, and an energy absorber is mounted bridge wise as a diagonal member between the upper end portion of the front leg and the lower end portion of the rear leg, to constitute a leg structure. Accordingly to this leg structure, a striking energy is absorbed by an anti-plastic deformation force induced when the rear leg and the energy absorber is deformed plastically under an impact larger than a predetermined value, and the seat is held at its supported posture in normal use. This leg structure can be utilized not only in aircraft but also in automobiles and railway vehicles.

[0007] A major difference between the current invention and the prior art is the ability to determine the exact position of the system under any give load and direction of the load. In the prior art, different impacts will apply different forces on the energy absorbing components. Greater load applied on the rear leg, will change the orientation of the seat differently than forces applied mainly on the front leg.

[0008] The change in orientation will affect the forces transferred to the occupant from the energy absorbing components (legs and cylinder).

[0009] Thus, if a simple, analytical and repeatable system is desired with optimized energy absorption mechanism, it is better to use a system with only one deforming component (i.e. spiral).

[0010] Designing a system with specific force-deflection curve which transfers predetermined forces to the occupant requires careful design of the mechanism and the use of a highly controllable EA element such as the spiral.

[0011] US Patent application 20030209926 discloses a child seat device formed of a base to be placed on a seat of a car, a child seat body placed on the base, and a connecting member for connecting a rear bottom of the child seat body to a fixed portion. The connecting member increases a length thereof while absorbing a kinetic energy of the child seat body when a tension higher than a predetermined value is applied thereto from the child seat body.

[0012] Hence there is a long felt and unmet need to provide a simple and cheap vehicle passenger safety seat which absorbs energy in tension and compression suitable for mass production.

SUMMARY OF THE INVENTION

[0013] It is hence one object of the invention to an energy absorbing device adapted for carrying a passenger seat. The aforesaid device comprises (a) a base fixedly attached to a pre-existing vehicle; (b) a member displaceable relative to the base; and (c) at least one energy-absorbing arrangement interconnecting the base and displaceable member.

[0014] It is a core purpose of the invention to provide the energy-absorbing arrangement comprises a plastically deformable absorbing element in response to stresses greater than a predetermined threshold stress.

[0015] Another object of the invention is to disclose the plastically deformable absorbing element which is a helically configured ribbon having spaced-apart ribbon laps.

[0016] A further object of the invention is to disclose the plastically deformable absorbing element which is compressible or extendable.

[0017] A further object of the invention is to disclose the base connected to the vehicle by means of a connector meeting ISOFIX 13216.

[0018] A further object of the invention is to disclose the energy-absorbing arrangement comprising a hingely interconnected four-bar sub-arrangement configured be reshaped

Appendix I: Copy of Senior Design Conference Presentation Slides

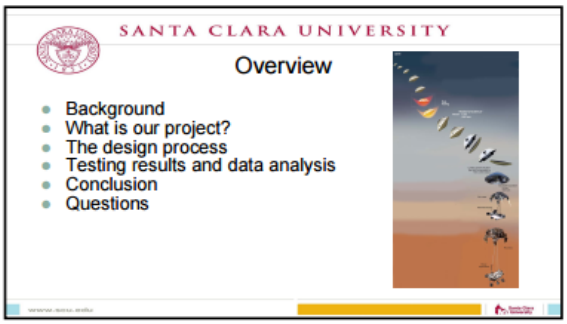

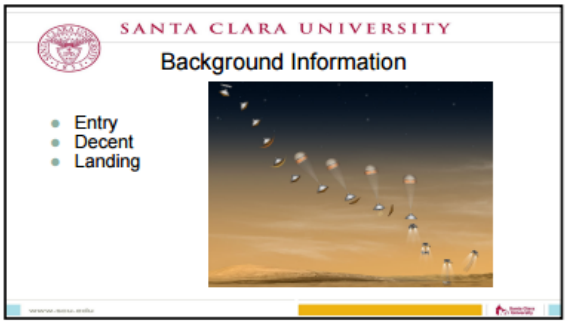

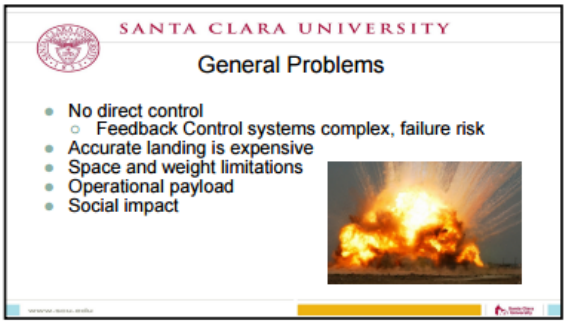

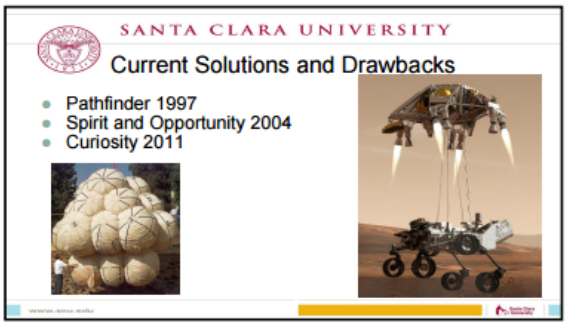

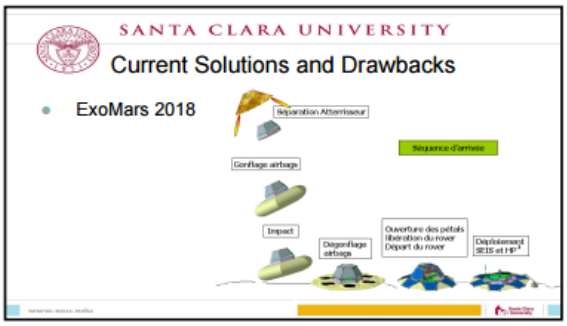

SANTA CLARA UNIVERSITY

Mission Statement

To design, build, and test a landing capsule test article that incorporates external crushable impact dampening in tandem with an internal suspension.

SANTA CLARA UNIVERSITY

Our Objective

- Low risk–Passive landing (No feedback control)
- Deliver a functioning payload
- Low cost
- High Accuracy

SANTA CLARA UNIVERSITY

Quantifying the Problem

- Cost Increase for Curiosity
  - Spirit/Opportunity $400 million each
  - Curiosity $2.5 billion
- Curiosity Accuracy Increase
  - Spirit/Opportunity 28 bounces 1km distance
  - Curiosity 0 bounces, perfectly accurate

SANTA CLARA UNIVERSITY

Design Requirements: Finding Parameters

- Scaling and comparing our design
  - Impact velocity is 13.89 m/s
  - Drop height 12.19 m
  - Mass of 533 kg
- Energy dissipated 51,416.4 J
  - Kinetic Energy = ½ mv^2

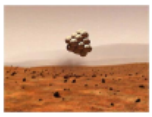

SANTA CLARA UNIVERSITY

Design Requirements: Finding Parameters

- Handling and testing constraints:
  - Desired weight < 50kg
  - Desired volume 1 m^3
  - Drop height < 4th story (12m)
- Potential Energy = mgh = 5,980.18 J
- Goal of 5,141.6 J
  - 10% of Spirit's impact energy
  - Required mass for final design is 43 kg
  - Test data → scale up design

SANTA CLARA UNIVERSITY

Design Process

- System level issues
- Priority matrix
- Brainstorming
- Sketching
- Design rating matrix
- Design decision

SANTA CLARA UNIVERSITY

Key Systems Level Issues

- Frame Geometry
  - What frame shape do we want for impact landing?
- Shock Absorption
  - How do we want to absorb energy?
- Landing Position
  - What final orientation do we want after impact for the rover to exit the capsule?

SANTA CLARA UNIVERSITY

Priority Matrix

	Criterion	1	2	3	4	5	6	7	8	9	SUM	FACTOR
1	Weight		1	1	0	0.5	1	0	0	0	3.5	10
2	Size	0		1	0	0.5	1	0	0	0	2.5	10
3	Aesthetics	0	0		0	0	0	0	0	0	0	1
4	Shock Absorption	1	1	1		1	1	1	1	0	7	75
5	Cost	0.5	0.5	1	0		1	0	0	0	3	10
6	Battery Life	0	0	1	0	0		0	0	0	1	5
7	Accuracy	1	1	1	0	1	1		0	0	5	35
8	Reliability	1	1	1	0	1	1	1		0	6	50
9	Safety	1	1	1	1	1	1	1	1		8	100

Highest Number Factor = Highest Priority

SANTA CLARA UNIVERSITY

Design Rating Matrix

CRITERIA	TARGET or FACTOR	DESIGN IDEAS: Pyramid External Crushable/ Floating Frame Springs		Pyramid External Crushable and Springs		Cylinder Design		Egg Design		Pyramid Bottom Crushable/ Floating Frame Springs		Pyramid Bottom Crushable/ Floating Frame Foam	
Time – Design		3		4		2		1		4		3	
Time – Build		3		4		2		1		4		3	
Time – Test		3		3		3		3		3		3	
Time Score	10		10		34.67		23.33		16.67		36.67		45.33
Weight	10	3	30	2	20	4	40	2	20	4	40	4	40
Size	10	3	30	2	20	4	40	2	20	4	40	4	40
Aesthetics	1	3	3	2	2	4	4	4	4	4	4	4	4
Shock Absorption	75	3	225	3	225	4	300	4	300	3	225	3	225
Cost	10	3	30	2	20	2	20	1	10	3	30	3	30
Battery Life	5	3	15	3	15	3	15	3	15	3	15	3	15
Accuracy	35	3	105	2	70	4	140	2	70	3	105	4	140
Reliability	50	3	150	3	150	2	100	3	150	3	150	4	200
Safety	100		300		200		300		300		300		300
	TOTAL		884.4		772		839		890.4		909.4		994.4
	RANK												
	% MAX		89.3%		77.9%		84.7%		89.9%		91.8%		100.0%

SANTA CLARA UNIVERSITY

Creative and Innovative Design Decision

- Pyramid shape
- Crushable base
- Internal suspension system for rover protection
- All door petals open after impact

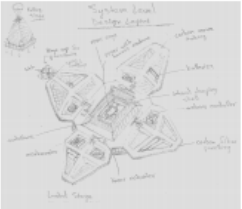

SANTA CLARA UNIVERSITY

First Mockup

- RC car restraining system
- Gap between the car level and petals

SANTA CLARA UNIVERSITY

Final Design

SANTA CLARA UNIVERSITY

Suspension Design

- Wanted to utilize bicycle shocks
  - Problem: Each designed for 80 kg person, need 4 for symmetry
    - Predicted capsule weight: 43kg
  - Original suspension design

SANTA CLARA UNIVERSITY

Suspension Design

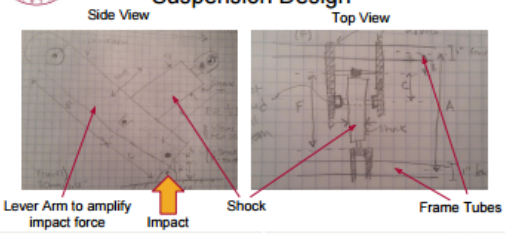

SANTA CLARA UNIVERSITY

Suspension Design

- DNM-22 bicycle shock:
  - compact
  - dashpot/damping + spring
- Two-fold advantage
  - Each shock will experience forces as designed
  - Total travel is doubled
- 4 of these assemblies used

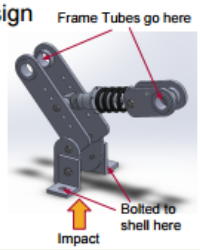

SANTA CLARA UNIVERSITY

Full Solidworks Model

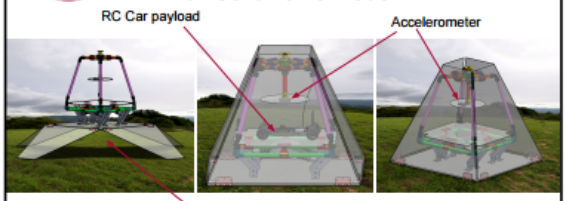

SANTA CLARA UNIVERSITY

Crushable Material Testing

- Pendulum test
- Energy absorbed
- Free Body Diagram

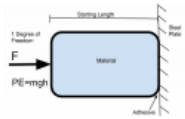

SANTA CLARA UNIVERSITY

Material Testing

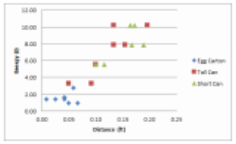

- Energy absorbed by each material
- Distance material crushed during impact

SANTA CLARA UNIVERSITY

Acceleration of Pendulum

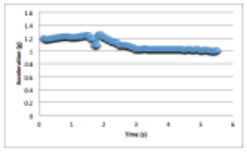

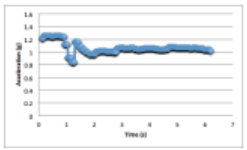

- Potential Energy of 7.54J
- Potential Energy of 20.10J

SANTA CLARA UNIVERSITY

Linear Approximation

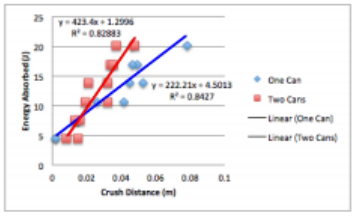

- Deformation is relatively linear
- Assumption: Adding more cans increases the buckling force linearly

SANTA CLARA UNIVERSITY

Cylindrical Shell Buckling Model

- Failure analysis of can model
  - Cylindrical shell buckling
- Assume perfect plastic deformation
  - Constant force
    - Energy absorption/dissipation
    - Time to buckle
    - Expected acceleration

SANTA CLARA UNIVERSITY

Cylindrical Shell Buckling Model

$$D = \frac{Et^3}{12(1-\mu^2)}$$

$$Z = \frac{l^2}{rt}\sqrt{1-\mu^2}$$

$$k_x = \frac{4\sqrt{3}}{\pi^2}\gamma Z$$

$$N_x = k_x \frac{\pi^2 D}{l^2}$$

- Wall flexural stiffness per unit width
- Curvature parameter for isentropic cylinder
- Buckling coefficient of a cylinder subject to axial loading
- Axial load per unit circumference

$$\gamma = 1 - 0.901(1 - e^{-\phi})$$

$$\phi = \frac{1}{16}\sqrt{\frac{r}{t}} \quad for \left(\frac{r}{t} < 1500\right)$$

- Correction factor

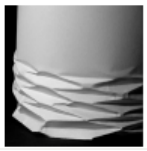

SANTA CLARA UNIVERSITY

Cylindrical Shell Buckling Analysis Results

- Force required to buckle one can:
  - Gradual Load: $N_x l = 1582\ N$ Impact Load: $\frac{N_x l}{2} = 791\ N$
- Energy absorbed by one can: $\frac{N_x l}{2} * L = 97\ J$
- Cans required to absorb 10% of the force of impact Spirit capsule assuming evenly crushed:

$$\#\ cans = \frac{5142\ J}{97\ J} = 53\ cans$$

SANTA CLARA UNIVERSITY

Frame Stress Analysis

Force applied was calculated from using 10% of impact energy of the Spirit capsule and knowing the distance over which the impact happened.

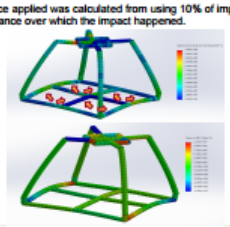

Loading caused by orientation of suspension

Weldments: ¾" nominal pipe size, sch 40 pipe

Yield Stress: 275 MPa

Analysis

Max Bending Stress: 130 MPa FOS ~ 2
Max Shear Stress: 12 MPa FOS ~ 23
Max Deflection: 0.02mm
No Failure

SANTA CLARA UNIVERSITY

Dynamic Suspension Analysis

- Performed a dynamic analysis on the suspension to predict how it would react to impact

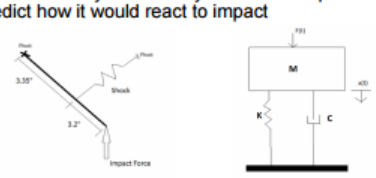

SANTA CLARA UNIVERSITY

Dynamic Suspension Analysis

- Simulink Code used to model, excited by an impulse

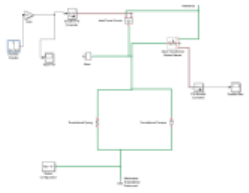

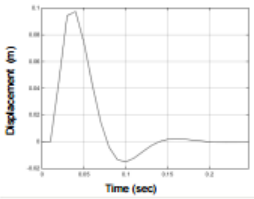

SANTA CLARA UNIVERSITY

First Test Mockup

- Accelerometer functionality
- Stiff base
- Better can adhesive

SANTA CLARA UNIVERSITY

Building the Final Test Article

- Used machine shop at SCU and SVG

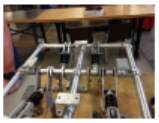

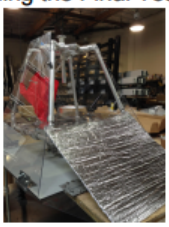

SANTA CLARA UNIVERSITY

Health and Safety

- Caution tape
- Educated public
- Hard hats, safety glasses, harness

SANTA CLARA UNIVERSITY

Testing Procedure

- Secure test article with quick release
- Check accelerometer functionality
- Lift test article to predetermined height
- Initiate drop with quick release
- Collect data
- Inspect and remove crushable base
- Recycle base sustainably
- Repeat 10, 20, 40 ft

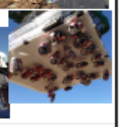

SANTA CLARA UNIVERSITY

Testing Procedure

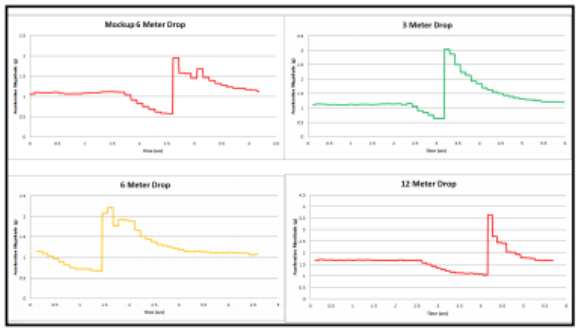

SANTA CLARA UNIVERSITY

Results

- Accelerometer Settings:
  - QCOMP filter: 185 Hz Sampling rate
  - Measured Corrected acceleration
- RC Car Payload worked after every test
- Capsule almost completely unbroken
  - One Cast Joint broke on last drop

SANTA CLARA UNIVERSITY

Scheduling Another Test

- Data recorded indicates insufficient sampling rate
  - Further testing to be done with higher sampling rate
  - New Accelerometer settings:
    - IMU Mode: 600 Hz sampling rate
    - Record Raw Acceleration data

SANTA CLARA UNIVERSITY

Comparing to Goal

- Model drag force as quadratic
  - c is aerodynamic constant from air properties and object coefficient of drag (due to shape)
- Solving differential equation yields v(t)
- Integrating v(t) gives y(t)

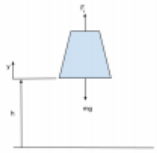

$$v(0) = 0\tfrac{m}{s}$$
$$y(0) = h$$
$$F_d - mg = ma$$
$$cv^2 - mg = m\tfrac{dv}{dt}$$
$$\rightarrow v(t) = \sqrt{\tfrac{mg}{c}}tanh[-gt\sqrt{\tfrac{c}{mg}}]$$
$$\rightarrow y(t) = \tfrac{m}{c}ln[cosh(-gt\sqrt{\tfrac{c}{mg}})] + h$$

SANTA CLARA UNIVERSITY

Comparing to Goal

- Get impact velocity from previous slide's equations
- Final mass 37.6kg
- Final impact energy 7.4% of Spirit's impact energy, near goal of 10%

	Imact Velocty	Mass	Impact Energy	% of Spirit Impact Energy
Expected	15.47 m/s	43 kg	5,141.6 J	10%
Actual	14.24 m/s	37.6 kg	3,812.2 J	7.40%

SANTA CLARA UNIVERSITY

Scaling Up Our Design

- Assume: crushable materials are evenly spaced, hollow cylinders that fail due to buckling

$$Energy\ Absorbed\ = F * d$$

- Cylinder geometry affects threshold force
- Suggested geometry for scaled up design

SANTA CLARA UNIVERSITY

Constraints from Spirit Geometry

- Approximate size of capsule is tetrahedron made from 3.45 meter equilateral triangles
- Bottom area available is 5.15 m^2
- Calculated thickness of deflated bag assembly is 0.1377 m
- Set this to length of cylinders

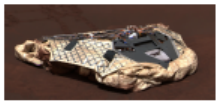

SANTA CLARA UNIVERSITY

Geometric Parameters

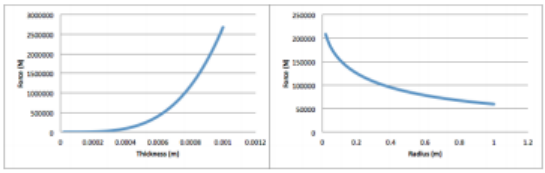

SANTA CLARA UNIVERSITY

Scaled Up Cylinder Assembly

Parameters	1nd	2rd	3th	4th	5th
Total Energy Absorbed (J)	51452.0308	51927.29126	51514.82334	51750.67172	51736.62733
Radius (m)	0.008	0.01	0.02	0.04	0.06
Thickness (m)	0.00178	0.0018	0.00184	0.00191	0.00196
# Cylinders	20000	12500	3200	800	350
Volume of Material	0.218994601	0.177148598	0.097198593	0.051618168	0.035029757
Area (m^2)	5.12	5	5.12	5.12	5.04

SANTA CLARA UNIVERSITY

Conclusion

- Design and build was a success
- RC car payload survived
- Could be used for any payload landing application: care packages, supply deliveries, etc.
- Expected completion by term's end
- IPPW Conference in Cologne, Germany for more info

SANTA CLARA UNIVERSITY

Special Thanks

- SCU School of Engineering
- Dr. Nikola Djordjevic
- Dr. Timothy Hight
- Dr. Calvin Tszeng
- Dr. Robert Marks
- Don MacCubbin
- Silicon Valley Glass Inc.
- Xchange Solutions Inc.

SANTA CLARA UNIVERSITY

Questions?

SANTA CLARA UNIVERSITY

References

Crisp, J. A., et al., Mars Exploration Rover mission, *J. Geophys. Res.*, 108, No. E12, 8061, doi:10.1029/2002JE002038, 2003.

Squyres, S. W., et al., Athena Mars rover science investigation, *J. Geophys. Res.*, 108, No. E12, 8063, doi:10.1029/2003JE002121, 2003.

Squyres, S. W., et al., The Spirit Rover's Athena science investigation at Gusev crater, Mars,*Science*, 305, No. 5685, 794-799, Aug. 2004.

Cook, R. A., The Mars exploration rover project, *Acta Astronaut.*, 57, No. 2-8, 116-123, 2005.

Arvidson, R. E., et al., Overview of the Spirit Mars Exploration Rover Mission to Gusev Crater: Landing site to Backstay Rock in the Columbia Hills, *J. Geophys. Res.*, 111, E02S01, doi:10.1029/2005JE002499, 2006.

Daggett, V. "Introduction to Special Issue 'Three Decades of Protein Engineering: Impact on Structural Biology and Therapy'" *Protein Engineering Design and Selection* 24.1-2 (2010): 1. PDH Center, 2012. Web. 10 May 2015.

NASA. "Buckling of Thin-Walled Circular Cylinders." [n.d.]: n. pag. NASA, 1968. Web. 10 May 2015.

Haynes, Williams (1949). "XVII: New Fibres: New Fabrics". *This Chemical Age*. London: Secker and Warburg. p. 217.

Seiford, S. B. "Critical Stress of Thin-Walled Cylinders in Axial Compression." *RTAW/TECH LIBRARY KAFB, NM* [n.d.]: n. pag. National Advisory Committee for Aeronautics, June 1947. Web. May 2015.

NASA. "Mars Exploration Rover Mission: The Mission." *Mars Exploration Rover Mission: The Mission*. NASA, n.d. Web. 12 May 2015.

SANTA CLARA UNIVERSITY

Material Failures

- Cast Aluminum joint
- Magnetic Closure

Appendix J: Technical Materials for Accelerometer

Technical Brief

YEI 3-Space Sensor™
Bluetooth

Miniature High-Performance Attitude & Heading Reference Systems / Inertial Measurement Units

Product Overview

The YEI 3-Space Sensor™ Bluetooth integrates a miniature, high-precision, high-reliability, Attitude and Heading Reference System (AHRS) / Inertial Measurement Unit (IMU) with a 2.4GHz Bluetooth v2.0+EDR Class 1 interface and a rechargeable lithium-polymer battery solution into a single low-cost end-use-ready unit. The Attitude and Heading Reference System (AHRS) uses triaxial gyroscope, accelerometer, and compass sensors in conjunction with advanced processing and on-board quaternion-based orientation filtering algorithms to determine orientation relative to an absolute reference in real-time.

Orientation can be returned in absolute terms or relative to a designated reference orientation. The gradient descent calibration process and high update rates increase accuracy and greatly reduce and compensate for sensor error. The YEI 3-Space Sensor system also utilizes a dynamic sensor confidence algorithm that ensures optimal accuracy and precision across a wide range of operating conditions.

The YEI 3-Space Sensor Bluetooth unit features are accessible via a well-documented open communication protocol that allows access to all available sensor data and configuration parameters using either 2.4Ghz Bluetooth or USB 2.0 interfaces. Versatile commands allow access to raw sensor data, normalized sensor data, and filtered absolute and relative orientation outputs in multiple formats including: quaternion, Euler angles (pitch/roll/yaw), rotation matrix, axis angle, two vector (forward/up).

Applications

- Robotics
- Motion capture
- Positioning and stabilization
- Personnel / pedestrian navigation and tracking
- Unmanned air/land/water vehicle navigation
- Education and performing arts
- Healthcare monitoring
- Gaming and motion control
- Accessibility interfaces
- Virtual reality and immersive simulation

Key Features

The YEI 3-Space Sensor Bluetooth has many features that allow it to be a flexible all-in-one solution for your orientation sensing needs. Below are some of the key features:

- Small self-contained high-performance wireless AHRS at 35mm x 60mm x 15mm and 28 grams
- Integrated 2.4GHz Bluetooth v2.0 EDR Class 1 wireless interface allows high-performance at ranges up to 300'
- Integrated Lithium-Polymer battery and charge control allows battery life of 5+ hours at full performance
- Fast sensor update and filter rate allow use in real-time applications, including stabilization, virtual reality, real-time immersive simulation, and robotics
- Highly customizable orientation sensing with options such as tunable filtering, oversampling, and orientation error correction
- Advanced integrated Kalman filtering allows sensor to automatically reduce the effects of sensor noise and sensor error
- Robust open protocol allows commands to be sent in human readable form, or more quickly in machine readable form
- Orientation output format available in absolute or relative terms in multiple formats (quaternion, rotation matrix, axis angle, two-vector)
- Absolute or custom reference axes
- Access to raw sensor data
- Flexible communication options: USB 2.0 or wireless 2.4GHz Bluetooth SPP (FCC Certified)
- Bluetooth SPP requires no proprietary dongle hardware
- USB 2.0 and Bluetooth SPP communication via virtual COM port
- USB joystick/mouse emulation modes ease integration with existing applications
- Upgradeable firmware
- RGB status LED, two programmable input buttons
- Available in either hand-held or screw-down packaging

YEI Technology

www.3SpaceSensor.com

High-reliability MEMS technology combined with advanced processing and multiple quaternion-based filtering algorithms allows for accurate orientation outputs across a wide range of performance conditions.

Block Diagram

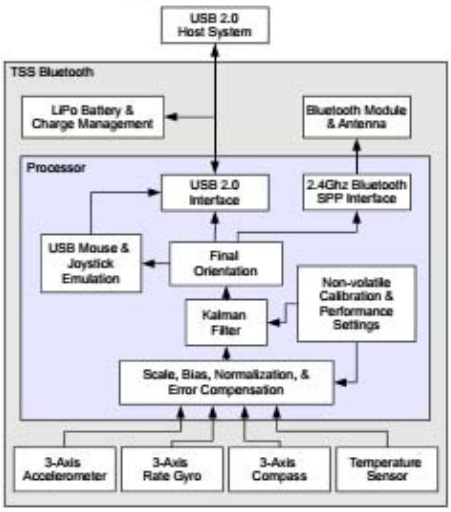

Hardware Overview

Case Dimensions

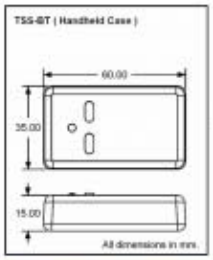

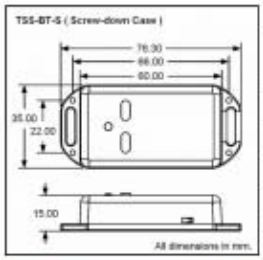

Specifications

General	
Part number	TSS-BT (Handheld Sensor Unit) TSS-BT-S (Screw-down Sensor Unit)
Dimensions	35mm x 60mm x 15mm (1.38 x 2.36 x 0.59 in.)
Weight	28 grams (0.98 oz)
Supply voltage	+5v USB
Battery technology	rechargeable Lithium-Polymer
Battery lifetime	5+ hours continuous use at full performance
Communication interfaces	USB 2.0, 2.4GHz Bluetooth SPP (FCC Certified)
Wireless communication range	up to 300' (Bluetooth v2.0+EDR, Class 1)
Filter update rate[1]	up to 250Hz USB/185Hz Bluetooth with Kalman AHRS up to 850Hz USB/420Hz Bluetooth with QCOMP AHRS up to 1350Hz USB/600Hz Bluetooth in IMU mode
Orientation output	absolute & relative quaternion, Euler angles, axis angle, rotation matrix, two vector
Other output	raw sensor data, corrected sensor data, normalized sensor data, temperature
Shock survivability	5000g
Temperature range	-40C ~ 85C (-40F ~ 185F)
Sensor	
Orientation range	360° about all axes
Orientation accuracy[2]	±1° for dynamic conditions & all orientations
Orientation resolution	<0.08°
Orientation repeatability	0.085° for all orientations
Accelerometer scale	±2g / ±4g / ±8g selectable for standard models ±6g / ±12g / ±24g selectable for HH models ±100g / ±200g / ±400g selectable for H3 models
Accelerometer resolution	14 bit, 12 bit(HH), 12 bit(H3)
Accelerometer noise density	99μg/√Hz, 650μg/√Hz(HH), 15mg/√Hz(H3)
Accelerometer sensitivity	0.00024g/digit-0.00096g/digit 0.003g/digit-0.012/digit(HH) 0.049g/digit-0.195g/digit(H3)
Accelerometer temperature sensitivity	±0.008%/°C, ±0.01%/°C(HH, H3)
Gyro scale	±250/±500/±1000/±2000 °/sec selectable
Gyro resolution	16 bit
Gyro noise density	0.009°/sec/√Hz
Gyro bias stability @ 25°C	2.5°/hr average for all axes
Gyro sensitivity	0.00833°/sec/digit for ±250°/sec 0.06667°/sec/digit for ±2000°/sec
Gyro non-linearity	0.2% full-scale
Gyro temperature sensitivity	±0.03%/°C
Compass scale	±0.88 Ga to ±8.1 Ga selectable (±1.3 Ga default)
Compass resolution	12 bit
Compass sensitivity	0.73 mGa/digit
Compass non-linearity	0.1% full-scale

1. Depends upon communication mode, filter mode, Bluetooth adapter
2. Average value when calibrated.

Specifications are subject to change.
Version: 3.0r1

YEI Technology
630 Second Street
Portsmouth, Ohio 45662 USA
ph: 1-888-395-9029
fax:1-740-354-1170

www.YeiTechnology.com
www.3SpaceSensor.com

Patents Pending
©2014 YEI Corporation